Archaeological and Anthropological Sciences

Geochemical characterisation of pozzolanic obsidian glasses used in the ancient mortars of Nora Roman theatre (Sardinia, Italy): provenance of raw materials and historical-archaeological implications

--Manuscript Draft--

Manuscript Number:	
Full Title:	Geochemical characterisation of pozzolanic obsidian glasses used in the ancient mortars of Nora Roman theatre (Sardinia, Italy): provenance of raw materials and historical-archaeological implications
Article Type:	Original Paper
Section/Category:	Geoarchaeology
Corresponding Author:	Stefano Columbu, MD Universita degli Studi Di Cagliari Cagliari, CA ITALY
Corresponding Author Secondary Information:	
Corresponding Author's Institution:	Universita degli Studi Di Cagliari
Corresponding Author's Secondary Institution:	
First Author:	Stefano Columbu, MD
First Author Secondary Information:	
Order of Authors:	Stefano Columbu, MD
	Anna Maria Garau, PhD
	Carlo Luglié, PhD
Order of Authors Secondary Information:	
Funding Information:	
Abstract:	The study focused on the volcanic glass used in the production of bedding mortars and concrete of the Roman theatre (I cent. AD) of the Nora site. The volcanic glasses were frequently used as aggregate and with pozzolanic function in all hydraulic mortars of the different sectors of the building (e.g., concretes of tribunalia vaults and external niches, jointing and foundation mortars of cavea tier ashlars, brick bedding, etc.), together with mainly quartz-feldspar sands, local Oligo-Miocenic dacitic volcanics, Paleozoic and Tyrrhenian sedimentary rocks. These volcanic glasses show characteristics closer to obsidian than to natural pozzolan normally used in the Roman period. They have definitely not sourced locally, unlike the other components that make up the aggregate. To identify their provenance, a petrochemical comparison between several samples taken from the theatre mortars and the volcanic outcrops of some probable Sardinian source areas is made. The use of the not local pozzolanic glass is a technical innovation in the mortars of the Nora archaeological site, and considered the wide use of obsidians in the prehistoric periods for the production of tools, significant considerations about its origin, procurement and use are made.
Suggested Reviewers:	Domingo Gimeno Torrente Full professor of Geoquímica and Petrologia, Universitat de Barcelona d.gimeno.torrente@gmail.com
	Maria Pilar Lapuente, Geological Sciences Full professor, Universidad de Zaragoza plapuent@unizar.es
	Anna Maria De Francesco

	Associate professor, University of Calabria defrancesco@unical.it
	Dagmara Wielgosz-Rondolino University of Warsaw dagmara.wielgosz@uw.edu.pl
	Jacopo Bonetto University of Padova jacopo.bonetto@unipd.it

Geochemical characterisation of pozzolanic obsidian glasses used in the ancient mortars of Nora Roman theatre (Sardinia, Italy): provenance of raw materials and historical-archaeological implications

Stefano Columbu[1]*, Anna Maria Garau[1], Carlo Lugliè[2]

[1] Dipartimento di Scienze Chimiche e Geologiche, Università degli Studi di Cagliari, Via Trentino 51, 09127 Cagliari, Italy

[2] Dipartimento di Dipartimento di Storia, Beni culturali e Territorio, Università degli Studi di Cagliari, Cittadella dei Musei, Piazza Arsenale 1, 09124 Cagliari, Italy

***Corresponding author:** E-mail: **columbus@unica.it**, Tel.: +39 070 6757766

ABSTRACT

The study focused on the volcanic glass used in the production of bedding mortars and concrete of the Roman theatre (I cent. AD) of the Nora site. The volcanic glasses were frequently used as aggregate and with pozzolanic function in all hydraulic mortars of the different sectors of the building (*e.g.*, concretes of *tribunalia* vaults and external niches, jointing and foundation mortars of *cavea* tier ashlars, brick bedding, etc.), together with mainly quartz-feldspar sands, local Oligo-Miocenic dacitic volcanics, Paleozoic and Tyrrhenian sedimentary rocks. These volcanic glasses show characteristics closer to obsidian than to natural pozzolan normally used in the Roman period. They have definitely not sourced locally, unlike the other components that make up the aggregate.

To identify their provenance, a petrochemical comparison between several samples taken from the theatre mortars and the volcanic outcrops of some probable Sardinian source areas is made.

The use of the not local pozzolanic glass is a technical innovation in the mortars of the Nora archaeological site, and considered the wide use of obsidians in the prehistoric periods for the production of tools, significant considerations about its origin, procurement and use are made.

Keywords: Pozzolan; Obsidian glass; Chemical analysis; Aggregate; Mt. Arci; Sardinian Neolithic

1. INTRODUCTION

The Roman theatre is one of the most important buildings of the Roman village of Nora, located in the Gulf of Cagliari (south-western Sardinia, Figs. 1, 2). Nora was founded by the Phoenicians around the mid-eighth century BC, although there is evidence of earlier settlements (AA.VV., 2000; Luglié, 2009b; Wilson, 1980). The theatre has a semi-circular isodomic front with a W-NW axis (Fig. 3) and was built during the Augustan or Giulio-Claudio period (first century AD; Bejor, 1999). According to the use in Roman times (Adam, 2006; Cagnana, 2000; Giuliani Cairoli, 2006), a variety of geomaterials (sandstones, conglomerates, volcanic rocks, marbles, bricks, etc.) and different kind of mortars (*i.e.*, Roman concrete, bedding and jointing mortars of ashlars and bricks, plasters) were employed to construct the theatre. In the mortars, several different raw materials (*i.e.* quartz-feldspatic sands, fine and coarse volcanic aggregate, etc.) were used, according to the mortar function and the different sectors of the building: structure-wall, *tribunalia* vaults, wall of external niches, foundation of *cavea* tiers, stage inner wall.

The volcanic glasses show characteristics similar to obsidian facies and not to natural pozzolan normally used in the Roman period for make the mortars. The use of these pozzolanic glasses, that at the outset does not show to share a local origin, is a novelty because, to date, they have never been found in the ancient mortars of the Nora archaeological site. Given the wide use of Sardinian obsidian in the Neolithic or Calcolithic periods for the production of tools and artifacts, significant considerations about its use, origin and exploitation can be made.

The archaeometric investigations on both the geochemical and petrographic features and origin of raw materials used in the ancient mortars are fundamental for understanding the ancient routes used by the Romans for the transport of stone materials and for obtaining information on the interconnection of Roman settlements and residential sites present in Sardinia. Moreover, these studies are useful to define the technologies and behaviours for the construction of ancient buildings in different historic times and to address the conservative interventions (Adriano *et al.*, 2009; Alvarez *et al.*, 2000; Antonelli *et al.*, 2014b; Bertorino *et al.*, 2002; Bianchini *et al.*, 2004; Bultrini *et al.*, 2006; Columbu, 2017, 2018; Columbu *et al.*, 2014a,b, 2015a,b, 2017a,b, 2018a,b,c; Columbu and Verdiani, 2014; De Luca *et al.*, 2013, 2015; Franzini *et al.*, 2000; Gutiérrez *et al.*, 2016; Lapuente, 2014; Lapuente *et al.*, 2012; Lezzerini *et al.*, 2016, 2018; Miriello *et al.*, 2010, 2015; Maravelaki-Kalaitzaki *et al.*, 2003; Moropoulou *et al.*, 2000, 2004; Riccardi *et al.*, 1998; Smith and Smith, 2009; Stanislao *et al.*, 2011; Verdiani and Columbu, 2010, 2012; Vola *et al.*, 2011).

To identify their geological provenance, the geochemical data of the glass samples were compared with those of new and literature data of acid volcanics (only the rhyolites and alkali-rhyolites were selected) for south and central Sardinia, where one may find similar lithologies: the island of St. Antioco and Mt. Arci, respectively. In the last of these areas, singled out as possible sources, there is no evidence of quarrying activity during the Roman period, but evidence from Neolithic working of obsidian.

More than 250 samples of rock samples from both the outcrops (Mt. Arci and St. Antioco areas) and volcanic glasses of mortars from main sectors of the theatre were analysed. The results of chemical analysis together with the petrographic characterisation were used in order to: i) geochemical classify the volcanic glasses from mortars of Nora theatre, according to different diagrams; ii) define compositional inhomogeneity internal to the same glass samples; iii) framing of glasses in the magmatic series, analysing the geochemical trend of trace elements and the rare earth pattern; iv) identify the geographical origin of these glasses employed in the mortars, to understand their supply in Sardinia in the Roman period.

2. MATERIALS AND ANALYTICAL METHODS

50 pozzolanic volcanic glass fragments of aggregate among 48 selected and representative samples of mortars were analysed and studied. The mortar samples come from the following sectors of the theatre: *tribunalia* (9 samples, divided into 7 concretes of two vaults, 2 bedding mortars of ashlar structure), *cavea* (14 jointing/foundation mortars of volcanic and sandstone ashlars), external niches (16 samples, divided into 9 bedding mortars of outer brick-walls, 3 concrete mortars of inner structure-wall, 2 concrete of basement of *via*, corridor around the external side of the *cavea*, 1 concrete of only one vault overlying the niche), *pulpitum* (7 bedding mortars and 4 samples of *arriccio* plasters of the *ribalta* wall and pillar of *hyposcenium*).

The mineralogical and petrographic analysis of volcanic rocks and mortars was performed on thin sections under the polarizing microscope (Zeiss photomicroscope Pol II).

The major chemical elements of volcanic glass from the mortars were analysed in thin section under an electron microprobe with a Cambridge S360 scanning electron microscope, equipped with an energy dispersive spectrometer Link QX2000, Pentafet detector and IBM 686 computer equipped with appropriate software for the acquisition of scanned images. Microanalyses were collected at 15 kV using a 3 μA beam current and a 25 μm spot size.

The analysis of the trace elements (including the full pattern of rare earth) of volcanic glasses included in the mortars were carried out with inductively coupled mass spectrometry combined with laser ablation as a sampling system. It has necessitated an ad hoc sample preparation: some volcanic glass fragments isolated from each mortar sample were embedded in two-component epoxy resin (RenLam M-1, viscosity 1300 mPa s at 25 °C) of cylindrical shape. The obtained test specimen was gradually treated with abrasives of silicon carbide and alumina powders to bring to the surface and polishing the embedded glass fragments. The diameter of the laser beam used is of 40 μm, with a frequency of 10 Hz and a fluence of about 15 J/cm^2. Data reduction was performed using software "Glitter" (Van Achterberg *et al.* 1999). As external standards, synthetic glass NIST 610 and BCR-2 basalt have used, while as a variable internal standard ^{44}Ca was used. In this method, the intensity signals of the elements depend both on the concentration changes, and the mass ablated in subsequent spot. To make independent analysis by mass variations you must use the internal standard technique with variable concentrations: the concentration of the analyte is a linear function of the intensity ratio of the analyte in the unknown sample relative to that of the reference standard for the same element, with a correction linearly dependent on the ratio of concentration of the same element (internal standard) content in the unknown sample with respect to a fixed concentration of the same element in the reference sample. Consequently, the knowledge for each point analysis of the concentration of internal standard assumes great importance. The glasses, which have been preliminarily subjected to analysis by electron microprobe, were given an average concentration for Ca element of 01.34 ± 0.13 at 1σ. The content ^{29}Si% was used as a variation index (see the diagrams of Figs. 13a, b, c). Nevertheless, clearly the concentrations in ^{29}Si% (average 49.14%) obtained by this method have a high standard deviation (± 16:24 at 1σ) in relation to the variability of the concentration of calcium in each fragment, and are consistently higher than those obtained in electron microprobe.

The chemical composition of volcanic rock samples from St. Antioco and (a part) from Mt. Arci were determined with a spectrometer in X-ray fluorescence Philips PW1400 with a Rh tube to analyse the major elements and some trace elements (Rb, Sr, Pb, Zn, Y, Nb, Zr), and with a W tube to analyse of Ni, Cr, Ba, V, La, Ce. Data reduction of major elements was performed by the method of Franzini *et al.* (1975). Data reduction of trace elements was performed by the method of Criss (1977), modified. The measurement accuracy is ± 1% for SiO_2, TiO_2, Al_2O_3, Fe_2O_3, CaO, K_2O and MnO and ± 4% for MgO, Na_2O and P_2O_5. The detection limits are about 3 ppm to 3σ for most of the elements; the accuracy of trace elements is ± 2 ÷ 3% to 1000 ppm; ± 5 ÷ 10% at 100 ppm and ± 10 ÷ 20% to 10 ppm. The weight loss for calcination (L.o.I., Loss on Ignition) was determined by calculating the loss in wt% at 1100 °C, while the FeO was determined by volumetric titration with $KMnO_4$ 10N in acid solution.

The analysis of the major elements of obsidians and perlites from Mt. Arci were performed by electron probe microanalysis using Wavelength Dispersive Spectrometry with a device ARL-SEMQ, using standards such as silicates and natural oxides; the data reduction was performed with the ZAF method (Colby, 1971). Detection limits of ~100 - 300 ppm are readily attained. During a typical multi-element analysis of a few minutes duration, 1σ precision of 0.3 - 1.5% relative is normally attained for major elements (*i.e.* those present at concentrations > 1% by weight). If desired, detection limits and precision may both be improved by increasing counting times, by increasing beam current, and/or by assigning multiple spectrometers to a single element.

3. CHARACTERISTICS OF MORTAR AGGREGATE

At the macroscopic observation, the mortars of the theatre (Fig. 4) show a reddish-grey-black and white/beige-grey aggregate (belonging to volcanic rock fragments and sialic mineral sands, respectively) with variable size and amounts, according to the different mortar function in the sectors.

The main compositional characteristics of the aggregate determined by microscopic modal analysis are reported in Tab. 1, along with the binder/aggregate ratio (B/A) expressed in vol.% (by modal analysis) and in wt% (after mechanical disintegration and acid attack of binder). The mortars show a greatest variability of vol.% B/A, due to the small size of the thin section that did not include the coarse fragments observed macroscopically, that probably do not reflect the real mixing proportions set by the manufacturer. B/A ratio calculated using the wt% data is much closer to those recommended by ancient sources (0.3–0.5 vol.%; *Vitruvius* Pollione, 15 BC).

The mortar aggregate consists mainly of quartz, orthoclase (Fig. 5e), microcline, plagioclase, black-grey volcanic glasses (Fig. 5a, b) and fragments of purplish volcanic rocks (Fig. 5c) with a local origin (according to Columbu and Garau, 2017). Subordinately, crystalline rocks from the Paleozoic basement (Fig. 5f), occasional mafic crystal-clasts (as pyroxene, Fig. 5d, biotite and opaque oxides), rare bioclasts and fragments of carbonate rocks (*e.g.* marble, limestone) were also used in the mortars. Not local volcanic glasses were used as aggregate but also with pozzolanic function, as highlighted by the reaction edges with the binder (Figs. 5a, 6b). Then, *cocciopesto* has also been used as pozzolanic material but overall in very low percentages (Tab. 1). The binder consists mainly of calcite, often present as spherules (Fig. 6d), where occasionally there are immersed lumps of bad-carbonated lime (Fig. 6c).

The local volcanic rocks belong to the Sarroch-Pula volcanism (Conte, 1989), related to the Late Eocene-Miocene Sardinian magmatic activity occurred between 38 and 15 Ma (Advokaat E.L. *et al.*, 2014a,b; Antonelli *et al.*, 2014a; Beccaluva *et al.*, 1985, 1989, 1994, 2005a, 2005b, 2011; Cherchi *et al.*, 2008; Columbu *et al.*, 2011; Lustrino *et al.*, 2004, 2009, 2011, 2013). Considering the medium-coarse size it's probably that the purplish volcanic rocks were used mainly as (inert-) aggregate, although they also show pozzolanic characteristics (Figs. 5c, 6a) (see Türkmenoglu and Tankut, 2002).

The different distribution of the main components in the aggregate has been showed in the ternary diagram of Fig. 7 where reported the modal percentages of quartz (Qz), feldspar (Fds) and volcanic glass (V). The volcanic glasses were used in almost all samples in varying proportions, according to the function of mortar in the theatre; they are less present in the plasters while they are more abundant in the structural concretes of *cavea* foundation and of the *tribunalia* vaults, where in some cases represent about the 90% of the aggregate.

The sandy component is wide used in the bedding mortars of the wall bricks and in the plasters (Fig. 7), while it is found less frequently in the concretes of the *tribunalia* vaults and variously present in the *cavea* samples and external niches. It shows an almost constant ratio of quartz and feldspar (2:1, Fig. 7) in almost all mortar samples thus highlighting a unique sampling point of these sands (Columbu and Garau, 2017).

Regarding the particle size, according to the Folk classification (1968), the aggregate is made from sand, slightly gravelled sands, gravelly sands and, in some cases, sandy gravel, while according to the Wentworth classification (1922), it is mostly composed of large and medium sands. The aggregate shows a moderately selected sorting (according to Folk 1954).

By analysis under a reflection microscope, the volcanic glass makes up the majority of the aggregate fraction below 2000 microns, along with the more rare andesitic-dacitic rocks aggregate from local volcanic outcrops. The sand fraction is mostly represented by quartz, feldspar, Palaeozoic rock fragments, Oligo-Miocenic volcanic rocks, volcanic glass and rare *cocciopesto*.

4. RESULTS

4.1 Petrographic features of volcanic rocks

In the mortars and concretes of theatre were employed two different kind of volcanic stones: 1) medium welded rocks, mainly used as medium-coarse aggregate; 2) grey-black obsidian glasses with not local origin, used as aggregate and also as pozzolanic material.

1) by macroscopic observation, the first rocks, characterized by chromatisms varying from grey-reddish to purplish-brown, show an evident self-clastic structure typical of a volcanic autobreccia, with from sub-centimetric lava-clasts. By microscopic analysis these volcanic rocks show a hypo-crystalline porphyritic structure (with variable porphyritic index between 5 and 8) for phenocrysts of early opaque, dominant plagioclase, pyroxene and hornblende. Due to the squat form, the opaque minerals are formed, presumably, by titan-magnetite or magnetite.

On the base of volcanological and petrographic features, these rocks show a similarity with the dacitic rocks of territory around the Nora village (e.g., "Perdu Pranu" outcrop, NE to the site) and especially with the volcanic stones used for the tiers of the theatre (*cavea*, see Fig. 3) belonging to the ancient quarry of "Su Casteddu" (Melis and Columbu, 2000; Columbu and Garau, 2017; Columbu, 2018). This latter is a volcanic structure (of which today essentially remains just the neck) located about 1.5 km at north-west from Nora site. In fact, the outcrop rock shows the same characteristics already observed in the volcanic coarse aggregates, characterised by the chaotic presence of large lava-clasts (usually sharp-edged) and smaller lava-clasts with rounded contour, with maximum dimensions of 1 cm immersed in a glassy matrix with a lower degree of welding, compared to the clasts.

2) the grey-black obsidian glasses show a hyaline structure with rare phenocrysts of plagioclase and biotite. These glasses are characterized by pearlitic fractures, or from a vacuolar and/or fluidal texture. In some cases there are typical devitrification structures as spherulites (in agreement with Lofgren, 1971). These volcanic fragments are always characterized by the presence of reaction rims between the glass and the binder of mortar (Fig. 6b).

4.2 Geochemical characteristics of obsidian glasses

4.2.1 Analysis of major elements and rock classification

Tabs. 2a, b show the results of the chemical analysis of the glasses used in the mortars of Roman theatre, where are reported the analytical values of major elements and the C.I.P.W. norm (according to Cross *et al.*, 1903). Tabs. 3a, b show the results of chemical analysis on the volcanics (perlites and obsidians) of Mt. Arci (Fig. 1). Tab. 3c shows the analytical values of the volcanics from St. Antioco area (Fig. 1).

Tab. 4 shows a summary of the rock classification of the glasses from the theatre mortars and volcanic samples from Mt. Arci and St. Antioco, according to the diagrams of Middlemost, 1975 (Fig. 8) and De La Roche *et al.* 1980 (Fig. 9). According to this latter diagram, the glasses of the mortars are classified as rhyolites. The samples of perlite and obsidian from Mt. Arci are classified as alkali-rhyolites and (as transition products) to the rhyolites. The acidic volcanics of St. Antioco constitute a separate group with respect to both the mortar glasses and the samples from the Mt. Arci outcrops.

According to the TAS (Total Alkali Silica) diagram of Le Maitre *et al.* (2002; Fig. 10), the most of the samples fall within the field of the rhyolites, while only some perlites from Mt. Arci and some volcanics from St. Antioco fall within the trachy-dacite and dacite fields.

All samples fall under the dashed discriminant line of Irvine and Baragar (1971) between the alkaline and subalkaline series, that has been overlapped to the TAS diagram of Fig. 10.

Also the diagram of De La Roche *et al.* (Fig. 9) shows the subalkaline character of the volcanics which, falling between the line of the critical plane of unsaturation (and away from it) and the abscissa axis, are strongly supersaturated.

In the classification diagram of Peccerillo and Taylor (1976; Fig. 11) the most of the samples falls within the field of shoshonitic series and subordinately of K-high series. Almost all samples are classified as rhyolites, except some perlites of Mt. Arci and Sant'Antioco, which are classified as trachytes of shoshonitic series.

Fig. 12 reports the variation diagrams of major elements *versus* the differentiation index (D.I.) of Thornton and Tuttle (1960). Regarding the volcanic glasses of the mortars, it's observe the typical trend of common magmatic series, with a decidedly positive correlation between SiO_2 and D.I.. Even the K_2O and Na_2O are positively correlated with D.I., although weakly. A negative correlation exists, however, between Al_2O_3 and P_2O_5, typical of the evolved rocks in which splits the apatite. Other oxides, such as MgO and TiO_2 are quite dispersed.

Almost always similar trends are even noted for the elements of obsidian and perlite samples from Mt. Arci, except for Al_2O_3 and CaO that remain almost constant. All diagrams of Fig. 12 show a different behaviour of the mortars glasses (that form a distinct group) compared to the samples from St. Antioco and Mt. Arci. Even among samples from Mt. Arci, it is possible to distinguish two different groups: the perlites and the obsidians. In particular, the perlite samples are characterized by higher values of Al_2O_3, CaO and K_2O and from lower values of P_2O_5 and Na_2O.

The behaviour of K_2O and Na_2O has already been highlighted by Cioni *et al.* (2001), according to which the interaction between the anhydrous volcanic glasses (obsidian) and the meteoric waters lead to the formation of hydrates glass (perlite) with leaching of Na_2O and relative enrichment in K_2O.

Instead, the samples of the Perdas Urias outcrops (eastern side of Mt. Arci) form a group almost always superimposed on the mortars glass samples, as already noted in the above diagrams, showing a certain similarity geochemistry with them.

4.2.2 Analysis of trace elements

Tabs. 5 and 6a-e show the results of the chemical analysis of trace elements of the obsidian glasses from the mortars, where are reported also some major elements. The analytical values are plotted in the diagrams of Figs. 13a-c *versus* ^{29}Si (expressed in % for graphic reasons). The patterns are comparable with those of common magmatic series, highlighting the validity of the ^{29}Si% as variation index.

There was a positive correlation between% ^{29}Si and: ^{23}Na, ^{66}Zn, ^{49}Ti, ^{85}Rb, ^{133}Cs, ^{137}Ba, ^{93}Nb, ^{139}La, ^{208}Pb and ^{238}U, while there is a negative correlation with the ^{88}Sr; the values of the other elements are dispersed.

The analytical values of some elements (Tabs. 6a-e) are far higher than the average of the same element in the other analysed points; these values, which may depend on the presence of phases within the micro volume of vaporized sample by the laser, or by a lack of homogeneity at the microscopic level in the distribution of the elements, were regarded as outsiders and therefore excluded from the variation diagrams.

The trends of some rare earth elements normalized to chondrites (factors taken from Anders and Grevesse, 1989) are shown in Fig. 14a. They are characterized by a moderate variability (minimum: 157.47 ± 9:49 ppm / chondrite for Ce;

maximum: 13.66 ± 3.2 ppm / chondrite for Eu), indicating the belonging to a single magmatic series. Furthermore, while the light rare earths have parallel trends and that do not intersect between them, the trends of the heavy rare earths are less correlated and tend to interbreed. Tab. 7 shows the correlation matrix for the rare earths showed in Fig. 14a; the maximum correlation for light rare earths coarsely tends to decrease for heavy rare earths, as highlighted by the variation diagrams *vs*. ^{29}Si% in the Fig.s 13a, b, c.

In general, the patterns are characterized by a negative peak in correspondence with europium, which indicates in all probability the fractionation of plagioclase, in good agreement with the petrographic observations and chemical analysis of some plagioclase phenocrystals of mortars glasses; in fact, in the plagioclases there is a greater europium content with respect to the content of the same element in the glasses (Tab. 5). The Eu negative peak also indicates the apatite fractionation (Cox *et al.*, 1979), according to the trend of P_2O_5 *vs.* D.I. (Fig. 12).

The pattern of the rare earths is characteristic of the final stages of the magmatic series and it is comparable with the pattern already observed in Sardinia for the dacitic and comenditic rocks from Sulcis area (Morra *et al.*, 1994) and for dacites and rhyolites of Mt. Arci (Beccaluva *et al.*, 1984).

Similarly, the pattern of trace elements normalized to primitive mantle according to Wood 1979 (Fig. 14b) shows that the whole sequence analysis has a regular distribution, with a not very wide range of variation (minimum: 5.69 ± 0.31 ppm / primitive mantle for Sr; maximum: 13.22 ± 2.48 ppm / primitive mantle for Hf); only some samples deviate on the performance more generally in correspondence of the tantalum and niobium, hafnium and zirconium. The pattern is characterized by an enrichment of the lithophile elements with wide ionic radius (LILE). Some elements such as Sr and Ba show the negative peaks, surely due to the fractionation of plagioclase and K-feldspar. In fact, as can be seen from Tabs. 5 and 6, the value of Sr (in ppm) in plagioclase is much higher than the value of Sr present in the glass. It also shows an impoverishment compared to the primordial mantle, due probably to the fractionation of iron and titanium oxides.

4.3 Provenance of pozzolanic glasses

Considering that in the areas adjacent to Nora's site there are no rock outcrops with similar geochemical-petrographic characteristics, in order to identify the sources of supply, the composition geochemistry of these glasses with new and literature analytical data of similar volcanic rocks (rhyolites / alkali-rhyolites) from Mt. Arci and St. Antioco areas was compared, using the linear discriminant analysis.

4.3.1 Discriminant analysis using major elements

The discriminant analysis (performed using the Statistical Mac program) was applied to subdivide the groups defined a priori that are represented by the glasses used as aggregate and pozzolan in the theatre mortars, the volcanics samples (obsidians and perlites) from Mt. Arci and the volcanics coming from the St. Antioco.

In detail, 232 analyses (divided as in Tab. 8) were considered. The variables chosen for the discrimination of the groups are represented by the major elements: SiO_2, TiO_2, Al_2O_3, FeO_T, MnO, MgO, CaO, Na_2O, K_2O, P_2O_5. Among them, those that are found to be significant (based on the discriminant analysis) are: CaO, FeO, Al_2O_3 and P_2O_5.

The samples will be classified as belonging to the group that has the higher score (Tab. 9a).

The classification score of a sample for a group, for example from the Nora theatre (TN), is calculated as follows:

$$\text{Score (TN)} = -\,295\,945 + CaO + FeO_T * 16{,}546 * 63{,}419 + P_2O_5 * (191{,}734) * 37784 + Al_2O_3.$$

Tab. 9b shows the summary diagram of the classification results, according to the classification score groups. All analysis of the mortar glasses are properly classified as belonging to the "Theatre" group. Also all analysis of samples from "Mt. Arci" are properly classified. For "St. Antioco" samples, 92.86% of the total analysis was correctly classified, single analysis was attributed to the theatre group and a second one to the Mt. Arci group.

Tab. 10a shows the canonical functions, which are equal to the number of groups minus one. For each sample, each variable must be multiplied by the coefficient shown in the Tab. according to the scheme:

$$\text{Root 1} = 3.9207 + CaO + FeO_T * 4.52979 * (-0.79973) + Al_2O_3 + P_2O_5 * 10.70594 -0.54622.$$

In the diagram in Fig. 15 are projected the points of the canonical score R1 and R2, calculated according to the functions given in Tab. 10a.

In Tab. 10b the three equations (with $y = ax + b$) of straight lines dividing between the three groups are reported.

Observing the discriminating diagram of Fig. 15, the volcanic glasses used in the mortars constitute a distinct group compared with those of other samples from Mt. Arci and St. Antioco. The analysed samples from Perdas Urias outcrops (belonging to the Mt. Arci area), though falling within the field of St. Antioco group (Fig. 15), are very close to the analysis of mortar glasses.

4.3.2 Discriminant analysis using trace elements

The discriminant analysis was applied using the trace elements of the mortars glasses, obsidians of Mt. Arci and volcanics of St. Antioco.

163 analysis were considered, among which 112 relating to mortars glasses, 37 obsidians of Mt. Arci, and 12 related to St. Antioco. The variables chosen for the discrimination of the groups are represented by the following elements: Ti, V,

Cr, Zn, Rb, Sr, Y, Zr, Nb, Cs, Ba, La, Ce, Pb. Among them (based on discriminant analysis) those that perform most significant results are: Sr, Ce, V, Ba, Rb, Y. Similarly to the case of major elements, each sample is classified as belonging to the group that shows the higher score, calculated using the coefficients in Tab. 11a.

Tab. 11b shows a summary diagram of the classification results, according to the classification score groups. In the case of the mortar glasses, obsidians of Mt. Arci and volcanics of St. Antioco, the classification is correct in 100% of cases.

Tab. 12a shows the canonical functions, which, also in this case, are equal to two (number of groups minus one). For each sample, each variable must be multiplied by the coefficient shown, according to the scheme of previous paragraph. In Fig. 16 are projected the points of the canonical score R1 and R2. In Tab. 12b the three equations (with $y = ax + b$) of straight lines dividing between the three groups are reported.

The analysis of samples from the mortars of the theatre, from Mt. Arci and St. Antioco, constitute separate fields, while the analysis of samples from Perdas Urias fall under the volcanic glasses from the mortars of the theatre with a good overlap.

5. DISCUSSION OF RESULTS

Inside the Nora Roman theatre a great amount of obsidian glasses together with quartz / feldspar sands are mainly used as aggregate in the hydraulic mortars. These glasses have been also used as pozzolan materials, although their characteristics are different with respect to the natural pozzolans normally used in the Roman period. Thus, the volcanic glass gives good hydraulic characteristics to the mortars, as shown by the constant presence of reaction edges with the binder (Fig. 6b) with consequent chemical exchanges: a decrease of Si, Al and K and a simultaneous increase of Ca and volatiles compared with glass (Columbu *et al.*, 2017). Given the good pozzolanic characteristics of the volcanic glass, it is conceivable that the Romans voluntarily used this type of material in place of *cocciopesto* (scarcely present in the mortars, or absent in some samples) to make as much resistant mortar from the structure of the theatre, an open work subject to weathering processes.

The use of these volcanic glasses in the archaeological site of Nora, as well as in other Sardinian Roman monuments, at the moment was not known. Differently from the other components of the aggregate, these obsidian rocks do not belong to the vicinity of the Nora site, because there are no outcrops bearing these petro-volcanological characteristics. However, their wide use in the theatre mortars may suggests a not very distant origin. The geochemical comparison of data indicates that the mortar glasses have a source from the volcanic complex of Mt. Arci (central-western Sardinia; Fig. 1) where there are volcanic rocks with similar characteristics. As showed by statistical stepwise linear discriminant analysis, the samples from the locality of *Perdas Urias* (east of Mt. Arci volcanic complex) show a geochemical similarity (especially on the basis of trace elements) with the volcanic glasses from the mortars, suggesting a provenance from *Perdas Urias* of obsidian glasses used in the mortars of Nora theatre. The Mt. Arci obsidian deposits are well-known both in the archaeological and geological literature, (Barca *et al.*, 2007; De Francesco *et al.*, 2008, 2011; Freund, 2014; Freund and Batist, 2014; Le Bourdonnec *et al.*, 2006, 2010, 2015; Léa, 2012; Lilliu, 1988; Luglié, 2003, 2009a, 2010; Luglié *et al.*, 2006, 2007, 2008, 2011; Macciotta *et al.*, 2004; Mackey and Warren, 1983; Marchi *et al.*, 2005; Tykot, 1996, 1997, 2002; Tykot *et al.*, 2008). The obsidian rocks (prosaically called the "black gold" of the prehistoric period) is an important lithic raw material that has been used since the Early Neolithic with a high diffusion in many Neolithic to Calcolithic sites in Sardinia and in a part of the Western Mediterranean area. This type of volcanic material was commonly reduced to produce chipped tools (*e.g.* cutting tools such as axes, arrowheads, etc.).

From an archaeological point of view, two possible hypotheses on their procurement in the Roman period can be made: i) the obsidian was already present in the vicinity of the site of Nora (*e.g.* as a waste or residues of previous processing of the material); ii) it was extracted from an ancient quarry of Mt. Arci outcrops, that was well-known for the high presence of obsidians.

Considered the widespread Sardinian road network in the Roman time (Fig. 1; Mastino, 2005) and their intensive use in the theatre of Nora, it is likely to imagine a procurement of these obsidians from the Mt. Arci area. In fact, in agreement with the archaeological literature, the road connecting the Roman villages of *Karales* (today Cagliari city, south Sardinia; Fig. 1) and *Turris Lybisonis* (today Porto Torres, NW Sardinia; Fig. 1) passed near the eastward side of Monte Arci volcanic complex. Moreover, in the middle of this ancient road stood the archaeological site of *Forum Traiani* (today Fordongianus village; Fig. 1) and Roman village of Mulargia (Fig. 1), both well known for its thermal baths and for its ancient quarries of ignimbrite rocks, respectively. Mulargia is a very important Roman site for the production of Roman millstones, exported in various parts of the Mediterranean (*e.g.*, North Africa, Antonelli *et al.*, 2014a) and for the existence of ancient commercial routes of different kinds of stone. For these reasons it is not unlikely to assume a gathering and transportation activity, even if occasional, of obsidians along the Roman road network.

However, the first hypothesis of obsidian origin is by far more likely, because of the presence of some prehistoric settlement in the Nora area or its surroundings as in the *S'Abuleu* region (Migaleddu, 1996) and, possibly, in the same site of Nora (Luglié, 2009b), where obsidian reduction was a daily activity to produce a plentiful of artefacts. Moreover, there is evidence of obsidian tools in Nora territory also in later Nuragic times; in fact, to the north of Nora town there are many Nuragic sites, among which stands out the complex tower and village of *Antigori* (near to the Sarroch city). This is a large site occupied from the 14th-8th centuries B.C. (Russell, 2010; Balmuth, 1992) with castle-like structures, heavy multi-towered walls, and associated villages, which Webster (1996) labeled as one of 14 known Class III settlements in Sardinia.

6. CONCLUSIONS

The research allowed us to define the geochemical characteristics and the probable provenance of obsidian glasses used in the ancient mortars of the Roman Nora theatre.

This kind of volcanic glass, together with a quartz-feldspar sandy and subordinately local Oligo-Miocenic calcalkaline volcanics and Paleozoic rocks, was used as mortar aggregate for the different sectors of the theatre (*i.e.*, *tribunalia* vaults, *cavea* foundation, vaults and inner walls of the external niches, brick and stone walls). Considered its low bulk density, it's probable that it was used also to lighten some structures (*e.g.*, concrete of *tribunalia* vaults), together with sub-decimetric fragments of other local stones (*i.e.*, volcanic rocks and sandstones), even them with low bulk density due to their high porosity. Given its chemical-physical features, characterised by an amorphous state reacting with the binder, it was also used as pozzolan, conferring hydraulic properties and high mechanical strengths to the mortars and concretes of the monument, especially in the structural parts where it has been intensively used.

Given the good hydraulic features and their massive use in the theatre, it's probable that the Romans intentionally used the volcanic glasses in place of *cocciopesto*, to make the mortars much resistant to weathering. Moreover, the unusual presence of volcanic fine aggregate in the plasters of the open-air *cavea* sector of the theatre confirms the intention of Roman constructors to improve the hydraulic characteristics of the mortars and their resistance to decay processes. It is not accident that the theatre, an open construction designed without roofing, is also one of the best preserved buildings in Nora site.

The use of these obsidian glasses as pozzolan today represents a novelty in the production of Roman mortars in the archaeological site of Nora, especially considering that in the area surrounding Nora there obsidian is not available as a raw material.

The results of discriminant analysis highlights that the volcanic glasses show a geochemical similarity with the volcanics of *Perdas Urias* outcrops, indicating a provenance from Mt. Arci volcanic complex, a well known source as early as the Neolithic period (Lilliu, 1988; Lugliè, 2009a). Since is still lacking an archaeological evidence for the obsidian procurement directly from the source in Roman times, this hypothesis of the origin of glasses opens new scenarios from a historical and cultural point of view, raising up new and interesting issues.

From a technical-constructive point of view, it opens up further interesting research topics to understand if the use of obsidian rocks as aggregate in the mortars of a theatre was: (i) a local experiment to make the hydraulic mortars of theatre or (ii) extends to other buildings of the Nora site and/or in other Sardinian Roman settlements. Considering that currently there is no archaeological evidence about both the use of these obsidian glasses in other Sardinian Roman sites and the presence of Roman procurement in the raw material source area, at the moment it is unlikely to suppose that the Romans supplied obsidians directly from Mt. Arci. Assuming the first case, Romans probably used shatter from a local pre-existing source of obsidian, coming from an earlier production activity in previous Neolithic times in the Nora area. In fact, the obsidian processing-wastes are usually abundant in these prehistoric sites and well known in the archaeological literature, so it is easy to think of a later reuse of crushed earlier obsidian artefacts as temper for the mortars to be used in a single building like the theatre.

In any case, the discovery of these glasses inside the mortars of the theatre raises a strong interest in the development of new archaeological investigation and further geochemical and petrographic studies either to check the possible use of Mt. Arci obsidians in other Roman Sardinian sites or, more likely, to find the evidence of their storage and processing in the Nora area in prehistoric times.

Acknowledgments

Special thanks to the University of Cagliari for funding this research; the Superintendence for Archaeological Heritage for the Provinces of Cagliari and Oristano for authorization to sample the materials from the monument; the staff and tourist guides of the archaeological site of Nora for their willingness regarding the study activities of the Roman theatre.

REFERENCES

AA.VV. (2000) Ricerche su Nora - I (anni 1990-1998). Tronchetti, C. (Ed.). Cagliari: Sainas Ed.

Adam JP (2006) L’arte di costruire presso i romani, materiali e tecniche vol 10. Longanesi

Adriano P, Santos Silva A, Veiga R, Mirão J, Candeias AE (2009) Microscopic characterization of old mortars from Santa Maria Church in Évora. Material Characterization 60,7:610-620

Advokaat EL, Van Hinsbergen DJJ, Maffione M, Langereis CG, Vissers RLM, Cherchi A, Schroeder R, Madani H, Columbu S (2014) Eocene rotation of Sardinia, and the paleogeography of the western Mediterranean region. Earth and Planetary Science Letters, 401:183-195

Alvarez JI, Navarro I, Martin A, Garcia Casado PJ (2000) A study of the ancient mortars in the north tower of Pamplona’s San Cernin Church. Cement and Concrete Research, 30:1413-1419

Anders E, Grevesse N (1989) Abundances of the elements: meteoric and solar. Geochim. Cosmochim. Acta, 53:197-214

Antonelli F, Columbu S, De Vos Raaijmakers M, Andreoli M (2014) An archaeometric contribution to the study of ancient millstones from the Mulargia area (Sardinia, Italy) through new analytical data on volcanic raw material and archaeological items from Hellenistic and Roman North Africa. Journal of Archaeological Science 50: 243–261

Antonelli F, Columbu S, Lezzerini M, Miriello D (2014b) Petrographic characterization and provenance determination of the white marbles used in the Roman sculptures of Forum Sempronii (Fossombrone, Marche, Italy). Applied Physics A 115:1033–1040

Barca D, De Francesco AM, Crisci GM (2007) Application of Laser Ablation ICP-MS for characterization of obsidian fragments from peri-Tyrrhenian area. Journal of Cultural Heritage, 8,2:141-150

Beccaluva L, Bianchini G, Bonadiman C, Coltorti M, Macciotta G, Siena F, Vaccaro C (2005b) Within-plate Cenozoic Volcanism and Lithospheric Mantle Evolution in the Western-central Mediterranean Area. In: Finetti, I. (Ed.), Elsevier Special Volume, “Crop Project — Deep Seismic Exploration of the Central Mediterranean and Italy”, pp. 641–664

Beccaluva L, Bianchini G, Coltorti M, Siena F, Verde M (2005a) Cenozoic Tectono- magmatic Evolution of the Central-western Mediterranean: Migration of an Arc- interarc Basin System and Variations in the Mode of Subduction. In: Finetti, I. (Ed.), Elsevier Special Volume, “Crop Project — Deep Seismic Exploration of the Central Mediterranean and Italy”, pp. 623–640

Beccaluva L, Bianchini G, Natali C, Siena F (2011) Geodynamic control on orogenic and anorogenic magmatic phases in Sardinia and Southern Spain: Inferences for the Cenozoic evolution of the western Mediterranean. Lithos 123:218-224

Beccaluva L, Brotzu P, Macciotta G, Morbidelli L, Serri G, Traversa G (1989) Cainozoic tectono-magmatic evolution and inferred mantle sources in the Sardo-Tyrrenian area, in: Boriani, A., Bonafede, M., Piccardo, G.B., Vai, G.B. (Eds.), The lithosphere in Italy. Advances in Earth Science Research. Atti Conv. Acc. Naz. Lincei 80, pp. 229-248

Beccaluva L, Civetta L, Macciotta G, Ricci CA (1985) Geochronology in Sardinia: results and problems. Rend. Soc. It. Min. Petr., 40:57–72

Beccaluva L, Coltorti M, Galassi B, Macciotta G, Siena F (1994) The Cainozoic calcalkaline magmatism of the western mediterranean and its geodynamic significance. Boll. di Geofisica Teorica e Applicata, Vol. XXXVI, 141-144, 293-308.

Beccaluva L, Macciotta G, Manetti P, Peccerillo A, Poli G (1984) Pliocene-Quaternary alkaline to subalkaline volcanism in Sardinia: magma genesis and evolution. Dip. Sc. Terra, Firenze, pp. 50

Bejor G (1999) L’area del teatro, in: AA. VV. Ricerche su Nora-I (anni 1990-1998). Tronchetti, C. (Ed.), Cagliari: Sainas Ed.

Bertorino G, Franceschelli M, Marchi M, Luglié C, Columbu S (2002) Petrographic characterisation of polished stone axes from Neolithic Sardinia, archaeological implications. Per. Mineral., Special Issue: Archaeometry and Cultural Heritage, 71:87-100

Bianchini G, Marrocchino E, Vaccaro C (2004) Chemical and mineralogical characterisation of historic mortars in Ferrara (NE, Italy). Cement and Concrete Research, 34,8:1471-1475

Bultrini G, Fragala I, Ingo GM, Lanza G (2006) Minero-petrographic, thermal and microchemical investigation of historical mortars used in Catania (Sicily) during the XVII century A.D. Applied Physics A 83,4:529-536

Cagnana A (2000) Archeologia dei materiali da costruzione. SAP Società Archeologica S.r.l., Mantova

Cherchi A, Mancin N, Montadert L, Murru M, Putzu MT, Schiavinotto F, Verrubbi V (2008) The stratigraphic response to the Oligo-Miocene extension in the western Mediterranean from observations on the Sardinia graben system (Italy). Bulletin de la Societe Geologique de France, 179:267-287

Cioni R, Macciotta G, Marchi M, Padalino G, Simeone R, Palomba M (2001) Water-rock interaction in genesis of perlite at Monte Arci volcanic complex (West Sardinia, Italy). In: Cidu (Ed.), Water-Rock Interaction 2001, (pp. 693-696). Lisse: Swets & Zeitlinger.

Colby JW (1971) Magic IV: a computer program for quantitative electron microprobe analysis. Bell Telephone Laboratories Inc., Allentown, Pensylvania

Columbu S, Piras G, Sitzia F, Pagnotta S, Raneri S, Legnaioli S, Palleschi V, Lezzerini M, Giamello M (2018b) Petrographic and mineralogical characterization of volcanic rocks and surface-depositions on Romanesque monuments. Mediterranean Archaeology and Archaeometry, in press

Columbu S, Antonelli F, Sitzia F (2018a) Origin of Roman worked stones from St. Saturno Christian Basilica (south Sardinia, Italy). *Mediterranean Archaeology and Archaeometry*, in press

Columbu S, Sitzia F, Ennas G (2017b) The ancient pozzolanic mortars and concretes of Heliocaminus baths in Hadrian’s Villa (Tivoli, Italy). Archaeol Anthropol Sci., 9:523-553

Columbu S (2017) Provenance and alteration of pyroclastic rocks from the Romanesque Churches of Logudoro (north Sardinia, Italy) using a petrographic and geochemical statistical approach. Applied Physics A, Materials Science & Processing, 123 (3), 165:1-28, DOI: 10.1007/s00339-017-0790-z

Columbu S (2018) Petrographic and geochemical investigations on the volcanic rocks used in the Punic-Roman archaeological site of Nora (Sardinia, Italy). Earth Environmental Sciences, in press

Columbu S, Antonelli F, Lezzerini M, Miriello D, Adembri B, Blanco A (2014a) Provenance of marbles used in the *Heliocaminus* Baths of Hadrian's Villa (Tivoli, Italy). Journal of Archaeological Science 49: 332-342

Columbu S, Cruciani G, Fancello D, Franceschelli M, Musumeci (2015a) Petrophysical properties of a granite-protomylonite-ultramylonite sequence: insight from the Monte Grighini shear zone, central Sardinia, Italy. European Journal of Mineralogy 27,4:471-486

Columbu S, Garau AM (2017) Mineralogical, petrographic and chemical analysis of geomaterials used in the mortars of Roman Nora theatre (south Sardinia, Italy). Ital. J. Geosci., 136,2:238-262

Columbu S, Garau AM, Macciotta G, Marchi M, Marini C, Carboni D, Ginesu S, Corazza G (2011) Manuale sui materiali lapidei vulcanici della Sardegna centrale e dei loro principali impieghi nel costruito. Iskra Edizioni, Ghilarza (OR), p. 302

Columbu S, Gioncada A, Lezzerini M, Marchi M (2014b) Hydric dilatation of ignimbritic stones used in the church of Santa Maria di Otti (Oschiri, northern Sardinia, Italy). Ital. J. Geosci. 133:149-160

Columbu S, Lisci C, Sitzia F, Buccellato G (2017a) Physical-mechanical consolidation and protection of Miocenic limestone used on Mediterranean historical monuments: the case study of Pietra Cantone (southern Sardinia, Italy). Environmental Earth Sciences, 76(4), 148, DOI:10.1007/s12665-017-6455-6

Columbu S, Palomba M, Sitzia F, Murgia M (2018c) Geochemical and mineral-petrographic studies of stones and mortars from the Romanesque Saccargia Basilica (Sardinia, Italy) to define their origin and alteration. *Italian Journal of Geosciences*, in press

Columbu S, Sitzia F, Verdiani G (2015a) Contribution of petrophysical analysis and 3D digital survey in the archaeometric investigations of the Emperor Hadrian’s Baths (Tivoli, Italy). Rendiconti Lincei 26,4:455-474

Columbu S, Verdiani G (2014) Digital Survey and Material Analysis Strategies for Documenting, Monitoring and Study the Romanesque Churches in Sardinia, Italy, Lecture Notes in Computer Science, Springer 8740: 446-453

Cox KG, Bell JD, Pankhurst RJ (1979) The interpretation of igneous rocks. George Allen & Unwin, London, pp. 450.

Criss JW (1977) NRLXRF: a fortran program for X-Ray fluorescence analisys. Cosmic, Athens, Georgia

Cross W, Iddings JP, Pirsson LV, Washington HS (1903) Quantitative classification of igneous rocks. University of Chicago Press

De Francesco AM, Bocci M, Crisci GM (2011) Non-destructive applications of wavelength XRF in obsidian studies. X-Ray Fluorescence Spectrometry (XRF) in Geoarchaeology, 81-107

De Francesco AM, Crisci GM, Bocci M (2008) Non-destructive analytic method using XRF for determination of provenance of archaeological obsidians from the mediterranean area: A comparison with traditional XRF methods. Archaeometry, 50,2:337-350

De La Roche H, Leterrier J, Grandclaude P, Marchal M (1980) A classification of volcanic and plutonic rocks using R1-R2 diagram and major-element analyses - Its relationships with current nomenclature. Chemical Geology, 29:183-210

De Luca R, Cau Ontiveros MA, Miriello D, Pecci A, Le Pera E, Bloise A, Crisci GM (2013) Archaeometric study of mortars and plasters from the Roman City of Pollentia (Mallorca-Balearic Islands). Per. Mineral. 82: 353-379

De Luca R, Miriello D, Pecci A, Domìnguez-Bella S, Bernal-Casasola D, Cottica D, Bloise A, Crisci GM (2015) Archaeometric Study of Mortars from the Garum Shop at Pompeii, Campania, Italy. Geoarchaeology: An International Journal, 30:330-351

Folk RL (1954) The distinction between grain size and mineral composition in sedimentary rock nomenclature. Journal of Geology, 62,4:344-359

Folk RL (1968) Petrology of sedimentary rocks. Texas: Hemphill’s Austin.

Franzini M, Leoni L, Lezzerini M, Sartori F (2000) The mortar of the “Leaning Tower” of Pisa: the product of a medieval technique for preparing high-strenght mortars. Eur. J. Mineral., 12:1151-1163

Franzini M, Leoni L, Saitta M (1975) Revisione di una metologia analitica per fluorescenza-X, basata sulla correzione completa degli effetti di matrice. Soc. It. Min. Petrol. – Rendiconti, 31,2:365-378

Freund KP (2014) Obsidian consumption in Chalcolithic Sardinia: A view from Bingia 'e Monti. Journal of Archaeological Science, 41:242–250

Freund KP, Batist Z (2014) Sardinian obsidian circulation and early maritime navigation in the Neolithic as shown through social network analysis. Journal of Island and Coastal Archaeology, 9,3:364-380

Giuliani Cairoli F (2006) L’edilizia nell’antichità. Carocci, Roma

Gutiérrez GMA, Plumed HR, Soutelo SG, Savin MC, Lapuente P, Chapoulie, R. (2016) The marble of O Incio (Galicia, Spain): Quarries and first archaeometric characterisation of a material used since roman times. ArcheoSciences, 40,1:103-117

Irvine TN, Baragar WRA (1971) A guide to the chemical classification of the common volcanic rocks. Can. J. Earth Sci., 8:523-548

Kuno H (1968) Differentiation of basalt magma. In: the Poldervaart treatise on rocks of basaltic composition. Ed. H. Hess, A. Poldervaart, Vol. II, Wiley & Sons, New York, 623-688

Lapuente P (2014) Archaeometry on stones. Multi-method approach to investigate stone provenance. studied cases from Roman Hispanic marmora. Archeometriai Műhely (1786-271X), 11,3:149-158

Lapuente P, (2014) White marble sculptures from the National Museum of Roman Art (Mérida, Spain): sources of local and imported marbles. European Journal of Mineralogy, 26,2:333-354

Lapuente P, León P, Nogales T, Royo H, Preite-Martinez M, Blanc Ph (2012) White sculptural materials from Villa Adriana: study of provenance. In: Gutiérrez Garcia A, Lapuente P, Rodà I (Eds.), Interdisciplinary Studies on Ancient Stone. Proceedings of the IX ASMOSIA Conference, Tarragona, pp. 364-375

Le Bourdonnec FX, Bontempi JM, Marini N, Mazet S, Neuville PF, Poupeau G, Sicurani J (2010) SEM-EDS characterization of western Mediterranean obsidians and the Neolithic site of A Fuata (Corsica). Journal of Archaeological Science, 37,1:92-106

Le Bourdonnec FX, D’Anna A, Poupeau G, Lugliè C, Bellot-Gurlet L, Tramoni P, Marchesi H (2015) Obsidians artefacts from Renaghju (Corsica Island) and the Early Neolithic circulation of obsidian in the Western Mediterranean. Archaeological and Anthropological Sciences, 7,4:441-462

Le Bourdonnec FX, Poupeau G, Lugliè C (2006) SEM-EDS analysis of western Mediterranean obsidians: a new tool for Neolithic provenance studies. Comptes Rendus - Geoscience, 338,16:1150-1157

Le Maitre RW, Streckeisen A, Zanettin B, Le Bas MJ, Bonin B, Bateman P, Bellieni G, Dudek A, Efremova S, Keller J, Lamere J, Sabine PA, Schmid R, Sorensen H, Woolley AR (2002) Igneous Rocks: A Classification and Glossary of Terms. Recommendations of the International Union of Geological Sciences, Subcommission of the Systematics of Igneous Rocks. Cambridge University Press, Cambridge

Léa V (2012) The diffusion of Obsidian in the Northwestern Mediterranean: Toward a new model of the Chassey culture?. Journal of Mediterranean Archaeology, 25,2:147-173

Lezzerini M, Antonelli F, Columbu S, Gadducci R, Marradi A, Miriello D, Parodi L, Secchiari L, Lazzeri A (2016) The Documentation and Conservation of the Cultural Heritage: 3D Laser Scanning and Gis Techniques for Thematic Mapping of the Stonework of the Façade of St. Nicholas Church (Pisa, Italy). International Journal of Architectural Heritage: Conservation, Analysis, and Restoration, 10,1:9-19.

Lezzerini M, Pagnotta S, Raneri S, Legnaioli S, Palleschi V, Columbu S, Neri NF, Mazzoleni P (2018) Examining the reactivity of volcanic ash in ancient mortars by using a micro-chemical approach. Mediterranean Archaeology and Archaeometry, in press

Lilliu G. (1988) La civiltà dei sardi: dal paleolitico all’età dei nuraghi. Torino: Nuova ERI.

Lofgren G (1971) Experimentally Produced Devitrification Textures in Natural Rhyolitic Glass. Geological Society of America Bulletin, 82:111-124

Lugliè C (Ed.) (2010) L'ossidiana del Monte Arci nel Mediterraneo: nuovi apporti sulla diffusione, sui sistemi di produzione e sulla loro cronologia: Proceedings of V° International Congress (Pau, Italia, 27-29 giugno 2008). Ales: Nur.

Lugliè C (2003) First report on the study of obsidian prehistoric workshops in the eastern side of Monte Arci (Sardinia). Les Matières Premières Lithique en Préhistoire, Actes de la Tab.-Ronde d’Aurillac (Préhistoire du Sud-ouest, Supplément 5), pp. 207-209.

Lugliè C (2009a) L’obsidienne néolithique en Méditerranée occidentale. In: Moncel, M.H., Frohlich, F., (Eds.), L’Homme et le Précieux Matières Minérales Précieuses, BAR International Series 1934, Oxford: BAR, pp. 199-211.

Lugliè C (2009b) I manufatti litici preistorici. In: Bonetto J., Falezza G., Ghiotoo A.R., Nora. Il foro romano. Storia di un'area urbana dall'età fenicia alla tarda antichità 1997-2006. II.1 I materiali preromani. Padova, Università di Padova, pp. 1-2.

Lugliè C, Le Bourdonnec FX, Poupeau G (2011) Neolithic obsidian economy around the Monte Arci source (Sardinia, Italy): The Importance of integrated provenance/technology analyses. In: Turbanti-Memmi, I., (Ed.), Berlin: Springer, Proceedings of the 37th International Symposium on Archaeometry, 12th–16th May 2008, Siena, Italy, pp. 255-260.

Luglié C, Le Bourdonnec FX, Poupeau G, Atzeni E, Dubernet S, Moretto P, Serani L (2007) Early neolithic obsidians in Sardinia (western Mediterranean): The Su carroppu case. Journal of Archaeological Science, 34,3:428-439

Lugliè C, Le Bourdonnec FX, Poupeau G, Bohn M, Meloni S, Oddone M, Tanda G (2006) A map of the Monte Arci (Sardinia Island, Western Mediterranean) obsidian primary to secondary sources. Implications for Neolithic provenance studies. Comptes Rendus - Palevol, 5,8:995-1003

Lugliè C, Le Bourdonnec FX, Poupeau G, Congia C, Moretto P, Calligaro T, Sanna I, Dubernet S (2008) Obsidians in the Rio Saboccu (Sardinia, Italy) campsite: Provenance, reduction and relations with the wider Early Neolithic Tyrrhenian area. Comptes Rendus - Palevol, 7,4:249-258

Lustrino M, Duggen S, Rosenberg CL (2011) The Central-Western Mediterranean: anomalous igneous activity in an anomalous collisional tectonic setting. Earth-Science Reviews 104:1-40

Lustrino M, Fedele L, Melluso L, Morra V, Ronga F, Geldmacher J, Duggen S, Agostini S, Cucciniello C, Franciosi L, Meisel T (2013) Origin and evolution of Cenozoic magmatism of Sardinia (Italy). A combined isotopic (Sr–Nd–Pb–O–Hf–Os) and petrological view. Lithos, 180–181, 138–158

Lustrino M, Morra V, Fedele L, Franciosi L (2009) Beginning of the Apennine subduction system in central western Mediterranean: constraints from Cenozoic “orogenic”magmatic activity of Sardinia, Italy. Tectonics 28, TC5016.

Lustrino M, Morra V, Melluso L, Brotzu P, d'Amelio F, Fedele L, Franciosi L, Lonis R, Petteruti Liebercknecht AM (2004) The Cenozoic igneous activity of Sardinia. Per. Mineral., 73:105-134

Macciotta G, Columbu S, Garau AM, Marchi M (2004) Obsidian in the geochemical-petrographical Evolution of Plio-Quaternary volcanics from Monte Arci. In: Castelli, P. (Ed.), Proceedings of 1st International Conference «L'ossidiana del Monte Arci nel Mediterraneo: recupero dei valori di un territorio». Oristano-Pau (Italy), 29 November – 1 December 2002, pp. 35-46

Mackey M, Warren SE (1983) The identification of obsidian sources in the Monte Arci region of Sardinia. In: Aspinall, A., Warren, S.E. (Eds.), Proceedings of the 22nd Symposium on Archaeometry, University of Bradford, Bradford, pp. 420-431

Maravelaki-Kalaitzaki P, Bakolas A, Moropoulou A (2003) Physico-chemical study of Cretan ancient mortars. Cem. Concr. Res., 33:65-61

Marchi M, Garau AM, Columbu S, Macciotta G (2005) Definizione, nel Monte Arci, di possibili siti di provenienza di manufatti ossidianacei, mediterranei, per mezzo della loro caratterizzazione petrografica e geochimica. In: Proceedings of 3rd International Conference «L'ossidiana del Monte Arci nel Mediterraneo: le vie dell’ossidiana nel Mediterraneo ed in Europa». Oristano-Pau (Italy), 25-26 September 2004, PTM Editor.

Mastino, A., 2005. Storia della Sardegna antica. Sassari: Ed. Il Maestrale.

Melis S, Columbu S (2000) Matériaux de construction en époque romaine et aves les anciennes carrières: l’exemple du théâtre de Nora (Sardaigne SO, Italie). In: Lorenz, J., Tardy, D., Coulon, G. (Eds.), La pierre dans la ville antique et médiévale. Analyse méthodologie et apports, Argentoun sur Creuse. St.-Marcel: Musée d'Argentomagus (Ed.), pp. 103-117

Middlemost EAK (1975) The basalt clan. Earth-Science Reviews, 11:337-364

Migaleddu M (1996) Nora IV. Ricognizione. L'insediamento preistorico di S.Abuleu. Quaderni della Soprintendenza Archeologica per le Provincie di Cagliari e Oristano, 13:189-209

Miriello D, Antonelli F, Apollaro C, Bloise A, Bruno N, Catalano E, Columbu S, Crisci GM, De Luca R, Lezzerini M, Mancuso S, La Marca A (2015) New data about the ancient mortars from the archaeological site of Kyme (Turkey): compositional characterization. Per. Mineral. 84:497-517.

Miriello D, Barca D, Bloise A, Ciarallo A, Crisci GM, De Rose T, Gattuso C, Gazineo F, La Russa F (2010a) Characterisation of archaeological mortars from Pompeii (Campania, Italy) and identification of construction phases by compositional data analysis. Journal of Archaeological Science 37:2207-2223

Moropoulou, A., Bakolas, A., Aggelakopoulou, E. (2004) Evaluation of pozzolanic activity of natural and artificial pozzolans by thermal analysis. Thermochimica Acta, 420:135-140.

Moropoulou, A., Bakolas, A., Bisbikou, K. (2000) Investigation of the technology of historic mortars. Journal of Cultural Heritage, 1:45–58.

Morra, V., Secchi, F.A., Assorgia, A., 1994. Petrogenetic significance of peralkaline rocks from Cenozoic calk-alkaline volcanism from SW Sardinia, Italy. Chemical geology, 118, 109-142.

Peccerillo A, Taylor SR (1976) Geochemistry of Eocene calc-alkaline volcanic rocks from the Kastamonu area, northern Turkey. Contrib. Mineral. Petrol., 58:63-81

Pollione MV (15 BC) De Architecture. Vol. II. In: Cesariano C, De Architectura Libri Dece, 1521, Como

Riccardi MP, Duminuco P, Tomasi C, Ferloni P (1998) Thermal, microscopic and X-ray diffraction studies on some ancient mortars. Thermochimica Acta 321:207-214

Shand SJ (1951) Eruptive rocks; their genesis, composition, classification, and their relation to ore-deposits, with a chapter on meteorites. 4th ed, Wiley, New York.

Smith P, Smith RM (2009) Bricks and Mortar: A Method for Identifying Construction Phases in Multistage Structures. Historical Archaeology, 43:40-60

Stanislao C, Rispoli C, Vola G, Cappelletti P, Morra V, De Gennaro M (2011) Contribution to the knowledge of ancient Roman seawater concretes: Phlegrean pozzolan adopted in the construction of the harbour at Soli-Pompeiopolis (Mersin, Turkey). Periodico di Mineralogia, 80,3:471-488

Thornton CP, Tuttle OF (1960) Chemistry of igneous rocks, I. Differentiation index. American Journal of Science, 258:664-684

Türkmenoglu AG, Tankut A (2002) Use of tuffs from central Turkey as admixture in pozzolanic cements. Assessment of their petrographical properties. Cement and Concrete Research, 32:629-637

Tykot RH (1996) Obsidian procurement and distribution in the central and western Mediterranean. Journal of Mediterranean Archaeology, 9,1:39-82

Tykot RH (1997) Characterization of the Monte Arci (Sardinia) obsidian sources. Journal of Archaeological Science, 24,5:467-479

Tykot RH (2002) Chemical fingerprinting and source tracing of obsidian: The central mediterranean trade in black gold. Accounts of Chemical Research, 35,8:618-627

Tykot RH, Glascock MD, Speakman RJ, Atzeni E (2008) Obsidian subsources utilized at sites in Southern Sardinia (Italy). Materials Research Society Symposium Proceedings, Materials Issues in Art and Archaeology VIII, Boston, MA (United States), 1047:175-183

Van Achterbergh E, Ryan CG, Griffin WL (1999) Glitter: on-line interactive data reduction for the laser ablation ICP-MS microbrobe. Proc. 9th V.M. Goldschmidt Conf. (Boston)

Verdiani G, Columbu S, (2010) E. Stone, an archive for the Sardinia monumental witnesses. Third International Conference, EuroMed 2010, Lemessos, Cyprus, November 8-13, 2010. Book Chapter. 'Lecture Notes in Computer Science' (LNCS), Springer. Berlin-Heidelberg Vol. 6436:356-372

Verdiani G, Columbu S (2012) E.Stone, an archive for the Sardinia monumental witnesses. International Journal of Heritage in the Digital Era, 1,1:75-102

Vola G, Gotti E, Brandon C, Oleson JP, Hohlfelder RL (2011) Chemical, mineralogical and petrographic characterization of roman ancient hydraulic concretes cores from Santa Liberata, Italy, and Caesarea Palestinae, Israel, Periodico di mineralogia 80,2:317-338

Wentworth CK (1922) A scale of grade and class terms for clastic sediments. J. Geology 30:377-392

Wilson RJA (1980) Sardinia and Sicily during the Roman empire: aspect of the archeological evidence. Kokalos, XXVI-XXVII, 219-242

Wood DA (1979) A variably veined suboceanic upper mantle – Genetic significance for mid-ocean ridge basalts from geochemical evidence. Geology, 7:499-503

CAPTIONS OF FIGURES AND TABLES

Figure 1. Geological map of Sardinia with localization of the Roman Nora village and other important Punic-Roman city from the south to the north of island, *i.e. Karales* (today Cagliari), *Forum Traiani* (Fordongianus), *Turris Lybisonis* (Porto Torres); from Columbu and Garau, 2017.

Legend of patterns and colours refers to lithologies: white = recent alluvial sediments; light gray = Oligo-Miocene volcanics; dark gray = Plio-Pleistocene volcanics; gray stippled = Miocene marine sediments, gray crosses = Paleozoic crystalline basement and Mesozoic formations. Red continuous and dashed lines = faults.

Figure 2. Nora Roman theatre: (a) overview of Nora archaeological site with the theatre evidenced by red ellipse; (b) southwest view of the *hyposcenium* space under the stage (*palcoscenium*) and east-side *tribunalia* sector (see Fig. 3); (c)

southeast view of *orchestra*, west-side of *cavea* tiers and (down) part of *hyposcenium*; (d) view of east-side *tribunalia* sector (with recent cement rebuilt-consolidation under the vault); (e) detail of east-side *cavea* sector with greyish sandstone ashlars, original purplish volcanic ashlars and concrete of the tier foundation; (f) original mosaic decoration of *orchestra* floor.

Figure 3. Plan of the Nora Roman theatre. Legend of sectors: **a**: *cavea* (auditorium); **b**: *orchestra*; **c**: wall of stage; **d**: *hyposcenium* (space under the *palcoscenium*); **e**: front scene; **f**: portico behind the scene; **g**: west archway entrance; **h**: access ladder at the west *tribunalia*; **i**: west *tribunalia*; **l**: *parasceni*; **m**: external niches; **n**: enclosure; **o**: *via* (corridor atop the *cavea*); **p**: scalaria; **q**: *euripus* (underground channel for water drainage); **r**: *dolia*; **s**: small pillars under the *palcoscenium* (from Columbu & Garau, 2017, modified).

Figure 4. Mortar samples from different sectors of Nora theatre. (a) bedding mortar of Tirrenian sandstone ashlars of theatre structure with a flattened rock fragment of local Oligo-Miocenic volcanic stone; (b) bedding mortar of tier volcanic ashlars belonging to “Su Casteddu” outcrops (see: Melis and Columbu 2000, Columbu and Garau, 2017); (c) mortar sample from Roman concrete of *cavea* foundation; (d) entrapment mortar of *caementium* (Roman concrete) from east-side *tribunalia* vault; (e) entrapment mortar from Roman concrete of *cavea* foundation; (f) joint-mortar taken between the volcanic ashlars of *cavea* tiers.

Figure 5. Photograph details of mortar aggregate on polarized microscope. (a, b) plain polars: fragment of volcanic glass with evident vacuolar (and fluidal) structure and borders of reaction with the binder; (c) cross Nicol: fragment of local Oligo-Miocenic dacitic volcanic rock with binder-reaction borders; (d) plain polars: orthopyroxene crystal; (e) cross Nicol: altered orthoclase crystals; (f) cross Nicol: rounded fragment of meta-sandstone from Paleozoic crystalline basement.

Figure 6. Photograph details of mortars on electronic microscope (SEM). (a) binder-reaction borders between volcanic aggregate and binder; (b) binder-reaction borders between a fragment of volcanic glass and the binder; (c) lump of bad-carbonated lime; (d) spherules of calcite.

Figure 7. Aggregate compositional distribution of quartz (Qz), feldspar (Fds) and volcanic glass (V) in the mortars from different sectors of theatre (from Columbu & Garau, 2017, modified).

Figure 8. Na_2O *vs.* K_2O wt% classification diagram of Middlemost (1975) between the high-potash, potash and soda volcanic series, where plotted the volcanic samples from the outcrops and aggregate glasses from the mortars of the Nora theatre.

Abbreviations of the legend: K-Rhy = potash rhyolite; K-alRhy = potash alkali-rhyolite.

Figure 9. R_1 *vs.* R_2 classification diagram of De La Roche *et al.* (1980), where plotted the volcanic samples from the outcrops and aggregate glasses from the mortars of the Nora theatre. Symbols as legend of Figure 8.

Figure 10. Total Alkali-Silica diagram [(Na_2O+K_2O) *vs.* SiO_2 wt%] of Le Bas *et al.* (1986), where plotted the volcanic samples from the outcrops and aggregate glasses from the mortars of the Nora theatre. Symbols as legend of Figure 8.

Figure 11. K_2O *vs.* SiO_2 wt% classification diagram of Peccerillo and Taylor (1976) where plotted the volcanic samples from the outcrops and aggregate glasses from the mortars of the Nora theatre. Note: it was not possible to plot all analysis, because some samples have higher values of SiO_2% to 73%. Symbols as legend of Figure 8.

Figure 12. Variation diagrams: major elements (wt%) *vs.* differentiation index (D.I.) of Thornton and Tuttle, 1960 (where D.I. = normative Q +Ab + Or + Ne + Kp + Lc) for the volcanic samples from the outcrops and aggregate glasses from the mortars of the Nora theatre.

Figure 13a, b, c. Variation diagrams: selected major and trace elements (ppm) *vs.* ^{29}Si% for the volcanic samples from the outcrops and aggregate glasses from the mortars of the Nora theatre.

Figure 14a, b. Geochemical characteristics of the mortar glasses: (a) pattern of selected rare earths normalized to chondrite (factors from Anders and Grevesse, 1989); (b) spider diagram of selected elements normalized to primitive mantle, according to Wood (1979).

Figure 15. Discriminant diagram (Root 1 *vs.* Root 2) on the basis of the major elements of volcanic glasses from the mortars and volcanic samples from Mt. Arci and St. Antioco areas. Abbreviations as the legend of Fig. 8.

Figure 16. Discriminant diagram (Root 1 *vs*. Root 2) on the basis of the trace elements of volcanic glasses from the mortars and volcanic samples from Mt. Arci.

Table 1. Composition defined by polarized microscope analysis on thin sections of mortar samples taken from *tribunalia*, *cavea*, structure-walls and vault of niches, *hyposcenium* and *pulpitum* (stage) walls (from Columbu & Garau, 2017, modified). It has also been reported the binder/aggregate ratio (B/A as wt% after dissolution of binder and as vol.% by modal analysis).

Abbreviations: B = binder; A = aggregate; Qz = quartz; Fds = feldspar; Paleoz. Basem. = Paleozoic crystalline basement; □ = standard deviation; ±2s = absolute error.

Table 2a. Chemical analysis of volcanic glasses from the theatre mortars, where reported the rock classification (according to De La Roche *et al*., 1980), wt% of major elements and C.I.P.W. norm according to Cross *et al.* (1903).

Abbreviations: S.I. (wt% Solidification Index of Kuno, 1968) = (MgO•100)/ ($MgO+FeO_{tot}+Na_2O+K_2O$); A.I. (Agpaitic Index of Shand, 1951) = (Na_2O+K_2O)/Al_2O_3; D.I. (Differentiation Index of Thornton and Tuttle, 1960) = normative Q +Ab + Or + Ne + Kp + Lc; SAL = sum of sialic minerals; FEM = sum of mafic minerals; n.d. = not detected; Rhy = rhyolite; alRhy = alkali-rhyolite.

Table 2b. Chemical analysis of volcanic glasses from the theatre mortars, where reported the rock classification (according to De La Roche *et al.*, 1980), wt% of major elements and C.I.P.W. norm according to Cross *et al.* (1903).

Abbreviations as caption of Table 2a.

Table 3a, b. Chemical analysis of selected volcanic rocks from Monte Arci (central-western Sardinia), where reported the rock classification (according to De La Roche *et al.*, 1980), wt% of major elements and C.I.P.W. norm according to Cross *et al.* (1903).

Abbreviations as caption of Table 2a.

Table 3c. Chemical analysis of selected volcanic rocks from St. Antioco area (Sulcis, south-western Sardinia), where reported the rock classification (according to De La Roche *et al.*, 1980), wt% of major elements and C.I.P.W. norm according to Cross *et al.* (1903).

Abbreviations as caption of Table 2a.

Table 4. Distribution of analysed volcanic samples within sodium (Na), potassium (K) and high in potassium (HK) series, according to Middlemost (1975) and De La Roche *et al.* (1980) rock classification.

Abbreviations as caption of Table 2a.

Table 5. Chemical analysis of three plagioclase phenocrystals from the aggregate of theatre mortars.

Table 6a-e. Chemical analysis of trace (and some major) elements of volcanic glasses from the theatre mortars. The values are reported in ppm.

Table 7. Correlation matrix for some rare earths of volcanic glasses from the theatre mortars.

Table 8. Subdivision of 232 chemical analyses in the groups identified in advance to make the discriminant analysis on the basis of the major elements.

Table 9a, b. (a) Classificative functions for the discriminant analysis on the basis of the major elements.

(b) Summary of the classification of sample groups.

Abbreviations: TN = Nora Theater; MA = Mt. Arci; SA = St. Antioco; # = number of samples.

Table 10a, b. (a) Coefficients of canonical functions (Root 1 and Root 2) for the discriminant analysis on the basis of the major elements. (b) Equations (as y = ax + b) of dividing straight lines (1, 2, 3).

Table 11a, b. (a) Classificative functions for the discriminant analysis on the basis of the trace elements.

Abbreviations as caption of Figure 9.

Table 12a, b. (a) Coefficients of canonical functions (Root 1 and Root 2) for the discriminant analysis on the basis of the trace elements. (b) Equations (as y = ax + b) of dividing straight lines (1, 2, 3).

Figure 1

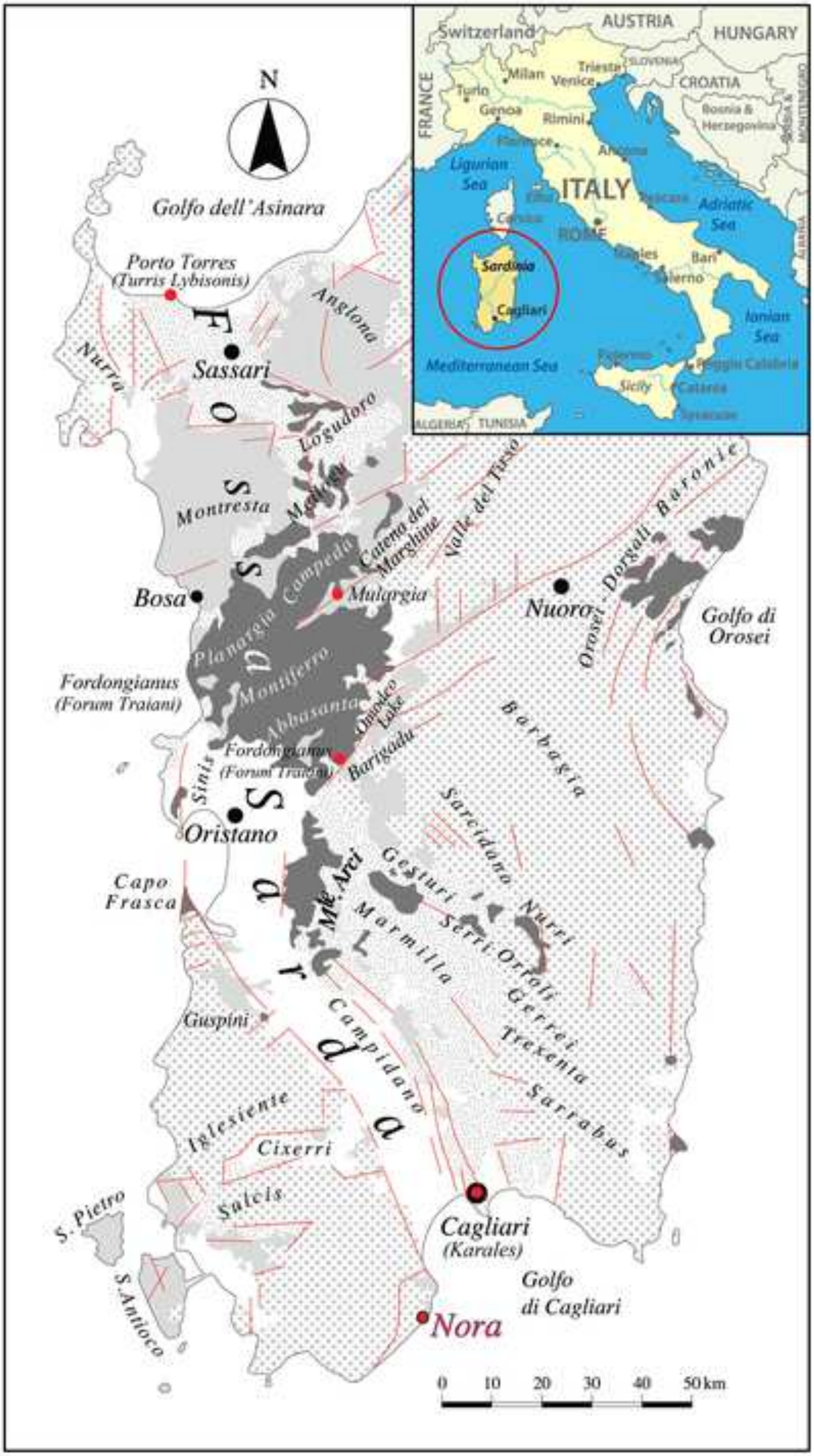
N
Golfo dell'Asinara
Porto Torres
(Turris Lybisonis)
Nurra
Anglona
Sassari
Logudoro
Montresta
Meilogu
Catena del Marghine
Valle del Tirso
Baronie
Bosa
Planargia
Campeda
Mulargia
Nuoro
Orosei - Dorgali
Golfo di Orosei
Fordongianus
(Forum Traiani)
Montiferro
Abbasanta
Omodeo Lake
Barigadu
Barbagia
Sinis
Oristano
Sarcidano
Capo Frasca
Gesturi
Mte Arci
Marmilla
Serri-Orroli
Nurri
Gerrei
Trexenta
Guspini
Campidano
Sarrabus
Iglesiente
Cixerri
Sulcis
S. Pietro
S. Antioco
Cagliari
(Karales)
Golfo di Cagliari
Nora
Fossa Sarda
0 10 20 30 40 50 km
Switzerland
AUSTRIA
HUNGARY
SLOVENIA
CROATIA
FRANCE
Milan
Trieste
Venice
Turin
Genoa
Rimini
Bosnia & Herzegovina
SERBIA & MONTENEGRO
Florence
Ancona
Ligurian Sea
ITALY
Elba
Pescara
Adriatic Sea
Corsica
ROME
ALBANIA
Sardinia
Naples
Bari
Salerno
Cagliari
Ionian Sea
Mediterranean Sea
Palermo
Reggio Calabria
Sicily
Catania
Syracuse
ALGERIA
TUNISIA


(a)
(b)
(c)
(d)
(e)
(f)

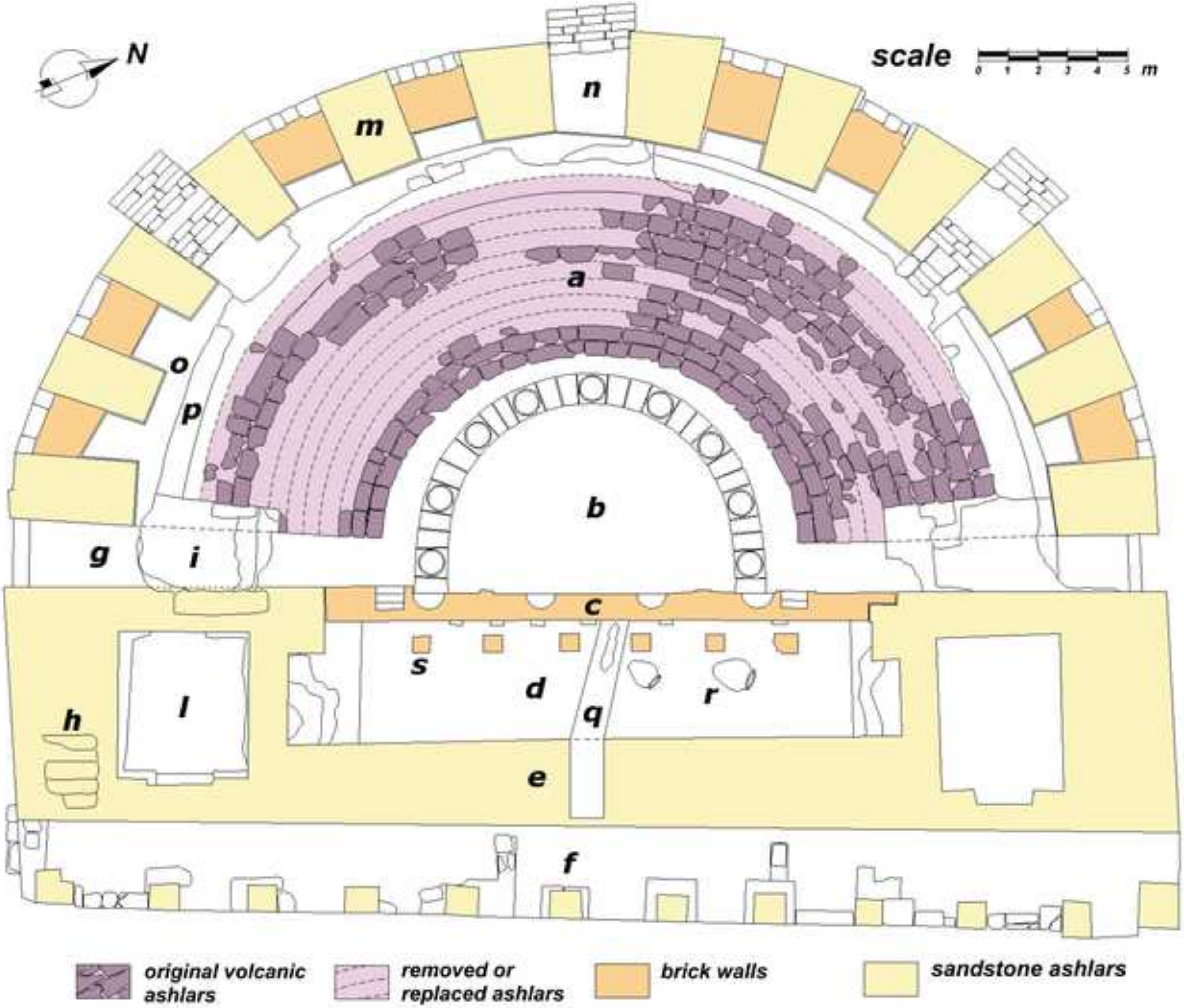
N
scale
0 1 2 3 4 5 m
n
m
a
o
p
b
g
i
c
s
d
q
r
h
l
e
f
original volcanic ashlars
removed or replaced ashlars
brick walls
sandstone ashlars

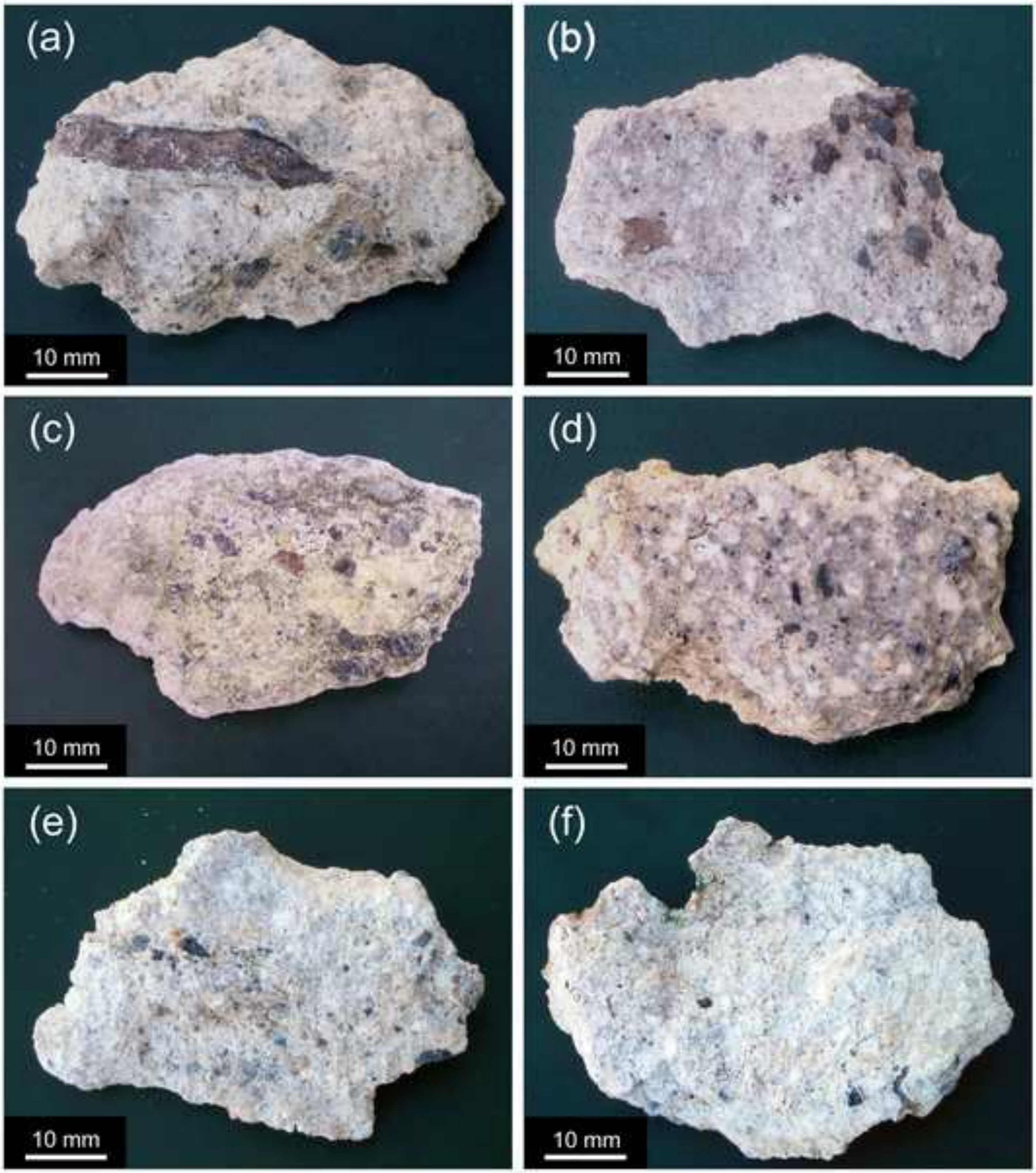
(a)
10 mm
(b)
10 mm
(c)
10 mm
(d)
10 mm
(e)
10 mm
(f)
10 mm

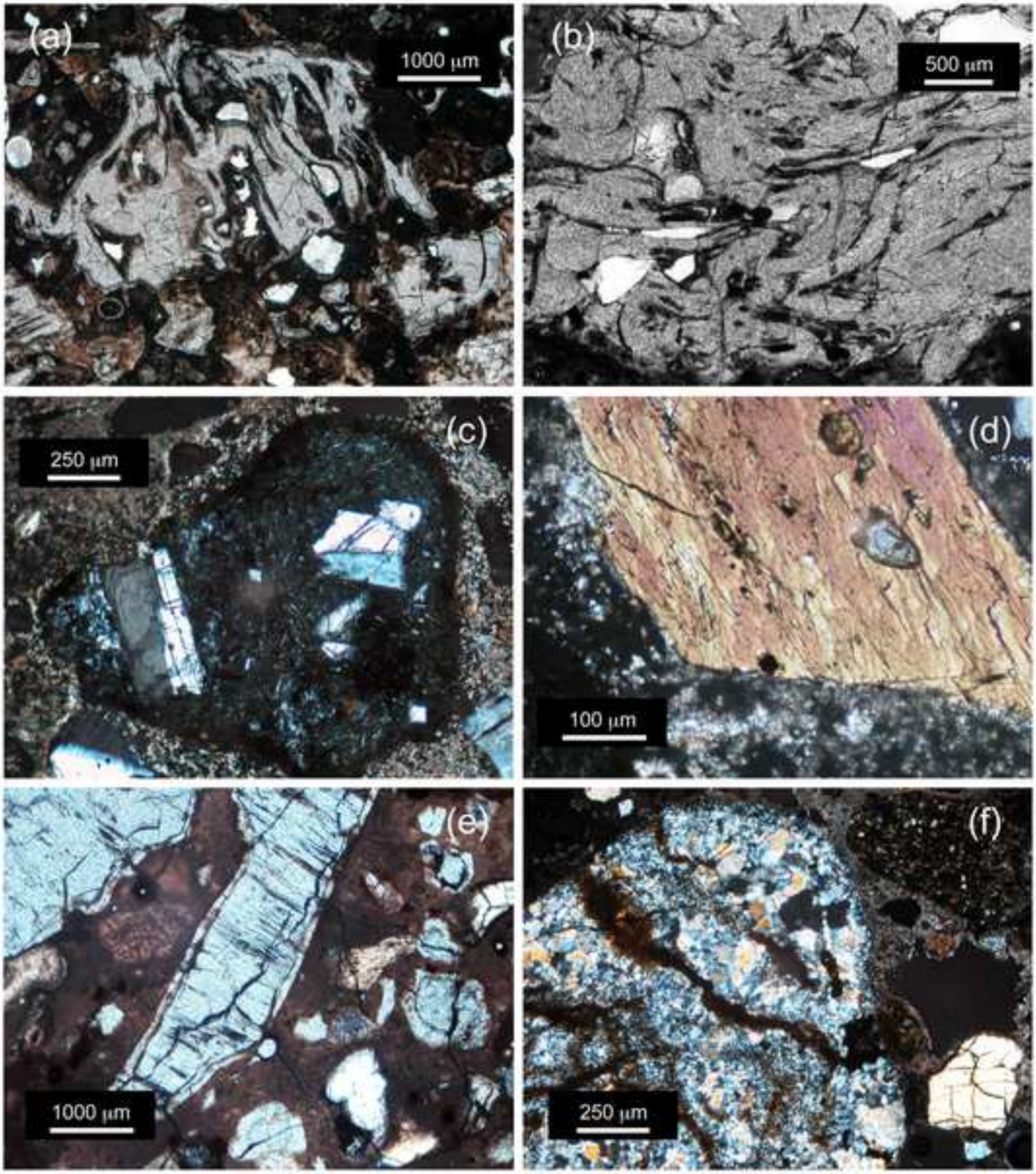
(a)
1000 µm
(b)
500 µm
(c)
250 µm
(d)
100 µm
(e)
1000 µm
(f)
250 µm

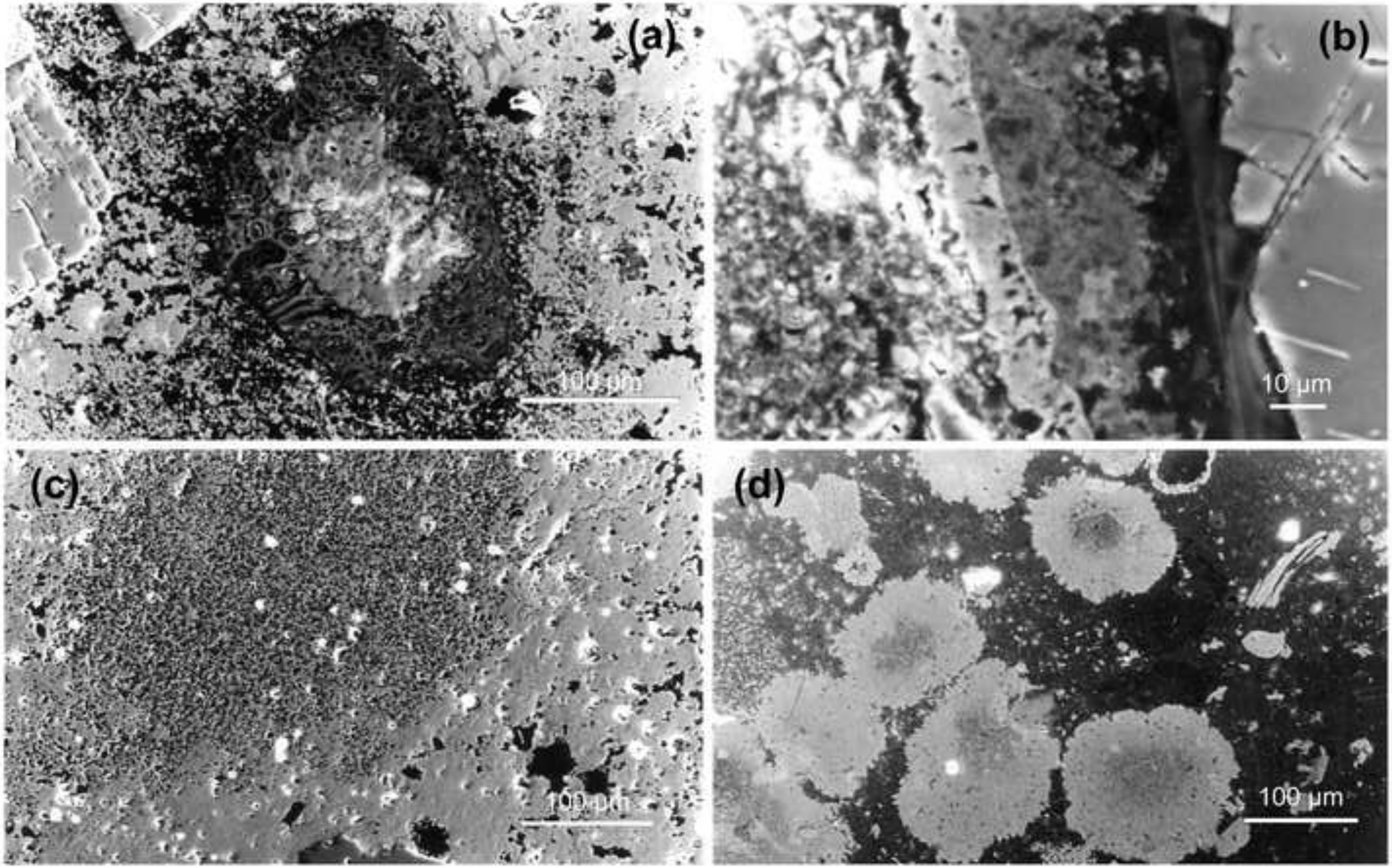
(a)
100 µm
(b)
10 µm
(c)
100 µm
(d)
100 µm

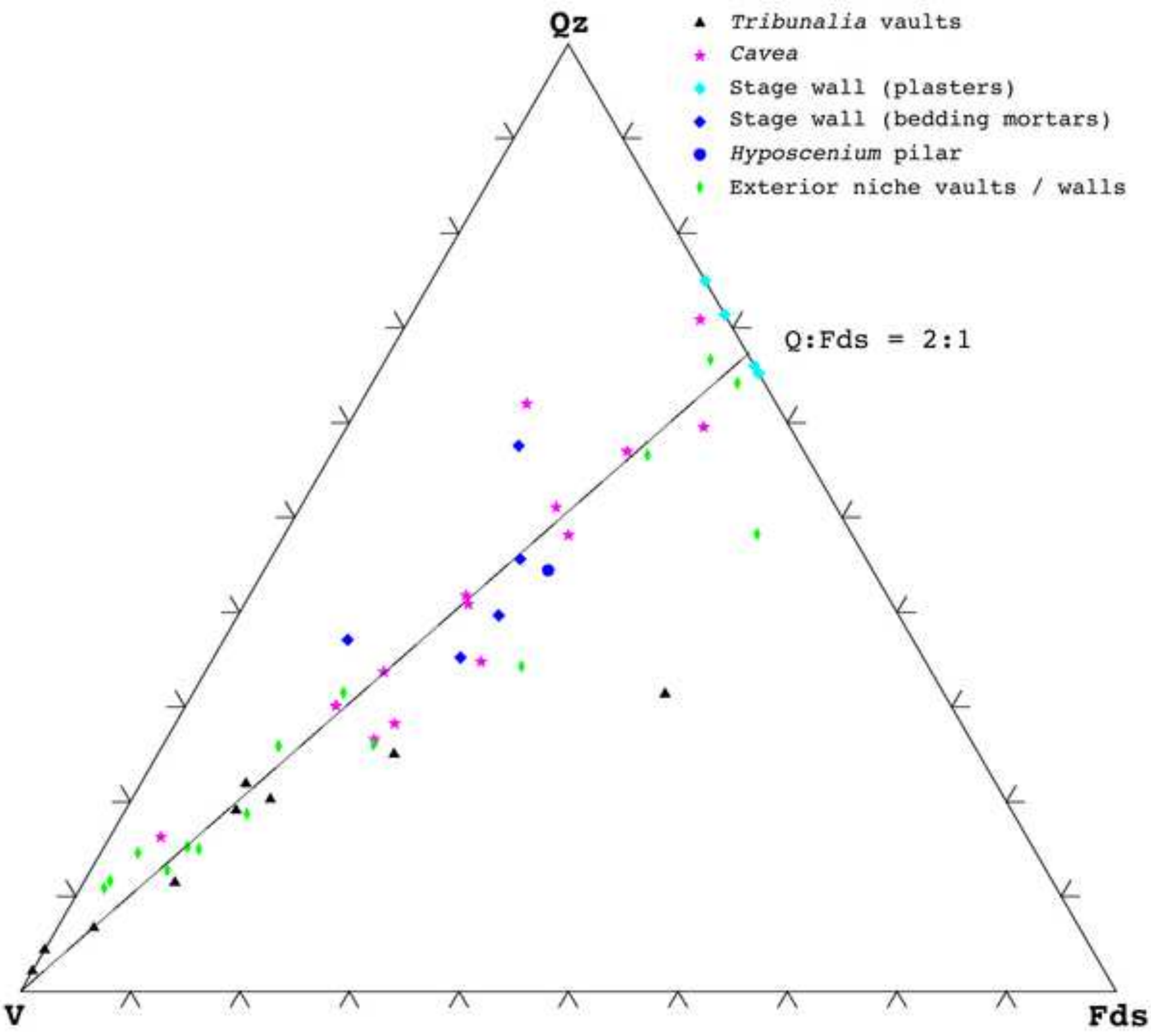
Qz
V
Fds
▲ *Tribunalia* vaults
★ *Cavea*
◆ Stage wall (plasters)
◆ Stage wall (bedding mortars)
● *Hyposcenium* pilar
◆ Exterior niche vaults / walls
Q:Fds = 2:1

Figure 8

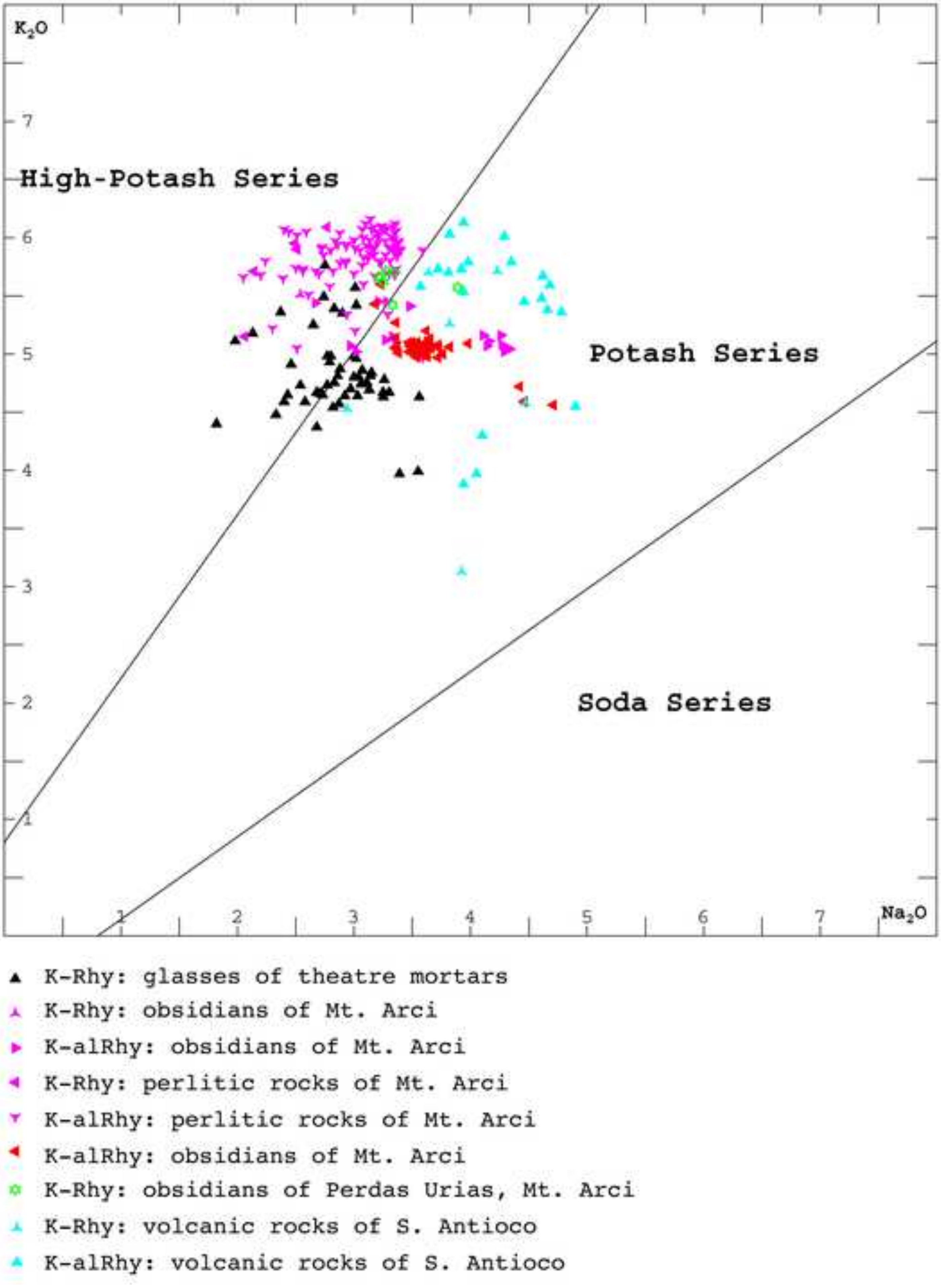
K₂O
Na₂O
1
2
3
4
5
6
7
High-Potash Series
Potash Series
Soda Series
▲ K-Rhy: glasses of theatre mortars
▲ K-Rhy: obsidians of Mt. Arci
▶ K-alRhy: obsidians of Mt. Arci
◀ K-Rhy: perlitic rocks of Mt. Arci
▼ K-alRhy: perlitic rocks of Mt. Arci
◀ K-alRhy: obsidians of Mt. Arci
✲ K-Rhy: obsidians of Perdas Urias, Mt. Arci
▲ K-Rhy: volcanic rocks of S. Antioco
▲ K-alRhy: volcanic rocks of S. Antioco

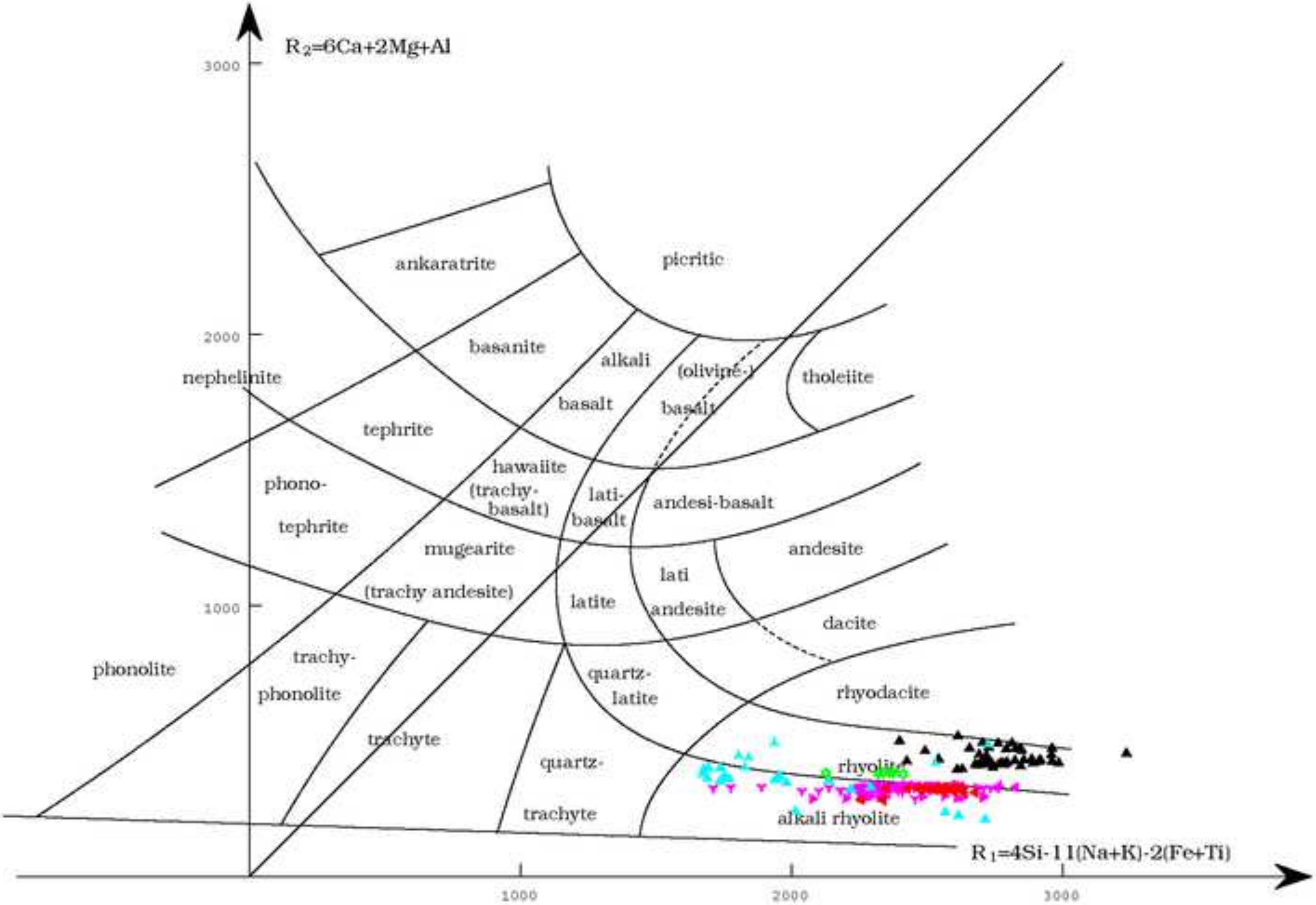
R_2=6Ca+2Mg+Al
3000
2000
1000
1000
2000
3000
R_1=4Si-11(Na+K)-2(Fe+Ti)
ankaratrite
picritic
basanite
alkali
basalt
(olivine-)
basalt
tholeiite
nephelinite
tephrite
hawaiite
(trachy-
basalt)
lati-
basalt
andesi-basalt
phono-
tephrite
mugearite
(trachy andesite)
latite
lati
andesite
andesite
dacite
phonolite
trachy-
phonolite
trachyte
quartz-
latite
rhyodacite
quartz-
trachyte
rhyolite
alkali rhyolite

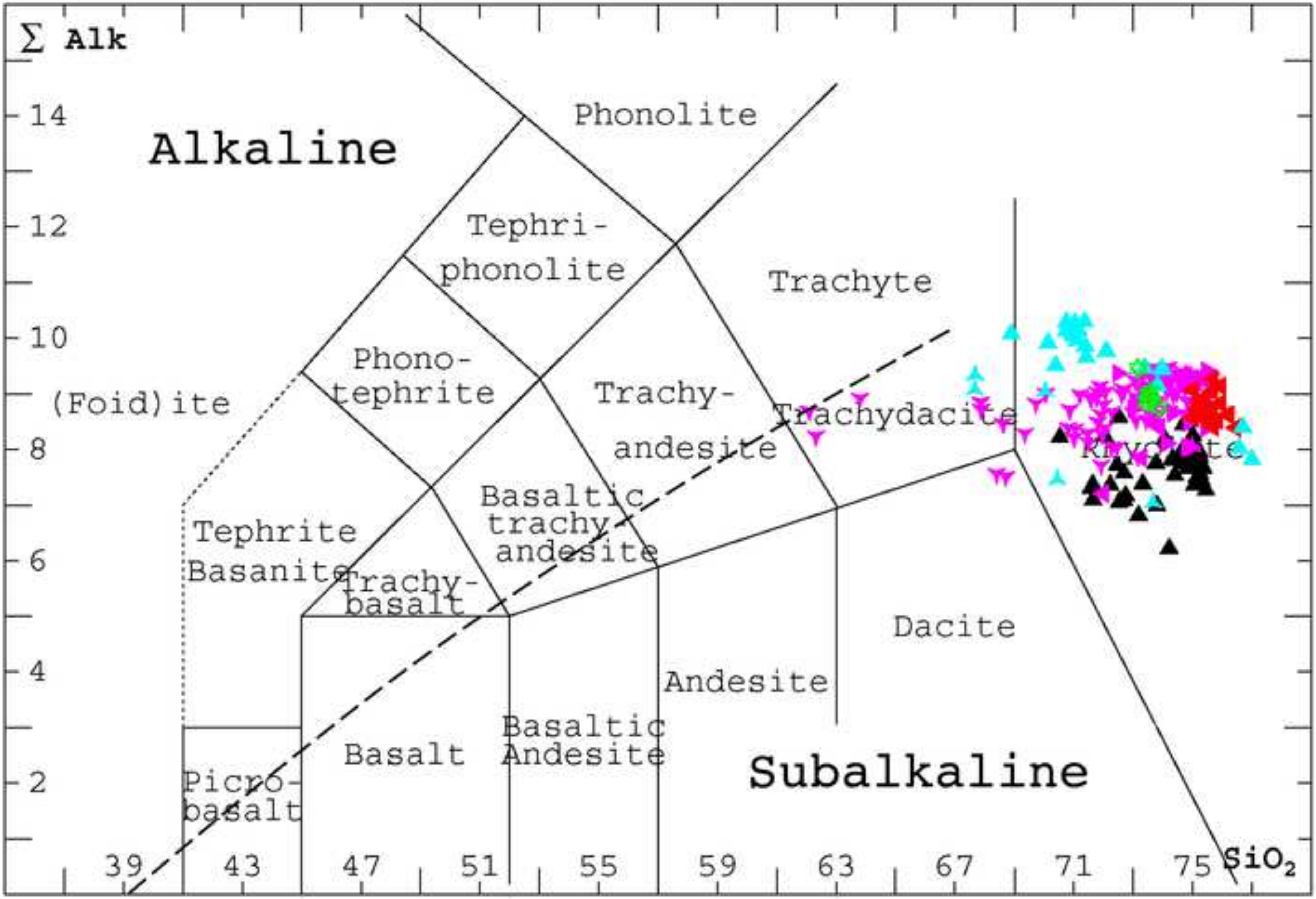
Σ Alk
14
12
10
8
6
4
2
39
43
47
51
55
59
63
67
71
75
SiO2
Alkaline
Subalkaline
Phonolite
Tephri-phonolite
Phono-tephrite
Trachyte
Trachy-andesite
Trachydacite
Rhyolite
(Foid)ite
Tephrite Basanite
Trachy-basalt
Basaltic trachy-andesite
Picro-basalt
Basalt
Basaltic Andesite
Andesite
Dacite

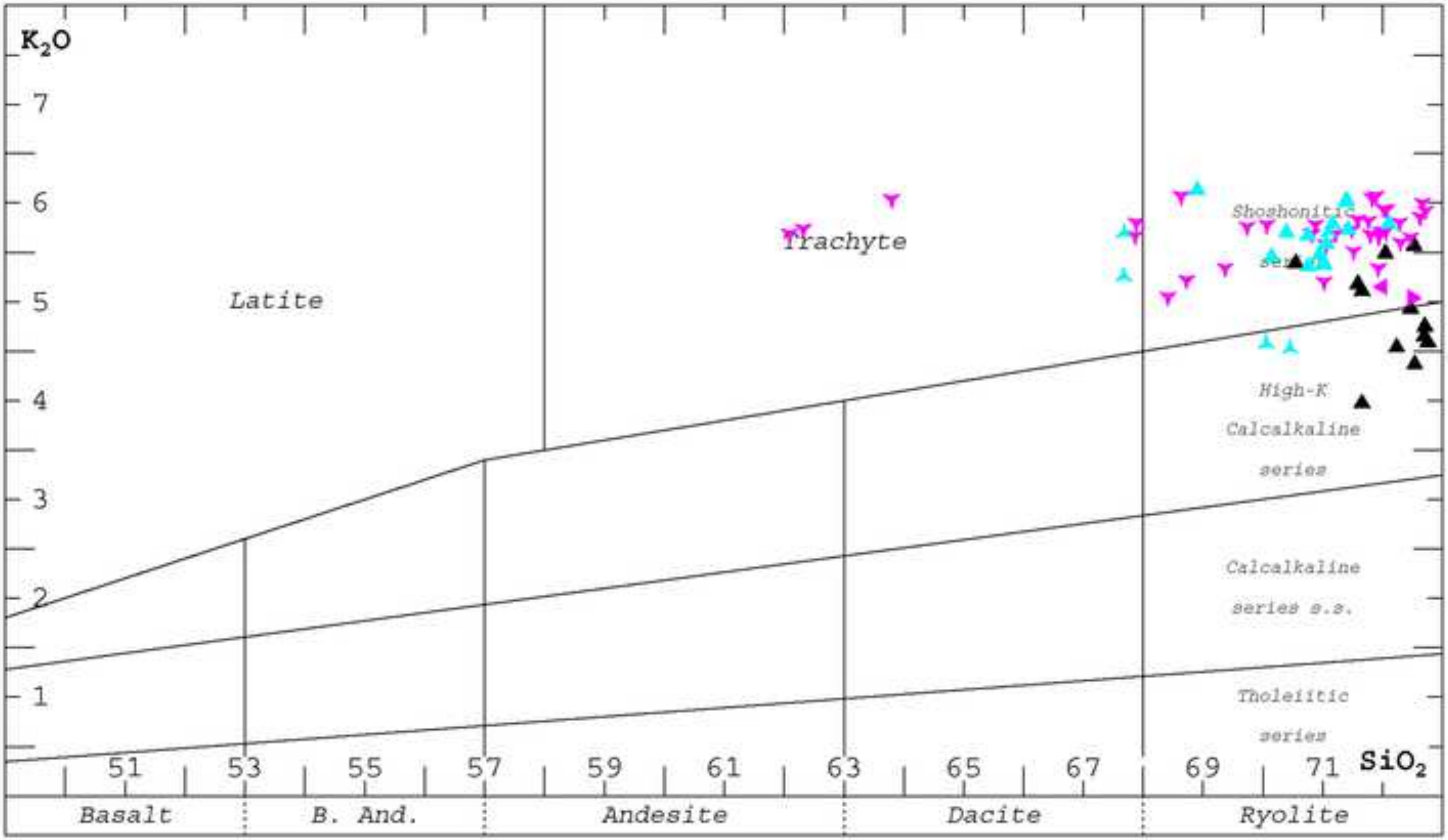
K_2O
7
6
5
4
3
2
1
Latite
Trachyte
Shoshonitic
series
High-K
Calcalkaline
series
Calcalkaline
series s.s.
Tholeiitic
series
51
53
55
57
59
61
63
65
67
69
71
SiO_2
Basalt
B. And.
Andesite
Dacite
Ryolite

Figure 12

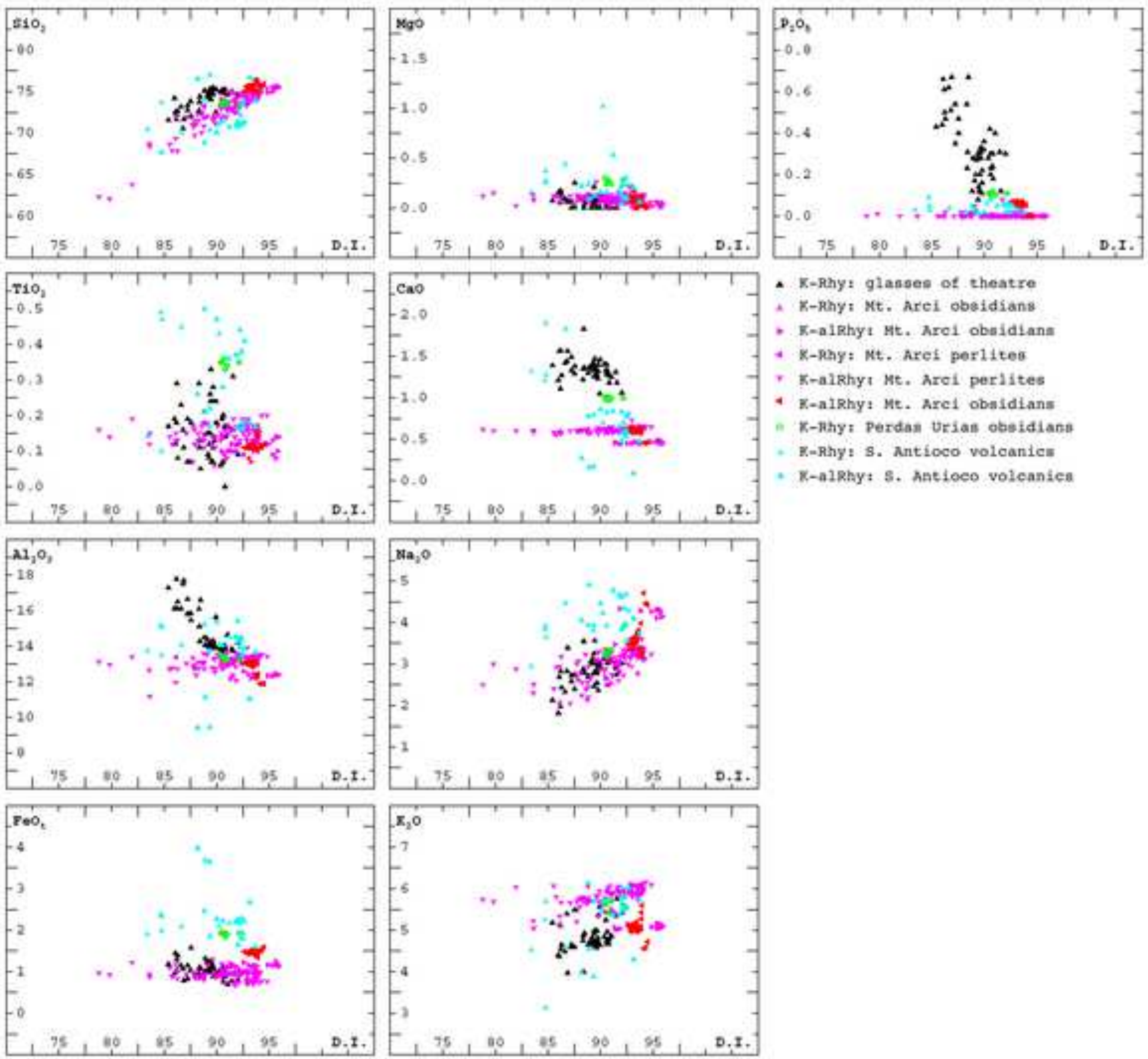
SiO2
80
75
70
65
60
MgO
1.5
1.0
0.5
0.0
P2O5
0.8
0.6
0.4
0.2
0.0
TiO2
0.5
0.4
0.3
0.2
0.1
0.0
CaO
2.0
1.5
1.0
0.5
0.0
Al2O3
18
16
14
12
10
8
Na2O
5
4
3
2
1
FeOt
4
3
2
1
0
K2O
7
6
5
4
3
75
80
85
90
95
D.I.
K-Rhy: glasses of theatre
K-Rhy: Mt. Arci obsidians
K-alRhy: Mt. Arci obsidians
K-Rhy: Mt. Arci perlites
K-alRhy: Mt. Arci perlites
K-alRhy: Mt. Arci obsidians
K-Rhy: Perdas Urias obsidians
K-Rhy: S. Antioco volcanics
K-alRhy: S. Antioco volcanics

Figure 13a

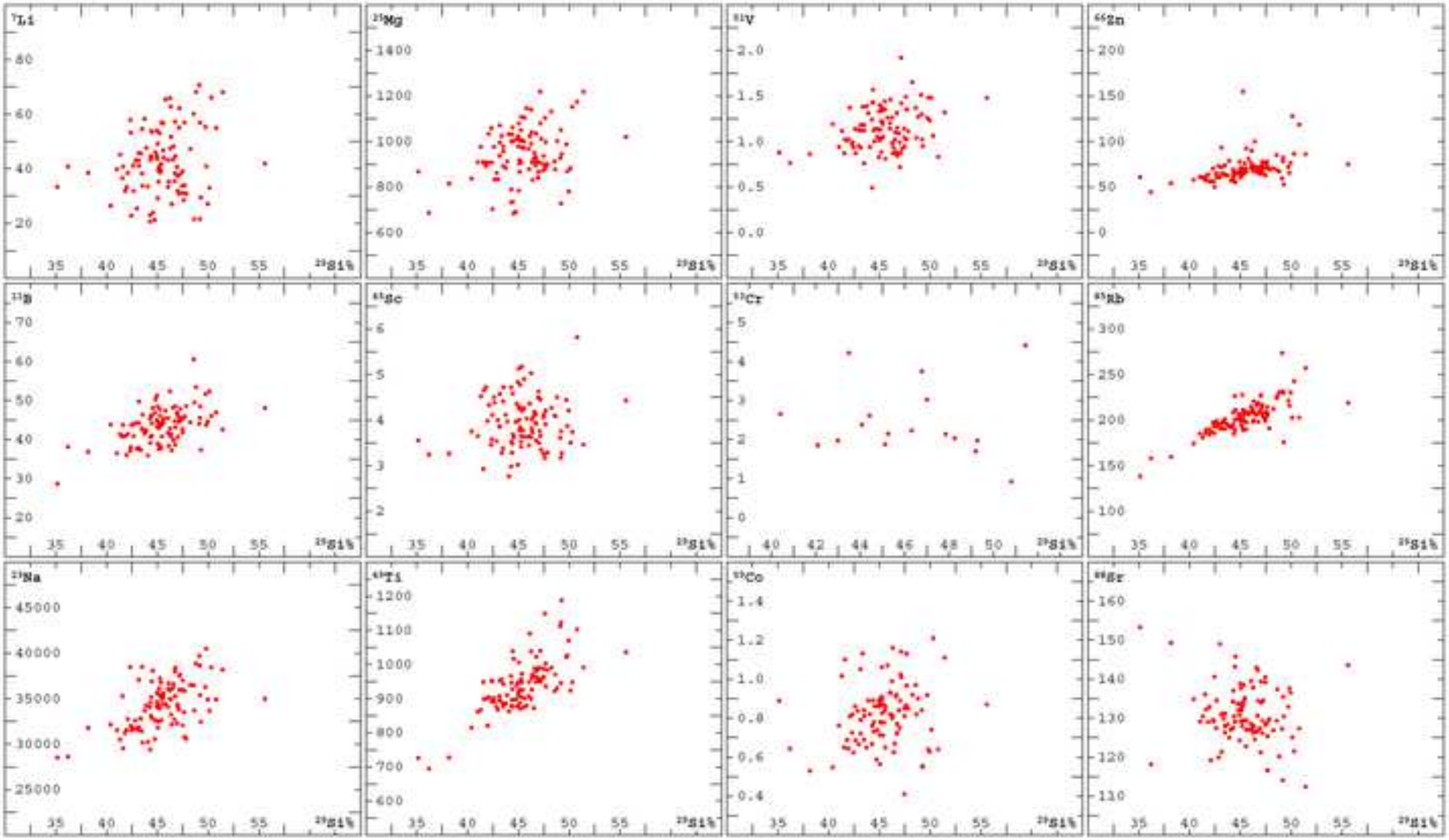
7Li
20
40
60
80
25Mg
600
800
1000
1200
1400
51V
0.0
0.5
1.0
1.5
2.0
66Zn
0
50
100
150
200
11B
20
30
40
50
60
70
45Sc
2
3
4
5
6
53Cr
0
1
2
3
4
5
40
42
44
46
48
50
85Rb
100
150
200
250
300
23Na
25000
30000
35000
40000
45000
49Ti
600
700
800
900
1000
1100
1200
59Co
0.4
0.6
0.8
1.0
1.2
1.4
88Sr
110
120
130
140
150
160
35
40
45
50
55
29Si%

Figure 13b

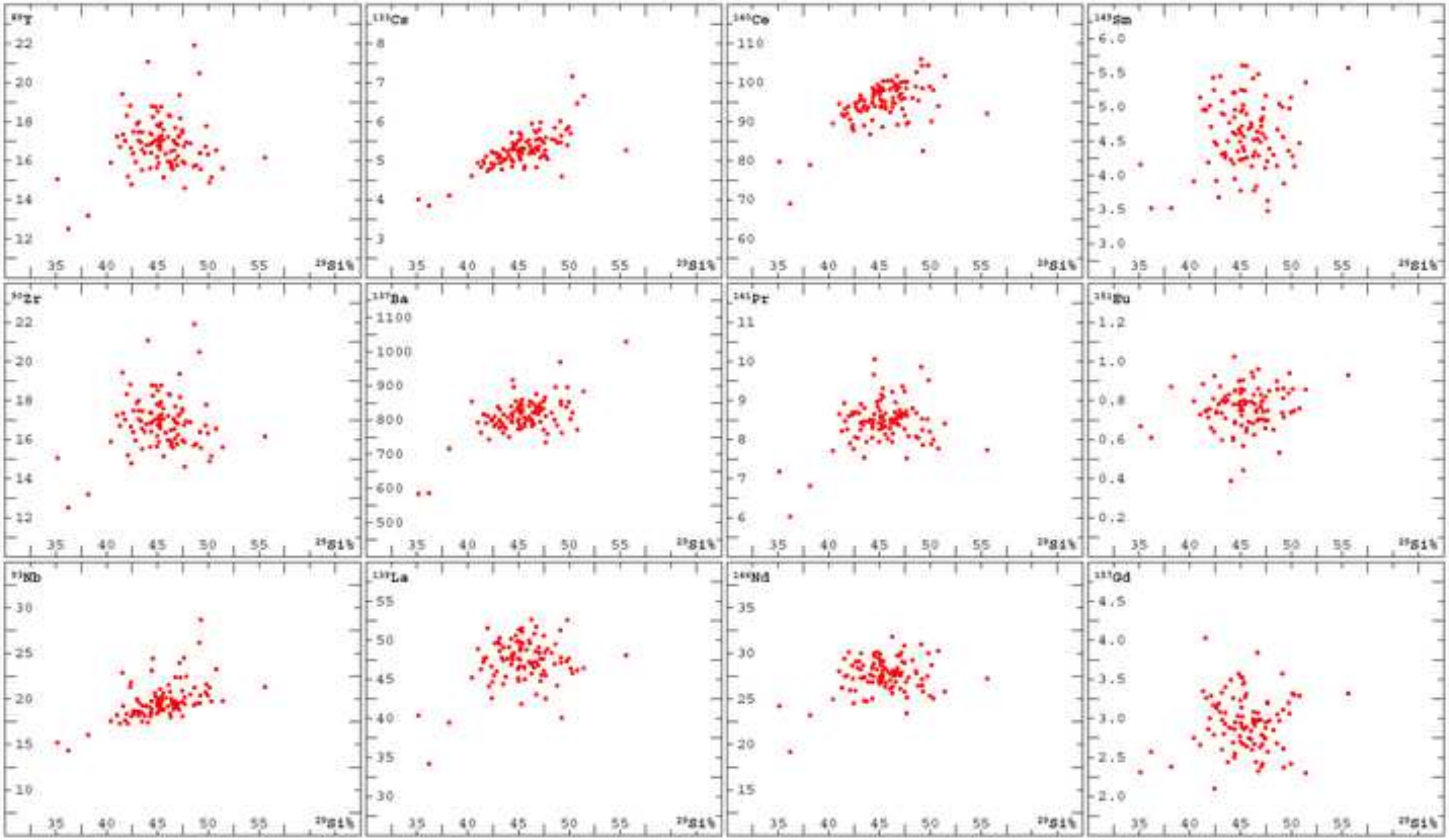
^{89}Y
12
14
16
18
20
22
^{133}Cs
3
4
5
6
7
8
^{140}Ce
60
70
80
90
100
110
^{147}Sm
3.0
3.5
4.0
4.5
5.0
5.5
6.0
^{90}Zr
12
14
16
18
20
22
^{137}Ba
500
600
700
800
900
1000
1100
^{141}Pr
6
7
8
9
10
11
^{151}Eu
0.2
0.4
0.6
0.8
1.0
1.2
^{93}Nb
10
15
20
25
30
^{139}La
30
35
40
45
50
55
^{146}Nd
15
20
25
30
35
^{157}Gd
2.0
2.5
3.0
3.5
4.0
4.5
35
40
45
50
55
^{29}Si%

Figure 13c

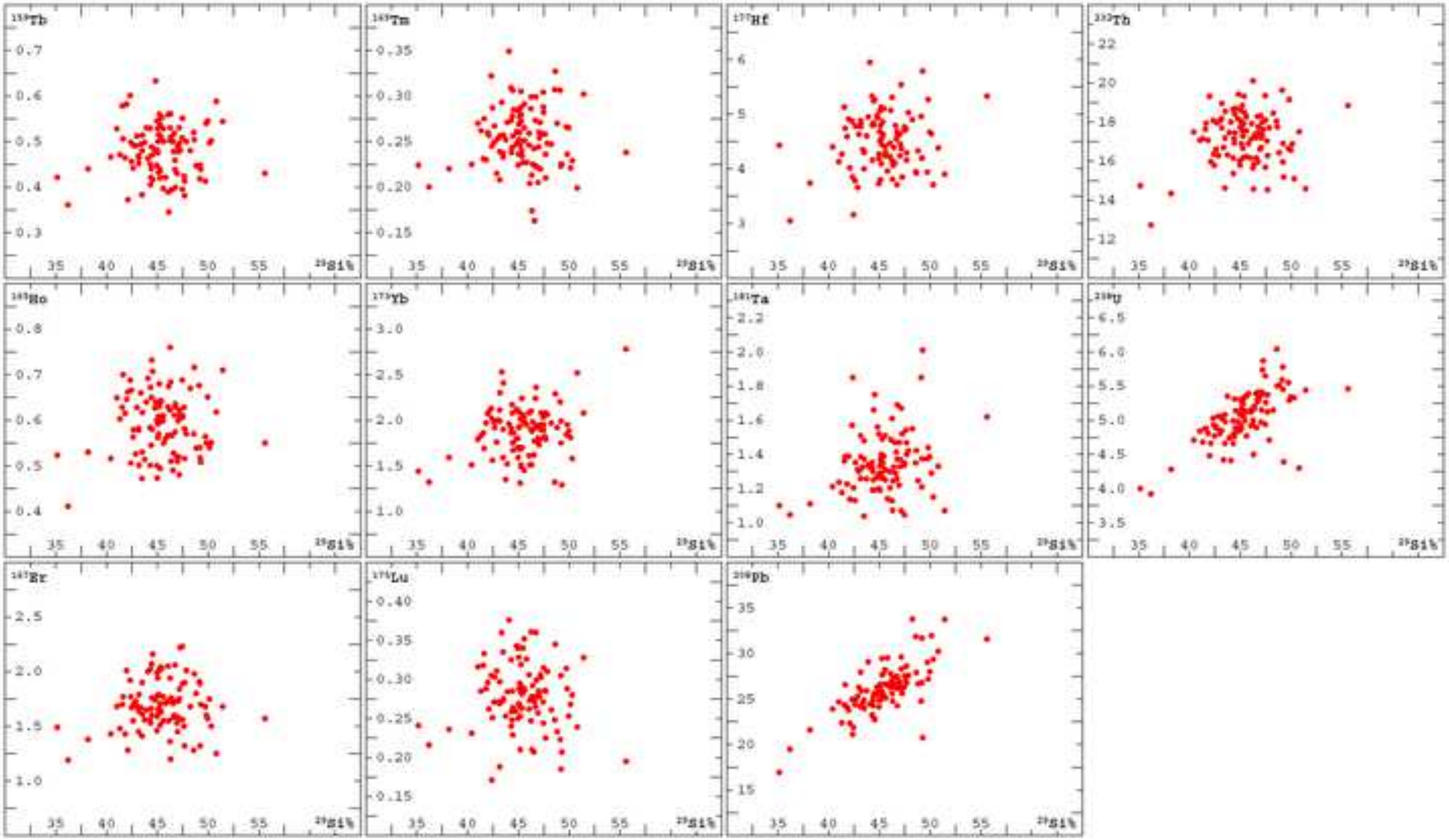
159Tb
0.7
0.6
0.5
0.4
0.3
169Tm
0.35
0.30
0.25
0.20
0.15
177Hf
6
5
4
3
232Th
22
20
18
16
14
12
165Ho
0.8
0.7
0.6
0.5
0.4
173Yb
3.0
2.5
2.0
1.5
1.0
181Ta
2.2
2.0
1.8
1.6
1.4
1.2
1.0
238U
6.5
6.0
5.5
5.0
4.5
4.0
3.5
167Er
2.5
2.0
1.5
1.0
175Lu
0.40
0.35
0.30
0.25
0.20
0.15
208Pb
35
30
25
20
15
35
40
45
50
55
29Si%

Figure 14a,b

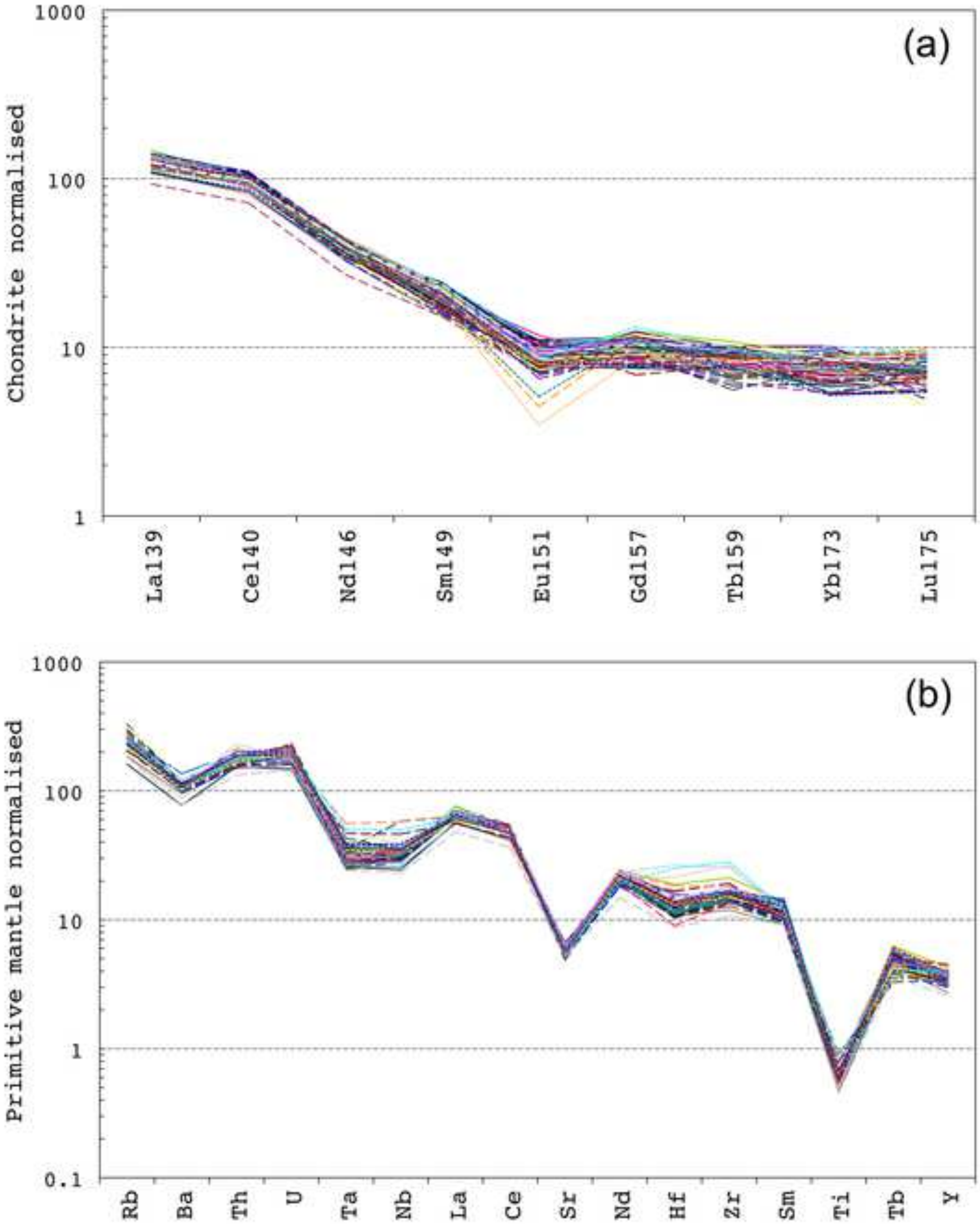
(a)
Chondrite normalised
1000
100
10
1
La139
Ce140
Nd146
Sm149
Eu151
Gd157
Tb159
Yb173
Lu175
(b)
Primitive mantle normalised
1000
100
10
1
0.1
Rb
Ba
Th
U
Ta
Nb
La
Ce
Sr
Nd
Hf
Zr
Sm
Ti
Tb
Y

Figure 15

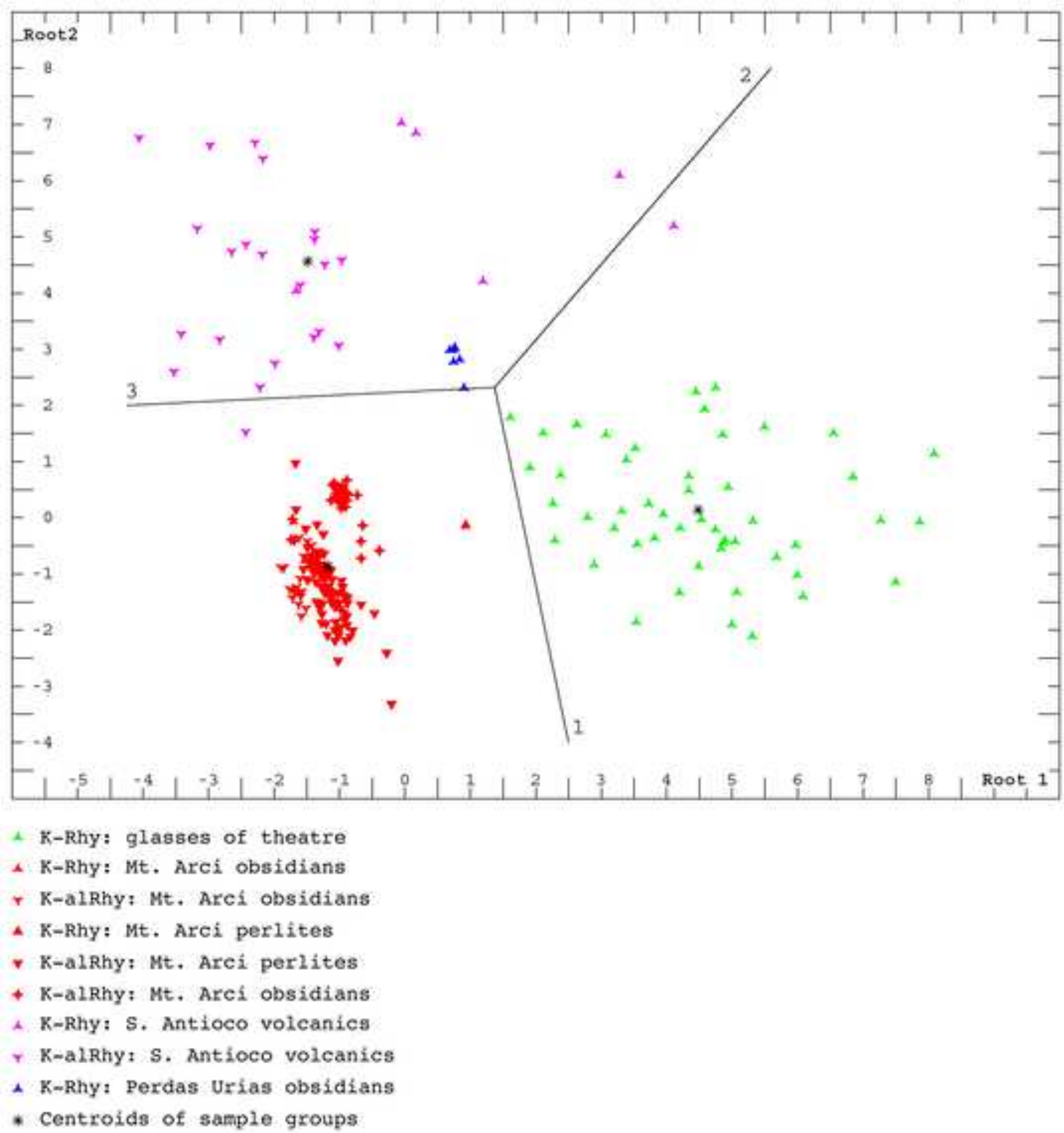
Root2
8
7
6
5
4
3
2
1
0
-1
-2
-3
-4
-5
-4
-3
-2
-1
0
1
2
3
4
5
6
7
8
Root 1
1
2
3
▲ K-Rhy: glasses of theatre
▲ K-Rhy: Mt. Arci obsidians
▼ K-alRhy: Mt. Arci obsidians
▲ K-Rhy: Mt. Arci perlites
▼ K-alRhy: Mt. Arci perlites
✦ K-alRhy: Mt. Arci obsidians
▲ K-Rhy: S. Antioco volcanics
▼ K-alRhy: S. Antioco volcanics
▲ K-Rhy: Perdas Urias obsidians
* Centroids of sample groups

Figure 16

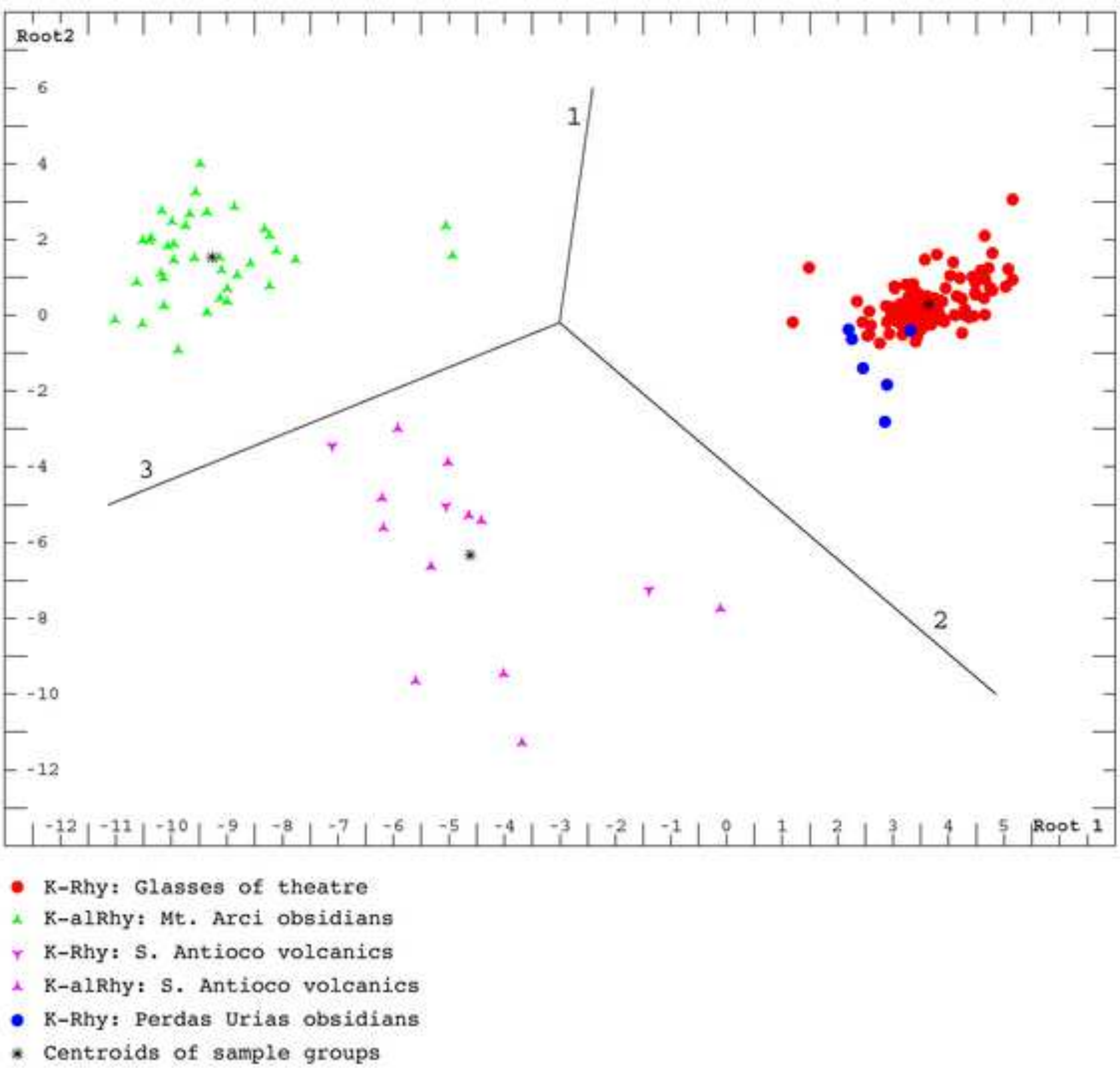
Root2
6
4
2
0
-2
-4
-6
-8
-10
-12
-12
-11
-10
-9
-8
-7
-6
-5
-4
-3
-2
-1
0
1
2
3
4
5
Root 1
1
2
3
K-Rhy: Glasses of theatre
K-alRhy: Mt. Arci obsidians
K-Rhy: S. Antioco volcanics
K-alRhy: S. Antioco volcanics
K-Rhy: Perdas Urias obsidians
Centroids of sample groups

Table 1

Theatre sector	**Mortar function**		**B/A wt%**	**B/A vol%**	**B**	**±2s**	**A**	**±2s**	**Qz**	**±2s**	**Fds**	**±2s**	**Qz/ Fds**	**Mafic cryst.**	**±2s**	**Glass**	**±2s**	**Volc. rocks**	**±2s**	**Paleoz. basem.**	**±2s**	**Coccio -pesto**	**±2s**	**Bioclast**	**±2s**
Tribunalia	Ashlar bedding, concrete	Mean	0.97	1.58	59.61	3.98	40.39	3.98	4.88	1.6	4.11	1.31	1.97	0.41	0.37	23.79	3.2	2.77	1.18	2.05	1.05	1.37	0.94	1.01	0.66
		± σ	0.41	0.61	9.25	0.89	9.25	0.89	3.92	0.83	4.17	1.04	1.45	0.69	0.47	16.29	1.21	2.25	0.6	1.93	0.61	0.66	0.31	1.05	0.53
Cavea	Bedding of ashlars	Mean	0.74	1.54	59.13	3.04	40.87	3.04	13.92	2.12	6.17	1.49	2.34	1.14	0.48	13.42	1.95	1.91	0.73	3.21	0.92	0.63	0.42	0.47	0.38
		± σ	0.21	0.49	8.49	0.22	8.49	0.22	5.66	0.37	1.61	0.22	0.85	2.27	0.53	10.17	0.7	1.83	0.46	3.55	0.58	0.72	0.32	0.4	0.21
Niche walls	Bedding of bricks	Mean	0.90	1.48	59.22	3.36	40.78	3.36	10.98	2.01	5.79	1.5	2.09	0.55	0.41	16.06	2.09	2.13	0.82	3.08	1.08	0.96	0.59	1.22	0.62
		± σ	0.40	0.26	4.25	0.76	4.25	0.76	7.8	0.89	3.7	0.6	1.03	0.52	0.39	12.03	1.08	2.15	0.57	2.62	0.69	0.76	0.3	1.92	0.73
Niche vaults	Roman concrete	Mean	0.80	1.36	57.16	3.21	42.84	3.21	9.24	1.84	4.32	1.25	2.87	0.45	0.4	21.24	2.41	4	1.21	2.2	0.83	0.71	0.48	0.68	0.43
		± σ	0.27	0.28	4.76	0.34	4.76	0.34	5.38	0.6	3.06	0.54	2.04	0.37	0.16	10.72	0.93	3.13	0.51	1.86	0.5	0.49	0.28	0.67	0.29
Hyposcenium	Bedding of brick/stone	Mean	0.95	1.03	49.07	3.1	50.93	3.1	14.41	2.19	6.94	1.55	2.21	0.43	0.31	11.26	1.91	7.72	1.68	6.89	1.45	1.17	0.58	2.02	0.88
		± σ	0.60	0.42	10.55	0.68	10.55	0.68	4.54	0.63	2.45	0.18	0.89	0.38	0.21	4.42	0.22	0.31	0.37	4.74	0.45	1.73	0.66	1.3	0.43
Stage wall	Plasters (*arriccio*)	Mean	2.52	2.38	66.15	2.77	33.85	2.77	15	1.97	5.91	1.37	2.33	0.47	0.36	0.08	0.09	4.68	1.31	4.77	1.27	0.98	0.56	1.97	0.84
		± σ	1.59	1.15	16.71	0.26	16.71	0.26	13.04	0.27	3.74	0.14	0.5	0.51	0.32	0.16	0.19	1.28	0.32	2.04	0.21	0.75	0.38	0.68	0.17

Table 2a

	1	2	3	4	5	6	7	8	9	10	11	12	13	14	15	16	17	18	19	20	21	22	23	24	25
Sample	Sp142	Sp19	Sp4	Sp120	Sp7	Sp129	Sp2	Sp22	Sp18	Sp1	Sp32	Sp3	Sp23	Sp35	Sp34	Sp138	Sp8	Sp144	Sp128	Sp143	Sp177	Sp114	Sp70	Sp125	Sp154
Class.	Rhy	Rhy	Rhy	Rhy	Rhy	Rhy	Rhy	Rhy	Rhy	Rhy	Rhy	Rhy	Rhy	Rhy	Rhy	Rhy	Rhy	Rhy	Rhy	Rhy	Rhy	Rhy	Rhy	Rhy	Rhy
SiO_2	71.58	74.22	72.53	71.65	72.23	72.69	73.19	70.54	71.65	72.75	73.33	73.81	72.04	72.70	73.78	74.41	72.46	75.13	75.07	74.45	74.49	74.32	75.04	75.17	74.79
TiO_2	0.17	0.19	0.12	0.18	0.29	0.08	0.23	0.16	0.11	0.19	0.07	0.07	0.18	0.29	0.11	0.13	0.05	0.21	0.21	0.15	0.09	0.15	0.08	0.12	0.15
Al_2O_3	17.27	16.13	16.13	17.78	16.13	16.50	16.11	17.49	17.69	16.65	15.82	15.84	15.47	16.09	15.11	14.28	16.60	14.48	14.07	14.42	14.09	14.09	13.96	14.11	14.16
Fe_2O_3	1.31	1.07	1.61	1.15	1.43	1.55	1.28	1.19	0.88	0.92	1.28	1.15	1.75	1.06	1.20	1.23	0.96	1.12	1.47	1.39	1.18	1.37	1.35	1.10	1.33
FeO	n.d.	n.d.	n.d.	n.d.	n.d.	n.d.	n.d.	n.d.	n.d.	n.d.	n.d.	n.d.	n.d.	n.d.	n.d.	n.d.	n.d.	n.d.	n.d.	n.d.	n.d.	n.d.	n.d.	n.d.	n.d.
MnO	0.05	0.14	0.02	0.05	0.07	0.04	0.02	0.11	n.d.	0.08	0.07	0.10	0.03	0.12	0.15	n.d.	n.d.	n.d.	n.d.	0.16	0.18	0.13	0.09	0.12	n.d.
MgO	0.07	0.15	0.16	0.05	0.17	0.12	0.09	0.06	0.07	0.06	n.d.	0.01	0.25	0.08	0.10	n.d.	0.04	0.13	0.07	n.d.	0.11	0.06	0.03	0.05	0.21
CaO	1.39	1.21	1.56	1.11	1.57	1.27	1.42	1.44	1.56	1.33	1.49	1.29	1.38	1.22	1.35	1.83	1.36	1.30	1.36	1.37	1.37	1.37	1.34	1.43	1.33
Na_2O	2.13	1.82	2.68	1.98	2.82	2.43	2.33	2.83	3.39	2.58	2.73	2.40	2.74	2.83	2.88	3.55	2.79	2.71	2.68	3.06	3.04	3.13	3.00	2.77	3.25
K_2O	5.18	4.40	4.37	5.11	4.54	4.65	4.48	5.39	3.97	4.59	4.65	4.59	5.49	4.75	4.87	3.99	4.93	4.66	4.67	4.74	4.80	4.69	4.80	4.73	4.63
P_2O_5	0.43	0.44	0.66	0.61	0.50	0.47	0.62	0.51	0.67	0.54	0.35	0.47	0.40	0.54	0.23	0.31	0.67	0.12	0.28	0.17	0.20	0.27	0.02	0.28	0.08
L.o.I.	--	--	--	--	--	--	--	--	--	--	--	--	--	--	--	--	--	--	--	--	--	--	--	--	--
Total	99.58	99.77	99.84	99.67	99.75	99.80	99.77	99.72	99.99	99.69	99.79	99.73	99.73	99.68	99.78	99.73	99.86	99.86	99.88	99.91	99.55	99.58	99.71	99.88	99.93
S.I.	0.82	2.04	1.84	0.61	1.92	1.39	1.12	0.64	0.85	0.74	0.00	0.12	2.48	0.93	1.12	0.00	0.46	1.53	0.80	0.00	1.22	0.66	0.33	0.58	2.26
A.I.	0.53	0.48	0.57	0.49	0.59	0.55	0.54	0.60	0.56	0.55	0.60	0.56	0.68	0.61	0.66	0.71	0.60	0.66	0.67	0.70	0.72	0.73	0.73	0.69	0.73
Q	36.78	44.59	37.58	39.23	35.52	38.26	40.43	31.01	34.72	38.27	36.65	40.09	31.92	36.32	35.21	34.79	35.73	38.36	38.63	35.18	35.09	35.06	35.51	37.92	34.52
C	6.66	7.23	5.74	8.43	4.92	6.29	6.33	5.60	6.58	6.31	4.43	5.70	3.47	5.37	3.20	1.54	5.81	2.90	2.80	2.17	1.88	2.02	1.44	2.50	1.58
Or	30.61	26.00	25.82	30.20	26.83	27.48	26.47	31.85	23.46	27.12	27.48	27.12	32.44	28.07	28.78	23.58	29.13	27.54	27.60	28.01	28.36	27.71	28.36	27.95	27.36
Ab	18.02	15.40	22.68	16.75	23.86	20.56	19.71	23.94	28.68	21.83	23.10	20.31	23.18	23.94	24.37	30.04	23.61	22.93	22.68	25.89	25.72	26.48	25.38	23.44	27.50
An	4.09	3.13	3.43	1.52	4.52	3.23	2.99	3.81	3.36	3.07	5.10	3.33	4.23	2.52	5.19	7.05	2.37	5.67	4.92	5.69	5.49	5.03	6.52	5.26	6.08
Ac	0	0	0	0	0	0	0	0	0	0	0	0	0	0	0	0	0	0	0	0	0	0	0	0	0
Ns	0	0	0	0	0	0	0	0	0	0	0	0	0	0	0	0	0	0	0	0	0	0	0	0	0
Di	0	0	0	0	0	0	0	0	0	0	0	0	0	0	0	0	0	0	0	0	0	0	0	0	0
Ed	0	0	0	0	0	0	0	0	0	0	0	0	0	0	0	0	0	0	0	0	0	0	0	0	0
Sl	0	0	0	0	0	0	0	0	0	0	0	0	0	0	0	0	0	0	0	0	0	0	0	0	0
En	0.17	0.37	0.40	0.12	0.42	0.30	0.22	0.15	0.17	0.15	0.00	0.02	0.62	0.20	0.25	0.00	0.10	0.32	0.17	0.00	0.27	0.15	0.07	0.12	0.52
Fs	1.59	1.40	2.02	1.36	1.59	2.05	1.39	1.56	1.01	1.08	1.75	1.63	2.13	1.18	1.73	1.46	1.22	1.17	1.65	1.94	1.79	1.85	1.87	1.52	1.56
Hy	1.76	1.77	2.42	1.48	2.02	2.35	1.62	1.71	1.19	1.23	1.75	1.66	2.76	1.38	1.98	1.46	1.32	1.50	1.82	1.94	2.06	2.00	1.94	1.64	2.08
Mt	0.23	0.18	0.28	0.20	0.25	0.27	0.22	0.21	0.15	0.16	0.22	0.20	0.30	0.18	0.21	0.21	0.17	0.19	0.25	0.24	0.20	0.24	0.23	0.19	0.23
Il	0.32	0.36	0.23	0.34	0.55	0.15	0.44	0.30	0.21	0.36	0.13	0.13	0.34	0.55	0.21	0.25	0.09	0.40	0.40	0.28	0.17	0.28	0.15	0.23	0.28
Ap	1.00	1.02	1.53	1.41	1.16	1.09	1.44	1.18	1.55	1.25	0.81	1.09	0.93	1.25	0.53	0.72	1.55	0.28	0.65	0.39	0.46	0.63	0.05	0.65	0.19
D.I.	85.4	86.0	86.1	86.2	86.2	86.3	86.6	86.8	86.9	87.2	87.2	87.5	87.6	88.3	88.4	88.4	88.5	88.8	88.9	89.1	89.2	89.3	89.3	89.3	89.4
SAL	96.2	96.3	95.2	96.1	95.7	95.8	95.9	96.2	96.8	96.6	96.8	96.6	95.3	96.2	96.8	97.0	96.6	97.4	96.6	96.9	96.6	96.3	97.2	97.1	97.0
FEM	3.3	3.3	4.5	3.4	4.0	3.9	3.7	3.4	3.1	3.0	2.9	3.1	4.3	3.4	2.9	2.6	3.1	2.4	3.1	2.9	2.9	3.2	2.4	2.7	2.8

Table 2b

	26	27	28	29	30	31	32	33	34	35	36	37	38	39	40	41	42	43	44	45	46	47	48	49	50
Sample	Sp140	Sp50	Sp51	Sp130	Sp83	Sp145	Sp126	Sp141	Sp152	Sp94	Sp134	Sp25	Sp169	Sp165	Sp121	Sp166	Sp155	Sp71	Sp77	Sp82	Sp91	Sp10	Sp81	Sp156	Sp101
Class.	Rhy	Rhy	Rhy	Rhy	Rhy	Rhy	Rhy	Rhy	Rhy	Rhy	Rhy	Rhy	Rhy	Rhy	Rhy	Rhy	Rhy	Rhy	Rhy	Rhy	Rhy	Rhy	Rhy	Rhy	Rhy
SiO_2	75.34	74.84	74.06	74.66	74.85	75.31	75.46	74.74	75.35	75.31	75.22	72.52	75.24	74.98	74.9	75.25	75.18	75.05	74.87	75.16	75.25	74.69	75.02	74.89	74.7
TiO_2	0.26	0.24	0.33	0.07	0.24	0.07	0.28	0.11	0.14	0.14	0.13	0.24	0.18	0.06	0.19	0.2	0.07	0.2	0.17	n.d.	0.14	0.17	0.16	0.31	0.09
Al_2O_3	14.09	14.12	13.88	14.24	14.22	14	14.1	14.31	13.88	14.06	13.93	15.63	13.92	13.85	13.7	13.89	13.82	13.92	14.02	13.86	13.91	14.64	13.84	13.75	14.22
Fe_2O_3	1.13	1.2	1.36	1.4	1.15	1.28	0.98	1.26	1.15	1.02	1.12	1.08	1.1	1.17	1.22	1.07	1.22	0.85	1.14	1.15	0.98	0.78	0.86	1.04	0.88
FeO	n.d.	n.d.	n.d.	n.d.	n.d.	n.d.	n.d.	n.d.	n.d.	n.d.	n.d.	n.d.	n.d.	n.d.	n.d.	n.d.	n.d.	n.d.	n.d.	n.d.	n.d.	n.d.	n.d.	n.d.	n.d.
MnO	0.06	0.02	0.26	n.d.	0.22	n.d.	0.07	n.d.	0.21	0.05	n.d.	0.14	n.d.	0.03	n.d.	0.01	0.07	0.1	0.04	0.11	0.14	n.d.	0.05	n.d.	n.d.
MgO	0.03	0.11	0.06	0.03	0.01	0.03	n.d.	0.09	0.05	0.02	0.07	0.13	n.d.	0.07	0.04	0.05	n.d.	0.05	0.02	0.1	0.07	n.d.	n.d.	n.d.	0.04
CaO	1.37	1.26	1.47	1.37	1.29	1.34	1.33	1.27	1.23	1.32	1.4	1.05	1.46	1.4	1.33	1.29	1.4	1.33	1.28	1.27	1.18	1.25	1.31	1.18	1.06
Na_2O	2.46	2.8	3.56	3	3.03	2.87	2.54	2.77	2.86	2.37	2.97	3.01	2.92	3.15	2.65	3.11	3.25	3.02	3.26	3.3	3.14	3.07	2.9	2.75	3.02
K_2O	4.91	4.98	4.63	4.98	4.64	4.57	4.73	4.98	4.81	5.36	4.7	5.57	4.64	4.84	5.25	4.75	4.67	4.96	4.78	4.67	4.81	4.86	5.35	5.76	5.42
P_2O_5	0.3	0.08	0.14	0.12	0.2	0.31	0.33	0.28	0.11	0.16	0.22	0.32	0.36	0.28	0.42	0.2	0.3	0.23	0.24	0.3	0.18	0.4	0.31	0.12	0.3
L.o.I.	--	--	--	--	--	--	--	--	--	--	--	--	--	--	--	--	--	--	--	--	--	--	--	--	--
Totale	99.95	99.65	99.75	99.87	99.85	99.78	99.82	99.81	99.79	99.81	99.76	99.69	99.82	99.83	99.70	99.82	99.98	99.71	99.82	99.92	99.80	99.86	99.80	99.80	99.73
S.I.	0.36	1.22	0.63	0.32	0.11	0.35	0.00	1.00	0.57	0.23	0.80	1.34	0.00	0.77	0.44	0.56	0.00	0.57	0.22	1.10	0.79	0.00	0.00	0.00	0.43
A.I.	0.66	0.71	0.78	0.73	0.70	0.69	0.66	0.70	0.71	0.69	0.72	0.70	0.71	0.75	0.73	0.74	0.75	0.74	0.75	0.76	0.75	0.70	0.76	0.78	0.76
Q	39.56	36.28	31.98	34.70	36.54	38.35	40.21	36.81	37.13	38.04	36.88	31.55	37.84	35.12	37.06	36.19	35.49	35.77	34.91	35.27	35.84	36.33	35.29	34.25	34.43
C	2.96	2.02	0.67	1.71	2.35	2.64	3.17	2.72	2.00	2.34	1.94	3.51	2.30	1.55	2.25	1.77	1.59	1.72	1.73	1.79	1.82	3.01	1.64	1.13	2.18
Or	29.01	29.43	27.36	29.43	27.42	27.00	27.95	29.43	28.42	31.67	27.77	32.91	27.42	28.60	31.02	28.07	27.60	29.31	28.25	27.60	28.42	28.72	31.61	34.04	32.03
Ab	20.81	23.69	30.12	25.38	25.64	24.28	21.49	23.44	24.20	20.05	25.13	25.47	24.71	26.65	22.42	26.31	27.50	25.55	27.58	27.92	26.57	25.98	24.54	23.27	25.55
An	4.84	5.73	6.38	6.01	5.09	4.62	4.44	4.47	5.38	5.50	5.51	3.12	4.89	5.12	3.85	5.09	4.99	5.10	4.78	4.34	4.68	3.59	4.47	5.07	3.30
Ac	0	0	0	0	0	0	0	0	0	0	0	0	0	0	0	0	0	0	0	0	0	0	0	0	0
Ns	0	0	0	0	0	0	0	0	0	0	0	0	0	0	0	0	0	0	0	0	0	0	0	0	0
Di	0	0	0	0	0	0	0	0	0	0	0	0	0	0	0	0	0	0	0	0	0	0	0	0	0
Ed	0	0	0	0	0	0	0	0	0	0	0	0	0	0	0	0	0	0	0	0	0	0	0	0	0
Sl	0	0	0	0	0	0	0	0	0	0	0	0	0	0	0	0	0	0	0	0	0	0	0	0	0
En	0.07	0.27	0.15	0.07	0.02	0.07	0.00	0.22	0.12	0.05	0.17	0.32	0.00	0.17	0.10	0.12	0.00	0.12	0.05	0.25	0.17	0.00	0.00	0.00	0.10
Fs	1.22	1.27	1.78	1.78	1.57	1.62	1.00	1.53	1.72	1.25	1.31	1.33	1.20	1.54	1.34	1.14	1.67	1.01	1.34	1.77	1.36	0.78	1.00	0.90	1.05
Hy	1.29	1.54	1.93	1.86	1.60	1.70	1.00	1.75	1.84	1.30	1.48	1.65	1.20	1.72	1.44	1.27	1.67	1.13	1.39	2.01	1.53	0.78	1.00	0.90	1.15
Mt	0.19	0.21	0.23	0.24	0.20	0.22	0.17	0.22	0.20	0.18	0.19	0.19	0.19	0.20	0.21	0.18	0.21	0.15	0.20	0.20	0.17	0.13	0.15	0.18	0.15
Il	0.49	0.46	0.63	0.13	0.46	0.13	0.53	0.21	0.27	0.27	0.25	0.46	0.34	0.11	0.36	0.38	0.13	0.38	0.32	0.00	0.27	0.32	0.30	0.59	0.17
Ap	0.70	0.19	0.32	0.28	0.46	0.72	0.76	0.65	0.25	0.37	0.51	0.74	0.83	0.65	0.97	0.46	0.70	0.53	0.56	0.70	0.42	0.93	0.72	0.28	0.70
D.I.	89.4	89.4	89.5	89.5	89.6	89.6	89.7	89.7	89.8	89.8	89.8	89.9	90.0	90.4	90.5	90.6	90.6	90.6	90.7	90.8	90.8	91.0	91.5	91.6	92.0
SAL	97.2	97.2	96.5	97.2	97.0	96.9	97.3	96.9	97.1	97.6	97.2	96.6	97.2	97.0	96.6	97.4	97.2	97.4	97.3	96.9	97.3	97.6	97.6	97.8	97.5
FEM	2.7	2.4	3.1	2.5	2.7	2.8	2.5	2.8	2.6	2.1	2.4	3.0	2.6	2.7	3.0	2.3	2.7	2.2	2.5	2.9	2.4	2.2	2.2	2.0	2.2

Table 3a

	1	2	3	4	5	6	7	8	9	10	11	12	13	14	15	16	17	18	19	20	21	22	23	24	25
Class.	Rhy	alRhy	alRhy	alRhy	alRhy	alRhy	alRhy	alRhy	alRhy	alRhy	alRhy	alRhy	alRhy	alRhy	alRhy	alRhy	alRhy	alRhy	alRhy	alRhy	Rhy	Rhy	Rhy	Rhy	Rhy
SiO_2	74.99	72.49	75.53	75.58	74.07	74.93	75.47	75.54	75.65	75.02	75.12	75.53	74.88	75.45	74.93	74.80	73.04	73.00	74.34	74.12	71.99	73.28	73.76	73.91	75.47
TiO_2	0.10	0.10	0.09	0.08	0.16	0.12	0.14	0.14	0.10	0.13	0.13	0.07	0.09	0.11	0.10	0.10	0.12	0.08	0.12	0.10	0.13	0.18	0.14	0.09	0.16
Al_2O_3	13.64	12.08	12.32	12.44	12.21	12.34	12.46	12.41	12.39	12.36	12.43	12.21	12.58	12.43	12.38	12.18	13.26	13.24	13.56	13.28	13.38	13.03	13.37	13.32	13.47
Fe_2O_3	1.24	1.25	1.27	1.32	1.27	1.29	1.39	1.25	1.30	1.28	1.27	1.24	1.36	1.29	1.29	1.33	1.24	1.22	1.18	1.17	1.12	1.02	1.14	1.04	0.94
FeO	n.d.	n.d.	n.d.	n.d.	n.d.	n.d.	n.d.	n.d.	n.d.	n.d.	n.d.	n.d.	n.d.	n.d.	n.d.	n.d.	n.d.	n.d.	n.d.	n.d.	n.d.	n.d.	n.d.	n.d.	n.d.
MnO	0.10	0.02	0.09	0.06	0.06	0.08	0.07	0.06	0.07	0.03	0.08	0.09	0.07	0.08	0.08	0.07	0.03	0.05	0.08	0.08	0.07	0.08	0.03	0.03	0.04
MgO	0.08	0.06	0.05	0.05	0.02	0.02	0.02	0.05	0.01	0.06	0.05	n.d.	0.05	0.02	0.06	0.07	0.09	0.04	0.08	0.06	0.06	0.12	0.14	0.09	0.07
CaO	0.60	0.44	0.47	0.49	0.45	0.47	0.45	0.45	0.47	0.48	0.46	0.47	0.45	0.45	0.46	0.46	0.60	0.61	0.60	0.58	0.59	0.62	0.62	0.64	0.65
Na_2O	2.54	4.33	4.32	4.31	4.29	4.27	4.26	4.16	4.14	4.11	3.63	3.36	3.33	3.27	3.02	2.97	3.48	3.28	3.21	2.67	2.06	2.14	2.49	2.51	2.77
K_2O	5.51	5.04	5.05	5.05	5.02	5.08	5.16	5.11	5.07	5.16	5.11	5.10	5.15	5.12	5.02	5.07	5.41	5.45	5.45	5.44	5.15	5.71	5.95	5.90	6.09
P_2O_5	n.d.	n.d.	n.d.	n.d.	n.d.	n.d.	n.d.	n.d.	n.d.	n.d.	n.d.	n.d.	n.d.	n.d.	n.d.	n.d.	n.d.	n.d.	n.d.	n.d.	n.d.	n.d.	n.d.	n.d.	0.02
L.o.I.	--	--	--	--	--	--	--	--	--	--	--	--	--	--	--	--	--	--	--	--	--	--	--	--	--
Total	98.80	95.81	99.19	99.38	97.55	98.60	99.42	99.17	99.20	98.63	98.28	98.07	97.96	98.22	97.34	97.05	97.27	96.97	98.62	97.50	94.55	96.18	97.64	97.53	99.68
S.I.	0.86	0.57	0.47	0.47	0.19	0.19	0.19	0.48	0.10	0.57	0.50	0.00	0.51	0.21	0.65	0.75	0.89	0.40	0.82	0.65	0.72	1.35	1.46	0.95	0.72
A.I.	0.74	1.04	1.02	1.01	1.02	1.01	1.01	1.00	0.99	1.00	0.93	0.90	0.88	0.88	0.84	0.85	0.87	0.85	0.82	0.77	0.67	0.74	0.79	0.79	0.83
Q	36.95	27.99	30.22	29.89	29.28	29.65	29.77	30.49	30.81	30.04	32.64	34.67	33.93	35.06	36.29	36.23	29.98	30.96	32.70	35.73	38.29	36.91	34.35	34.63	34.12
C	2.41	0.00	0.00	0.00	0.00	0.00	0.00	0	0	0	0.09	0.31	0.71	0.69	1.14	0.97	0.59	0.84	1.29	1.95	3.34	2.20	1.71	1.64	1.19
Or	32.56	29.78	29.84	29.84	29.66	30.02	30.49	30.20	29.96	30.49	30.20	30.14	30.43	30.25	29.66	29.96	31.97	32.20	32.20	32.15	30.43	33.74	35.16	34.86	35.99
Ab	21.49	34.07	35.25	35.87	34.85	35.19	35.36	35.20	35.03	34.78	30.71	28.43	28.18	27.67	25.55	25.13	29.44	27.75	27.16	22.59	17.43	18.11	21.07	21.24	23.44
An	2.98	0.00	0.00	0.00	0.00	0.00	0.00	0.10	0.25	0.04	2.28	2.33	2.23	2.23	2.28	2.28	2.98	3.03	2.98	2.88	2.93	3.08	3.08	3.17	3.09
Ac	0	0.43	0.44	0.45	0.44	0.44	0.48	0	0	0	0	0	0	0	0	0	0	0	0	0	0	0	0	0	0
Ns	0	0.48	0.19	0.02	0.22	0.10	0.03	0	0	0	0	0	0	0	0	0	0	0	0	0	0	0	0	0	0
Di	0	0.18	0.15	0.15	0.06	0.06	0.06	0.16	0.03	0.20	0	0	0	0	0	0	0	0	0	0	0	0	0	0	0
Ed	0	1.74	1.91	2.00	1.92	2.01	1.93	1.73	1.82	1.86	0	0	0	0	0	0	0	0	0	0	0	0	0	0	0
Sl	0	1.92	2.06	2.15	1.98	2.07	1.98	1.88	1.85	2.06	0	0	0	0	0	0	0	0	0	0	0	0	0	0	0
En	0.20	0.07	0.06	0.05	0.02	0.02	0.02	0.05	0.01	0.06	0.12	0.00	0.12	0.05	0.15	0.17	0.22	0.10	0.20	0.15	0.15	0.30	0.35	0.22	0.17
Fs	1.70	0.76	0.85	0.84	0.68	0.76	0.90	0.66	0.76	0.59	1.66	1.74	1.83	1.72	1.73	1.77	1.54	1.62	1.55	1.57	1.44	1.24	1.37	1.32	1.09
Hy	1.90	0.83	0.91	0.89	0.70	0.78	0.92	0.71	0.77	0.65	1.78	1.74	1.95	1.77	1.88	1.94	1.77	1.72	1.75	1.72	1.59	1.54	1.72	1.54	1.26
Mt	0.21	0.00	0.00	0.00	0.00	0.00	0.00	0.22	0.22	0.22	0.22	0.21	0.23	0.22	0.22	0.23	0.21	0.21	0.20	0.20	0.19	0.18	0.20	0.18	0.16
Il	0.19	0.19	0.17	0.15	0.30	0.23	0.27	0.27	0.19	0.25	0.25	0.13	0.17	0.21	0.19	0.19	0.23	0.15	0.23	0.19	0.25	0.34	0.27	0.17	0.30
Ap	0.00	0.00	0.00	0.00	0.00	0.00	0.00	0.00	0.00	0.00	0.00	0.00	0.00	0.00	0.00	0.00	0.00	0.00	0.00	0.00	0.00	0.00	0.00	0.00	0.05
D.I.	91.0	91.8	95.3	95.6	93.8	94.9	95.6	95.9	95.8	95.3	93.6	93.2	92.5	93.0	91.5	91.3	91.4	90.9	92.1	90.5	86.2	88.8	90.6	90.7	93.5
SAL	96.4	91.8	95.3	95.6	93.8	94.9	95.6	96.0	96.1	95.3	95.9	95.9	95.5	95.9	94.9	94.6	95.0	94.8	96.3	95.3	92.4	94.0	95.4	95.6	97.8
FEM	2.3	3.9	3.8	3.7	3.6	3.6	3.7	3.1	3.0	3.2	2.3	2.1	2.4	2.2	2.3	2.4	2.2	2.1	2.2	2.1	2.0	2.1	2.2	1.9	1.8

Table 3b

	1	2	3	4	5	6	7	8	9	10	11	12	13	14	15	16	17	18	19	20	21	22	23	24	25
Class.	alRhy	alRhy	alRhy	alRhy	alRhy	alRhy	alRhy	alRhy	alRhy	alRhy	alRhy	alRhy	alRhy	alRhy	alRhy	alRhy	alRhy	alRhy	alRhy	alRhy	alRhy	alRhy	alRhy	alRhy	alRhy
SiO_2	75.70	75.72	75.39	75.69	75.52	75.49	75.67	75.43	75.57	75.43	75.18	75.57	75.25	75.59	75.61	75.42	75.84	75.57	75.29	75.68	75.48	75.34	75.54	75.50	75.40
TiO_2	0.11	0.11	0.11	0.11	0.11	0.11	0.08	0.11	0.11	0.12	0.11	0.11	0.11	0.11	0.11	0.11	0.11	0.11	0.11	0.11	0.11	0.12	0.11	0.11	0.11
Al_2O_3	13.07	13.07	13.11	12.98	13.04	13.19	13.07	13.05	13.07	13.01	13.11	12.91	13.03	12.94	13.12	12.99	12.85	13.06	13.07	13.04	12.98	13.09	13.05	13.00	12.97
Fe_2O_3	0.31	0.17	0.32	0.31	0.32	0.29	0.32	0.39	0.33	0.30	0.37	0.34	0.44	0.22	0.27	0.48	0.39	0.32	0.42	0.30	0.24	0.58	0.23	0.30	0.24
FeO	1.18	1.30	1.20	1.21	1.18	1.22	1.16	1.14	1.16	1.23	1.13	1.14	1.11	1.27	1.25	1.05	1.11	1.17	1.16	1.19	1.23	0.99	1.28	1.20	1.25
MnO	0.07	0.07	0.07	0.07	0.07	0.08	0.07	0.07	0.07	0.07	0.07	0.07	0.07	0.07	0.07	0.07	0.07	0.07	0.07	0.07	0.07	0.07	0.07	0.07	0.07
MgO	0.07	0.11	0.09	0.08	0.10	0.08	0.07	0.11	0.09	0.08	0.10	0.17	0.08	0.07	n.d.	0.05	0.07	0.08	0.07	0.07	0.06	0.09	n.d.	0.07	0.08
CaO	0.60	0.60	0.61	0.62	0.64	0.60	0.61	0.61	0.60	0.61	0.60	0.59	0.62	0.59	0.60	0.61	0.60	0.59	0.62	0.59	0.60	0.60	0.60	0.60	0.59
Na_2O	3.35	3.37	3.50	3.36	3.54	3.48	3.47	3.53	3.50	3.54	3.64	3.63	3.65	3.60	3.50	3.63	3.52	3.62	3.62	3.58	3.72	3.72	3.58	3.66	3.76
K_2O	5.05	5.06	5.10	5.14	5.01	5.07	5.02	5.08	5.03	5.10	5.09	4.98	5.13	4.99	5.08	5.06	5.00	5.01	5.20	5.04	4.97	5.08	5.08	5.05	5.00
P_2O_5	0.07	0.07	0.06	0.06	0.07	0.06	0.06	0.07	0.06	0.06	0.06	0.06	0.06	0.06	0.06	0.06	0.06	0.06	0.07	0.06	0.06	0.06	0.07	0.07	0.06
L.o.I.	0.42	0.33	0.43	0.36	0.39	0.34	0.40	0.41	0.41	0.46	0.55	0.41	0.45	0.49	0.33	0.46	0.38	0.36	0.31	0.28	0.48	0.26	0.39	0.36	0.47
Total	100.00	99.98	99.99	99.99	99.99	100.01	100.00	100.00	100.00	100.01	100.01	99.98	100.00	100.00	100.00	99.99	100.00	100.02	100.01	100.01	100.00	100.00	100.00	99.99	100.00
S.I.	0.7	1.10	0.88	0.79	0.99	0.79	0.70	1.08	0.89	0.78	0.97	1.66	0.77	0.69	0.00	0.49	0.70	0.79	0.67	0.69	0.59	0.86	0.00	0.68	0.77
A.I.	0.84	0.84	0.86	0.85	0.86	0.85	0.85	0.87	0.86	0.87	0.88	0.88	0.89	0.88	0.86	0.88	0.87	0.87	0.89	0.87	0.89	0.89	0.87	0.88	0.89
Q	34.72	34.53	33.25	34.20	33.45	33.61	34.04	33.19	33.74	33.07	32.28	33.08	32.10	33.37	33.70	32.74	34.03	33.15	32.07	33.39	32.65	32.01	33.19	32.71	32.20
C	1.17	1.13	0.87	0.91	0.80	1.03	0.96	0.80	0.92	0.70	0.67	0.62	0.49	0.69	0.92	0.58	0.70	0.75	0.53	0.77	0.53	0.52	0.74	0.59	0.44
Or	29.84	29.90	30.14	30.37	29.60	29.96	29.66	30.02	29.72	30.14	30.08	29.43	30.31	29.49	30.02	29.90	29.55	29.60	30.73	29.78	29.37	30.02	30.02	29.84	29.55
Ab	28.34	28.51	29.61	28.43	29.95	29.44	29.36	29.87	29.61	29.95	30.80	30.71	30.88	30.46	29.61	30.71	29.78	30.63	30.63	30.29	31.48	31.48	30.29	30.97	31.81
An	2.52	2.52	2.63	2.68	2.72	2.58	2.63	2.57	2.58	2.63	2.58	2.53	2.68	2.53	2.58	2.63	2.58	2.53	2.62	2.53	2.58	2.58	2.52	2.52	2.53
Ac	0	0	0	0	0	0	0	0	0	0	0	0	0	0	0	0	0	0	0	0	0	0	0	0	0
Ns	0	0	0	0	0	0	0	0	0	0	0	0	0	0	0	0	0	0	0	0	0	0	0	0	0
Di	0	0	0	0	0	0	0	0	0	0	0	0	0	0	0	0	0	0	0	0	0	0	0	0	0
Ed	0	0	0	0	0	0	0	0	0	0	0	0	0	0	0	0	0	0	0	0	0	0	0	0	0
Sl	0	0	0	0	0	0	0	0	0	0	0	0	0	0	0	0	0	0	0	0	0	0	0	0	0
En	0.17	0.27	0.22	0.20	0.25	0.20	0.17	0.27	0.22	0.20	0.25	0.42	0.20	0.17	0	0.12	0.17	0.20	0.17	0.17	0.15	0.22	0	0.17	0.20
Fs	2.15	2.14	2.19	2.19	2.16	2.20	2.18	2.20	2.15	2.19	2.16	2.13	2.22	2.16	2.20	2.18	2.15	2.15	2.27	2.15	2.13	2.21	2.19	2.17	2.16
Hy	2.32	2.41	2.42	2.39	2.41	2.40	2.36	2.47	2.37	2.39	2.40	2.55	2.42	2.34	2.20	2.31	2.33	2.35	2.44	2.33	2.28	2.44	2.19	2.34	2.36
Mt	0.28	0.28	0.29	0.29	0.28	0.28	0.28	0.29	0.28	0.29	0.28	0.28	0.29	0.28	0.29	0.28	0.28	0.28	0.29	0.28	0.28	0.29	0.28	0.28	0.28
Il	0.21	0.21	0.21	0.21	0.21	0.21	0.15	0.21	0.21	0.23	0.21	0.21	0.21	0.21	0.21	0.21	0.21	0.21	0.21	0.21	0.21	0.23	0.21	0.21	0.21
Ap	0.16	0.16	0.14	0.14	0.16	0.14	0.14	0.16	0.14	0.14	0.14	0.14	0.14	0.14	0.14	0.14	0.14	0.14	0.16	0.14	0.14	0.14	0.16	0.16	0.14
D.I.	92.91	92.9	93.0	93.0	93.0	93.0	93.1	93.1	93.1	93.2	93.2	93.2	93.3	93.3	93.3	93.4	93.4	93.4	93.4	93.5	93.5	93.5	93.5	93.5	93.6
SAL	96.59	96.6	96.5	96.6	96.5	96.6	96.7	96.4	96.6	96.5	96.4	96.4	96.5	96.5	96.8	96.6	96.7	96.7	96.6	96.8	96.6	96.6	96.8	96.6	96.5
FEM	2.97	3.1	3.1	3.0	3.1	3.0	2.9	3.1	3.0	3.1	3.0	3.2	3.1	3.0	2.8	2.9	3.0	3.0	3.1	3.0	2.9	3.1	2.9	3.0	3.0

Table 3c

	1	2	3	4	5	6	7	8	9	10	11	12	13	14	15	16	17	18	19	20	21	22	23	24	25
Class.	Rhy	Rhy	Rhy	Rhy	Rhy	Rhy	alRhy	alRhy	alRhy	alRhy	alRhy	alRhy	alRhy	alRhy	alRhy	alRhy	alRhy	alRhy	alRhy	alRhy	alRhy	alRhy	alRhy	alRhy	alRhy
SiO_2	70.45	67.67	73.69	67.68	70.05	71.09	76.58	68.90	73.98	77.01	70.39	70.14	71.42	70.76	71.02	71.39	70.94	70.75	71.16	72.10	71.05	73.39	73.83	71.38	76.70
TiO_2	0.14	0.49	0.10	0.47	0.45	0.43	0.26	0.50	0.21	0.22	0.17	0.47	0.28	0.36	0.37	0.17	0.37	0.37	0.44	0.16	0.38	0.18	0.16	0.41	0.18
Al_2O_3	13.74	15.18	13.48	15.07	14.07	14.13	9.43	15.22	11.14	9.45	13.76	15.34	14.05	14.48	14.53	15.41	14.45	14.25	13.91	14.51	14.31	13.61	13.55	13.89	11.06
Fe_2O_3	2.12	2.65	0.70	2.59	2.33	2.33	4.38	2.49	4.09	4.05	2.06	2.53	2.38	2.41	2.10	1.82	2.09	1.09	1.27	2.00	2.31	2.15	2.00	0.83	2.97
FeO	n.d.	n.d.	1.36	n.d.	n.d.	n.d.	0.04	0.22	n.d.	n.d.	n.d.	n.d.	0.09	n.d.	0.30	n.d.	0.36	1.28	1.03	n.d.	0.21	n.d.	n.d.	1.46	n.d.
MnO	0.07	0.06	0.05	0.06	0.07	0.06	0.10	0.06	0.09	0.09	0.06	0.05	0.06	0.07	0.03	0.05	0.04	0.07	0.06	0.03	0.03	0.05	0.03	0.08	0.04
MgO	0.16	0.25	0.37	0.27	0.44	1.02	0.22	0.24	0.09	0.12	0.12	0.16	0.16	0.53	0.17	0.04	0.12	0.22	0.23	0.10	0.30	0.09	0.10	0.23	0.20
CaO	1.32	1.21	1.90	1.28	1.83	0.70	0.27	0.78	0.16	0.17	0.79	0.86	0.82	0.84	0.65	0.48	0.57	0.83	0.70	0.53	0.61	0.78	0.55	0.81	0.09
Na_2O	2.94	3.82	3.92	3.64	4.47	4.23	4.05	3.94	4.90	3.94	3.81	4.46	3.92	4.78	4.66	3.82	4.61	4.62	4.35	3.98	4.68	3.94	3.57	4.29	4.10
K_2O	4.53	5.26	3.13	5.70	4.58	5.71	3.97	6.13	4.55	3.88	5.70	5.45	5.73	5.36	5.38	6.03	5.48	5.67	5.79	5.79	5.59	5.53	5.58	6.01	4.30
P_2O_5	0.03	0.09	0.05	0.03	0.04	0.06	0.02	0.05	0.03	0.02	0.01	0.02	0.08	0.05	0.06	0.02	0.05	0.05	0.06	0.02	0.05	0.02	0.02	0.05	0.03
L.o.I.	4.51	3.32	1.26	3.20	1.69	0.24	0.66	1.48	0.76	1.06	3.13	0.52	1.01	0.36	0.73	0.79	0.91	0.79	0.99	0.77	0.48	0.25	0.61	0.56	0.34
Total	100.01	100.00	100.01	99.99	100.02	100.00	99.98	100.01	100.00	100.01	100.00	100.00	100.00	100.00	100.00	100.02	99.99	99.99	99.99	99.99	100.00	99.99	100.00	100.00	100.01
S.I.	1.67	2.13	3.92	2.26	3.79	7.80	1.79	1.87	0.68	1.03	1.04	1.29	1.33	4.12	1.37	0.35	0.96	1.72	1.83	0.86	2.33	0.78	0.90	1.80	1.77
A.I.	0.71	0.79	0.73	0.81	0.87	0.93	1.16	0.86	1.17	1.13	0.90	0.86	0.90	0.94	0.93	0.83	0.94	0.96	0.96	0.88	0.96	0.92	0.88	0.98	1.03
Q	31.77	21.29	33.10	20.34	21.77	20.70	38.33	19.27	30.07	39.40	23.43	20.07	23.55	19.07	20.60	24.03	20.60	19.40	21.20	24.43	19.77	26.46	29.30	20.82	34.78
C	1.67	1.22	0.31	0.66	0.00	0.00	0.00	0.81	0.00	0.00	0.00	0.59	0.10	0.00	0.00	1.77	0.02	0.00	0.00	0.78	0.00	0.00	0.69	0.00	0.00
Or	26.77	31.08	18.50	33.68	27.06	33.74	23.46	36.22	26.89	22.93	33.68	32.20	33.86	31.67	31.79	35.63	32.38	33.50	34.21	34.21	33.03	32.68	32.97	35.51	25.41
Ab	24.88	32.32	33.17	30.80	37.82	35.79	26.40	33.34	31.97	27.00	32.24	37.74	33.17	40.44	39.43	32.32	39.01	39.09	36.81	33.68	39.60	33.34	30.21	36.30	32.95
An	6.35	5.41	9.10	6.15	4.80	2.70	0.00	3.54	0.00	0.00	3.61	4.14	3.55	2.22	2.83	2.25	2.50	1.40	1.33	2.50	1.53	3.12	2.60	0.89	0.00
Ac	0	0	0	0	0	0	1.52	0	1.41	1.39	0	0	0	0	0	0	0	0	0	0	0	0	0	0	1.02
Ns	0	0	0	0	0	0	1.43	0	1.84	1.11	0	0	0	0	0	0	0	0	0	0	0	0	0	0	0.14
Di	0	0	0	0	1.13	0.17	0.10	0	0.02	0.04	0.02	0	0	0.48	0	0	0	0.37	0.30	0	0.23	0.05	0	0.46	0.03
Ed	0	0	0	0	2.29	0.15	0.97	0	0.51	0.59	0.19	0	0	0.89	0	0	0	1.71	1.22	0	0.78	0.50	0	1.97	0.19
Sl	0	0	0	0	3.42	0.31	1.06	0	0.53	0.63	0.21	0	0	1.37	0	0	0	2.08	1.52	0	1.01	0.55	0	2.43	0.22
En	0.40	0.62	0.92	0.67	0.57	2.46	0.50	0.60	0.21	0.28	0.29	0.40	0.40	1.10	0.42	0.1	0.30	0.38	0.43	0.25	0.64	0.20	0.25	0.36	0.49
Fs	2.78	2.90	2.93	2.85	1.33	2.49	5.68	3.00	5.50	5.38	2.53	2.75	3.02	2.33	2.75	2.28	2.84	2.02	2.02	2.51	2.47	2.45	2.51	1.76	4.00
Hy	3.18	3.52	3.85	3.52	1.91	4.95	6.19	3.60	5.72	5.67	2.81	3.15	3.41	3.43	3.17	2.38	3.14	2.40	2.45	2.76	3.11	2.65	2.76	2.11	4.48
Mt	0.37	0.46	0.38	0.45	0.40	0.40	0.00	0.47	0.00	0.00	0.36	0.44	0.43	0.42	0.42	0.31	0.43	0.43	0.42	0.34	0.44	0.37	0.34	0.42	0.00
Il	0.27	0.93	0.19	0.89	0.85	0.82	0.49	0.95	0.40	0.42	0.32	0.89	0.53	0.68	0.70	0.32	0.70	0.70	0.84	0.30	0.72	0.34	0.30	0.78	0.34
Ap	0.07	0.21	0.12	0.07	0.09	0.14	0.05	0.12	0.07	0.05	0.02	0.05	0.19	0.12	0.14	0.05	0.12	0.12	0.14	0.05	0.12	0.05	0.05	0.12	0.07
D.I.	83.4	84.7	84.8	84.8	86.7	90.2	88.2	88.8	88.9	89.3	89.4	90.0	90.6	91.2	91.8	92.0	92.0	92.0	92.2	92.3	92.4	92.5	92.5	92.6	93.1
SAL	91.4	91.3	94.2	91.6	91.5	92.9	88.2	93.2	88.9	89.3	93.0	94.7	94.2	93.4	94.7	96.0	94.5	93.4	93.5	95.6	93.9	95.6	95.8	93.5	93.1
FEM	3.9	5.1	4.5	4.9	6.7	6.6	10.7	5.1	10.0	9.3	3.7	4.5	4.6	6.0	4.4	3.1	4.4	5.7	5.4	3.5	5.4	4.0	3.5	5.9	6.3

Table 4

Origin of rock samples	**Geochemical characteristics**			
	Classification	Volcanic serie affinity		
		Na	K	HK
Volcanic glass aggregates from the mortars of Nora theater	Rhy	-	25	25
Volcanic rocks (perlites and obsidians) from Monte Arci outcrops (central-west Sardinia)	Rhy	-	1	5
	alRhy	-	17	94
	Subtotal	-	*18*	*99*
	alRhy	-	35	2
Volcanic rocks from Sant'Antioco outcrops (south-west Sardinia)	Rhy	-	6	-
	alRhy	-	20	-
	Subtotal	-	*26*	-
	Total samples	**-**	**104**	**126**

Table 5

Sample	**36_ob15-5**	**39_ob15-8**	**13_ob40-1**
^{7}Li	82.2	61.13	67.21
^{11}B	1.15	1.31	1.33
^{23}Na	96621.82	92136.09	89979.59
^{25}Mg	152.49	273.24	106.18
^{29}Si	614887.75	572032.5	556738.69
^{45}Sc	1.87	1.78	2.47
^{49}Ti	73.48	94.56	72.99
^{51}V	0.61	0.3	<0.1410
^{53}Cr	<1.20	10.94	<1.9300
^{59}Co	0.44	0.08	0.14
^{60}Ni	0.44	0.75	<0.0000
^{66}Zn	30.08	43.14	18.69
^{85}Rb	1.82	2.58	1.48
^{88}Sr	1372.23	1311.37	1512.18
^{89}Y	0.22	0.29	0.28
^{90}Zr	<0.0360	0.81	0.06
^{93}Nb	<0.0206	0.2	<0.031
^{133}Cs	<0.0107	0.03	0.01
^{137}Ba	545.66	560.16	580
^{139}La	19.86	19	20.86
^{140}Ce	31.11	28.86	29.18
^{141}Pr	1.93	1.86	1.89
^{146}Nd	5.3	4.26	4.66
^{149}Sm	0.13	0.27	0.19
^{151}Eu	4.03	3.82	4.37
^{157}Gd	0.1	0.33	<0.00
^{159}Tb	0.03	<0.0073	<0.0180
^{163}Dy	0.14	<0.0500	0.19
^{165}Ho	<0.0068	0.01	<0.0107
^{167}Er	<0.00	0.07	<0.0540
^{169}Tm	<0.00	0.01	<0.0099
^{173}Yb	<0.0410	<0.0440	0.09
^{175}Lu	<0.0116	<0.0073	<0.0075
^{177}Hf	<0.048	0.08	<0.055
^{181}Ta	<0.0072	0.06	<0.0142
^{208}Pb	17.41	14.43	15.55
^{232}Th	<0.0072	0.01	<0.0165
^{238}U	0.02	<0.0060	9.6

Table 6a

	1	2	3	4	5	6	7	8	9	10	11	12	13	14	15	16	17	18	19	20	21	22	23
^{7}Li	31.88	45.17	23.03	54.95	39.09	41.16	33.74	40.77	49.18	41.12	45.96	53.93	46.77	47.48	47.39	40.67	37.31	26.96	40.65	53.80	47.21	47.65	41.73
^{11}B	40.83	41.31	45.29	46.94	45.15	43.81	46.35	43.70	48.47	49.72	50.24	51.22	44.95	42.80	36.87	43.59	46.11	40.47	46.91	46.02	44.40	42.34	43.62
^{23}Na	31230	30511	29406	34897	30191	31725	30168	29524	34315	31528	32595	35654	34375	34979	23927	33908	34349	31520	32275	35156	36508	34222	32610
^{25}Mg	892	977	789	1174	924	976	956	904	1078	1070	1010	1022	1000	1140	2337	1002	866	911	841	1061	1132	912	973
^{29}Si	418274	413153	442866	507975	442950	426193	435235	416267	450405	431837	448281	449651	455746	462573	488815	451910	469982	500246	469368	444181	482501	439085	453683
^{45}Sc	4.72	4.52	4.72	5.82	4.81	4.50	4.72	4.65	5.13	4.57	4.36	4.83	4.90	5.03	6.01	4.77	4.63	5.05	4.50	3.48	4.27	3.97	5.17
^{49}Ti	899.78	866.32	965.88	1102.21	997.52	902.24	942.47	899.10	1006.13	952.63	938.47	947.30	876.03	1038.17	1337.02	947.98	958.46	989.39	985.65	927.68	990.51	909.72	947.54
^{51}V	1.01	1.11	1.24	0.83	2.90	1.14	1.12	1.02	1.40	0.93	1.05	0.83	1.35	1.26	1.65	0.88	0.99	5.30	1.09	1.43	1.65	1.31	1.05
^{53}Cr	<1.66	<1.37	<1.46	0.92	<1.28	<1.04	<1.40	<1.09	<0.98	<1.37	<1.23	<1.71	<0.95	<2.02	<1.24	<2.04	3.02	2.84	<1.77	2.61	2.03	<1.42	<1.67
^{59}Co	0.69	1.02	0.67	0.64	0.82	0.86	0.81	1.10	0.86	0.79	0.74	0.89	0.84	0.80	0.75	0.89	0.75	0.87	0.84	0.89	0.92	0.89	0.71
^{60}Ni	0.22	0.36	0.37	1.30	11.97	0.09	<0.124	0.25	0.56	0.74	0.26	0.41	0.11	<0.36	0.21	0.66	0.93	416.04	0.66	0.15	0.86	0.47	<0.24
^{66}Zn	63.69	60.44	60.27	118.45	72.70	64.90	63.50	61.44	68.36	71.67	65.43	68.95	70.00	67.44	68.61	67.33	64.45	52.89	65.01	67.81	70.30	78.64	66.13
^{85}Rb	189.74	180.90	194.30	202.84	209.53	193.68	196.53	189.33	201.87	196.62	206.41	200.45	209.38	198.02	157.58	227.75	226.74	185.90	209.93	200.20	212.24	192.92	206.25
^{88}Sr	128.98	130.47	134.21	127.31	129.22	127.43	131.16	132.26	129.25	131.15	131.96	130.75	122.79	137.82	115.68	129.06	121.24	135.96	127.40	130.49	126.86	125.02	134.47
^{89}Y	17.02	16.70	17.39	16.54	16.26	16.38	17.46	17.34	16.76	17.48	18.75	17.82	17.59	18.28	15.33	17.76	16.82	20.74	15.76	17.35	16.89	16.80	18.77
^{90}Zr	159.94	155.51	190.06	183.31	164.91	153.68	164.02	165.64	162.18	170.93	174.58	165.64	158.10	193.21	291.34	174.68	171.90	232.88	162.01	166.60	173.37	162.99	181.31
^{93}Nb	17.63	17.29	19.04	23.24	19.87	18.66	19.24	19.20	19.16	19.59	20.23	19.63	20.61	20.77	23.57	19.53	19.46	21.22	19.05	19.73	20.48	19.22	19.41
^{133}Cs	5.11	4.84	5.29	6.47	5.23	5.19	5.30	4.94	5.14	5.14	5.28	5.27	5.31	5.27	6.68	5.02	5.37	5.08	5.27	5.28	5.55	5.24	5.20
^{137}Ba	790.60	763.31	839.92	771.69	847.88	781.86	816.42	815.92	802.34	830.84	832.41	828.87	807.24	852.51	663.46	849.39	839.96	797.72	817.87	809.48	821.15	807.95	842.30
^{139}La	47.76	46.26	50.18	46.16	49.88	45.49	49.06	47.70	44.79	49.51	49.79	47.65	46.61	52.65	41.76	49.31	49.09	54.28	46.80	47.43	48.37	47.62	51.52
^{140}Ce	92.04	91.91	94.94	93.99	100.32	94.81	95.33	93.28	96.80	95.96	99.53	98.15	95.16	100.42	75.54	98.19	98.69	93.14	96.53	97.36	96.07	93.68	100.35
^{141}Pr	8.26	8.22	8.40	7.77	8.79	8.06	8.81	8.47	8.74	8.91	8.85	8.26	8.14	9.22	7.17	9.15	8.75	9.04	8.37	8.50	8.80	8.46	9.09
^{146}Nd	27.55	26.21	28.35	30.27	29.14	25.90	27.40	27.46	26.63	29.99	30.12	29.48	26.31	31.81	26.23	28.81	29.74	31.45	27.62	27.46	29.25	26.86	29.17
^{149}Sm	4.19	4.96	5.21	4.47	3.85	3.92	4.30	4.96	4.93	5.09	4.67	4.49	5.60	5.42	4.16	4.96	4.81	5.30	4.49	3.95	4.30	4.77	4.36
^{151}Eu	0.71	0.88	0.61	0.76	0.75	0.75	0.71	0.75	0.86	0.80	0.90	0.75	0.64	0.92	0.30	0.75	0.83	0.79	0.77	0.85	0.65	0.83	0.85
^{157}Gd	2.86	3.35	3.26	3.29	3.75	3.15	3.40	3.26	3.53	2.98	3.57	3.23	2.89	2.95	2.65	3.02	2.98	3.82	2.63	2.86	2.85	2.88	3.46
^{159}Tb	0.46	0.47	0.53	0.59	0.58	0.44	0.51	0.51	0.53	0.46	0.63	0.55	0.53	0.53	0.41	0.44	0.49	0.62	0.43	0.44	0.48	0.53	0.55
^{163}Dy	2.71	3.00	3.01	2.51	2.49	2.67	3.13	3.15	3.00	2.85	2.73	2.88	3.52	3.15	2.61	3.25	2.75	3.77	2.94	2.55	3.05	2.96	3.49
^{165}Ho	0.62	0.60	0.58	0.62	0.63	0.56	0.62	0.70	0.59	0.50	0.64	0.60	0.60	0.76	0.55	0.68	0.51	0.58	0.52	0.65	0.67	0.64	0.64
^{167}Er	1.43	1.48	2.02	1.25	1.30	1.55	1.61	1.77	1.78	1.79	1.76	1.99	1.55	1.94	1.39	2.01	1.45	1.95	1.53	1.60	1.68	1.65	1.63
^{169}Tm	0.23	0.26	0.31	0.20	0.24	0.25	0.26	0.28	0.24	0.24	0.26	0.28	0.27	0.30	0.23	0.29	0.24	0.32	0.21	0.28	0.25	0.27	0.23
^{173}Yb	1.97	1.83	1.86	2.52	1.94	1.98	2.41	1.69	1.92	2.30	2.12	1.80	1.45	2.10	1.75	2.01	1.77	2.21	1.80	2.08	1.97	1.52	1.70
^{175}Lu	0.29	0.29	0.33	0.24	0.27	0.27	0.28	0.33	0.27	0.30	0.34	0.34	0.35	0.36	0.31	0.25	0.29	0.36	0.26	0.29	0.26	0.28	0.26
^{177}Hf	4.59	4.27	5.33	4.38	4.38	3.78	4.32	4.74	4.68	4.83	4.93	4.19	4.41	5.31	7.51	4.09	4.63	6.59	4.62	4.80	4.90	4.95	4.63
^{181}Ta	1.23	1.18	1.35	1.33	1.29	1.13	1.37	1.39	1.29	1.39	1.56	1.52	1.51	1.61	2.14	1.29	1.47	1.78	1.22	1.25	1.55	1.34	1.26
^{208}Pb	24.09	22.38	23.26	30.22	27.29	24.38	23.97	26.56	26.45	25.88	25.50	24.85	28.21	25.57	22.90	25.87	26.92	28.07	26.46	25.26	33.76	29.06	27.73
^{232}Th	17.06	17.15	18.65	17.50	18.05	16.61	18.54	17.94	17.74	18.95	19.42	18.10	18.25	20.11	16.61	18.84	18.31	20.41	16.60	16.92	18.45	17.46	19.32
^{238}U	4.81	4.68	4.99	4.30	5.04	4.90	4.98	4.88	5.30	5.05	4.84	5.08	5.35	5.00	3.73	5.26	5.36	4.81	5.41	4.76	5.15	4.74	5.33

Table 6b

	24	25	26	27	28	29	30	31	32	33	34	35	36	37	38	39	40	41	42	43	44	45	46
^{7}Li	33.29	29.17	31.90	43.08	35.25	33.26	39.75	25.47	21.23	26.46	39.17	39.40	65.37	44.56	39.12	39.19	33.00	39.45	35.19	53.30	40.90	56.55	38.49
^{11}B	28.66	38.89	40.87	37.84	37.59	35.96	36.45	37.61	46.85	43.79	37.70	44.32	47.34	46.15	41.74	38.33	52.36	44.24	42.94	44.10	43.69	44.15	36.85
^{23}Na	28517	31811	31661	31869	32473	31556	31537	31741	30538	32138	36776	35556	34408	33091	37001	35013	33661	36102	34351	32829	40506	35604	31776
^{25}Mg	867	784	832	936	866	909	909	832	690	837	1005	903	1146	1032	873	993	882	1007	918	1000	869	973	815
^{29}Si	351543	450465	426647	431538	451171	419737	410243	429918	447503	404081	453428	450741	458061	443823	474845	437064	501317	451888	451195	444741	498190	455833	381816
^{45}Sc	3.55	4.26	4.38	3.85	4.29	3.98	3.65	4.00	3.96	3.75	4.20	4.00	4.03	3.28	4.12	3.60	3.50	3.84	3.78	3.68	3.87	4.26	3.26
^{49}Ti	725.47	923.99	889.74	894.00	922.49	820.94	861.24	866.36	897.40	814.90	972.53	907.27	879.11	896.18	962.50	874.46	923.25	869.91	886.81	876.39	1026.43	874.74	727.86
^{51}V	0.88	1.01	0.87	1.12	1.03	1.02	0.94	0.95	1.14	1.19	1.19	1.02	1.26	1.57	0.95	1.15	1.48	1.22	1.13	1.13	1.48	1.44	0.86
^{53}Cr	<1.54	<2.00	<1.77	<1.65	<1.55	<1.73	<1.42	1.97	<2.77	2.65	<2.04	<1.96	<0.86	<1.43	<1.73	40.88	<2.05	<1.72	1.88	<1.60	<2.06	<1.50	<2.83
^{59}Co	0.89	0.71	0.69	1.05	0.78	0.64	0.76	0.67	0.59	0.55	0.87	0.56	1.07	0.89	0.81	0.87	0.74	0.91	0.78	0.78	0.64	0.65	0.53
^{60}Ni	0.29	0.43	0.28	0.54	0.28	0.38	0.28	<0.30	0.28	<0.41	<0.39	0.32	0.58	0.51	0.32	0.41	<0.35	0.75	0.42	<0.31	0.47	<0.31	16.58
^{66}Zn	60.71	65.41	60.86	64.83	70.24	56.39	60.94	60.33	65.60	57.84	65.33	70.94	81.17	62.87	70.93	62.63	127.90	62.13	66.54	64.07	65.60	92.33	54.17
^{85}Rb	138.26	200.78	198.73	190.46	199.14	184.01	185.03	190.88	201.17	174.19	198.92	200.15	206.10	184.74	208.84	185.66	202.71	192.59	193.89	189.39	215.72	189.68	159.41
^{88}Sr	153.27	137.65	134.53	130.88	132.66	132.87	129.13	149.03	133.68	134.87	138.51	133.64	127.11	130.40	139.21	128.79	125.10	127.89	131.97	129.04	137.67	127.02	149.30
^{89}Y	15.05	18.52	17.48	17.98	17.19	18.32	17.24	17.88	17.02	15.90	17.93	17.77	16.35	16.41	17.45	17.07	14.89	17.03	15.89	16.90	17.78	17.06	13.19
^{90}Zr	147.70	177.94	174.26	170.63	175.95	179.35	166.91	171.49	175.07	161.05	174.72	164.96	150.50	164.40	175.40	165.55	175.46	159.19	163.76	167.95	184.45	164.59	131.31
^{93}Nb	15.18	19.33	18.29	18.17	19.81	18.34	18.20	19.95	20.68	17.56	20.19	19.95	20.10	18.30	19.68	18.87	21.24	19.78	18.63	18.74	21.60	18.75	16.05
^{133}Cs	4.01	5.21	4.91	5.10	5.71	4.74	4.95	5.06	5.42	4.61	5.33	5.71	5.48	4.85	5.46	4.99	5.70	5.07	5.29	4.98	5.40	4.79	4.11
^{137}Ba	584.06	841.11	810.20	799.36	822.03	812.24	792.28	838.50	855.53	854.40	859.27	839.82	800.07	792.79	855.21	796.37	802.97	825.83	785.69	821.43	895.81	789.84	716.37
^{139}La	40.38	51.34	49.58	50.29	48.74	51.55	48.87	49.79	50.57	45.21	51.05	49.88	48.78	47.72	50.58	46.85	46.37	47.49	46.70	48.04	52.59	46.43	39.44
^{140}Ce	79.75	98.73	93.85	96.72	95.60	93.86	94.61	95.20	97.65	89.49	100.41	97.68	100.48	96.16	100.21	93.35	90.07	94.18	93.68	96.91	104.48	93.97	78.93
^{141}Pr	7.18	8.42	8.70	8.43	8.60	8.60	8.66	8.67	8.96	7.71	9.31	9.01	8.02	8.39	8.66	8.59	7.88	8.61	8.55	8.64	9.52	8.67	6.81
^{146}Nd	24.19	29.16	29.07	28.21	28.70	30.12	28.03	29.12	28.24	24.96	27.55	29.93	27.99	28.66	28.94	26.87	28.69	26.92	27.50	29.98	30.00	28.37	23.20
^{149}Sm	4.16	4.62	4.45	4.91	4.72	5.02	5.14	5.45	4.35	3.91	4.57	5.25	4.68	4.85	5.17	4.69	4.28	5.61	4.23	4.96	4.98	4.90	3.52
^{151}Eu	0.67	0.76	0.74	0.74	0.67	0.76	0.73	0.87	0.78	0.80	0.80	0.77	0.69	1.03	0.82	0.85	0.86	0.85	0.72	0.68	0.94	0.79	0.87
^{157}Gd	2.31	2.94	3.13	3.33	3.14	3.00	2.66	3.08	3.03	2.75	2.86	3.14	2.75	2.50	2.95	2.71	3.32	3.52	2.89	2.95	3.06	3.31	2.38
^{159}Tb	0.42	0.48	0.49	0.47	0.52	0.58	0.53	0.51	0.48	0.47	0.51	0.50	0.42	0.42	0.55	0.48	0.50	0.56	0.43	0.47	0.54	0.40	0.44
^{163}Dy	2.51	2.90	3.22	3.01	3.09	3.34	2.65	2.76	3.21	2.89	2.98	2.94	2.74	3.07	2.93	3.11	3.14	2.87	2.59	3.06	2.86	2.99	1.97
^{165}Ho	0.52	0.56	0.58	0.58	0.61	0.65	0.65	0.63	0.63	0.52	0.64	0.60	0.56	0.55	0.61	0.66	0.54	0.63	0.57	0.58	0.55	0.61	0.53
^{167}Er	1.49	1.94	1.70	1.64	1.62	2.01	1.68	1.68	1.74	1.43	2.04	1.66	1.71	1.66	1.89	1.56	1.75	2.02	1.79	1.76	1.60	1.77	1.38
^{169}Tm	0.22	0.27	0.27	0.26	0.26	0.26	0.27	0.25	0.25	0.23	0.24	0.25	0.23	0.24	0.28	0.26	0.22	0.25	0.28	0.26	0.24	0.29	0.22
^{173}Yb	1.44	2.09	1.92	2.11	1.68	2.07	1.79	2.00	1.79	1.51	2.24	2.09	1.95	2.17	1.95	1.89	1.81	1.31	1.93	1.67	1.95	2.02	1.59
^{175}Lu	0.24	0.33	0.30	0.27	0.27	0.30	0.32	0.27	0.26	0.23	0.28	0.29	0.33	0.25	0.32	0.27	0.27	0.21	0.30	0.26	0.29	0.29	0.24
^{177}Hf	4.43	5.06	4.78	4.88	4.79	4.91	4.13	4.63	4.97	4.40	4.86	4.51	3.96	4.84	4.77	4.18	4.64	5.13	3.80	4.81	5.27	4.24	3.74
^{181}Ta	1.10	1.33	1.35	1.26	1.37	1.39	1.24	1.30	1.27	1.21	1.35	1.19	1.14	1.30	1.35	1.20	1.29	1.40	1.37	1.19	1.44	1.25	1.11
^{208}Pb	16.94	24.84	24.90	24.16	26.60	23.77	24.68	26.28	26.27	23.88	25.23	26.53	29.51	24.27	27.50	25.34	31.94	25.74	24.86	25.58	27.19	26.60	21.61
^{232}Th	14.74	18.60	17.96	18.18	17.98	19.32	17.07	18.06	18.16	17.48	17.91	17.67	16.89	17.13	18.10	16.71	16.87	17.57	16.88	17.44	19.15	17.55	14.34
^{238}U	4.00	4.92	4.88	4.85	5.17	4.48	4.84	4.80	4.98	4.71	5.05	5.09	5.39	4.80	5.26	4.88	5.33	5.13	4.89	4.89	5.29	5.13	4.28

Table 6c

	47	48	49	50	51	52	53	54	55	56	57	58	59	60	61	62	63	64	65	66	67	68	69
^{7}Li	44.02	55.10	54.57	43.35	60.07	30.83	41.92	29.06	51.73	52.95	30.86	28.53	39.91	21.59	43.05	33.92	57.23	21.58	27.12	20.64	45.55	31.99	43.18
^{11}B	45.28	45.72	42.80	48.19	60.58	48.54	48.13	41.54	41.38	47.68	44.54	45.65	46.14	49.45	44.27	45.81	48.50	48.43	44.60	39.12	37.31	40.64	40.58
^{23}Na	35214	37491	38501	36149	36460	30568	34978	29949	33239	33988	33804	33511	37220	33701	32593	30807	37980	35372	34886	34052	32806	34070	34568
^{25}Mg	1104	1219	977	926	911	901	1020	943	908	1050	909	1103	908	877	862	884	1035	727	781	732	1025	866	1001
^{29}Si	456129	471532	434988	465321	485840	478494	556002	485609	463397	452543	470865	476245	452636	486411	428616	476826	467360	492075	499628	442972	433669	470357	443228
^{45}Sc	3.63	3.65	4.41	4.09	4.10	3.28	4.43	4.85	4.02	3.65	3.76	3.17	3.52	4.08	3.53	3.91	4.13	3.75	4.21	2.98	3.28	3.49	3.52
^{49}Ti	900.82	948.85	876.34	872.10	922.27	983.47	1036.20	1036.02	926.49	904.61	950.27	1148.89	926.96	970.84	876.18	935.92	963.39	1123.02	1070.28	878.60	955.79	990.65	946.76
^{51}V	0.81	1.92	0.76	1.02	1.37	1.11	1.48	1.04	0.87	1.37	0.87	1.49	1.22	1.04	1.13	1.02	1.31	1.02	1.23	0.49	1.38	0.72	1.43
^{53}Cr	<1.57	<1.82	<2.10	<1.68	<1.14	2.14	<1.54	1.71	<1.92	2.15	<1.91	<1.58	<1.70	<1.60	<1.48	<1.38	<1.96	<1.72	<2.37	<1.91	<1.80	<1.90	<1.67
^{59}Co	0.86	1.14	0.84	0.67	0.97	0.85	0.87	0.73	0.81	1.06	1.02	0.87	0.83	0.82	0.84	1.13	0.72	0.55	0.63	0.76	1.13	0.89	0.76
^{60}Ni	0.55	0.85	<0.23	0.86	0.46	<0.26	1.11	<0.29	0.35	0.13	<0.163	0.99	<0.187	<0.181	0.99	12.05	<0.146	0.12	<0.50	<1.56	0.33	0.19	0.83
^{66}Zn	66.47	77.53	62.78	71.41	84.95	69.14	74.98	69.74	72.53	70.51	69.33	77.81	67.72	68.32	72.80	70.74	70.54	82.25	76.33	68.99	64.54	71.95	65.01
^{85}Rb	197.66	206.71	190.20	205.51	224.10	190.89	218.69	192.90	199.50	201.39	213.96	214.16	210.75	226.01	195.38	205.35	217.84	229.48	230.05	194.93	199.47	227.44	208.14
^{88}Sr	129.36	126.10	126.29	126.54	129.36	129.72	143.54	134.02	127.90	133.56	133.96	128.81	133.33	137.35	119.91	116.57	126.69	135.46	136.55	127.51	129.84	139.33	137.02
^{89}Y	15.15	17.29	16.56	15.57	15.71	16.94	16.16	18.22	15.67	16.89	17.21	16.75	16.57	21.91	15.94	14.60	16.04	16.40	16.32	15.62	16.95	16.24	16.84
^{90}Zr	155.72	160.47	162.47	158.91	159.14	180.64	181.98	279.43	159.36	166.21	168.44	162.19	163.31	168.38	154.16	154.62	155.19	170.65	166.50	164.06	167.19	171.63	161.01
^{93}Nb	18.85	18.81	18.46	19.33	19.30	22.46	21.30	23.37	20.02	18.78	19.48	24.48	19.03	21.24	18.63	20.18	19.28	20.37	20.36	18.04	18.48	19.02	18.43
^{133}Cs	4.86	5.08	5.04	5.20	5.84	5.04	5.27	5.17	5.21	5.55	5.80	5.27	5.66	5.53	5.19	5.12	5.53	5.64	5.86	5.04	4.78	5.57	5.72
^{137}Ba	782.07	795.02	783.51	789.44	800.44	758.93	1029.00	797.02	782.09	819.20	835.54	866.38	826.85	896.40	788.74	734.64	838.92	855.45	852.77	797.47	790.49	825.78	815.67
^{139}La	44.99	47.63	47.40	46.48	46.95	48.86	48.06	52.64	47.00	48.74	48.41	48.41	48.94	49.51	46.00	42.53	47.24	47.78	47.66	46.89	47.78	48.34	47.98
^{140}Ce	93.32	95.69	94.00	94.72	99.01	89.80	92.09	92.07	96.17	95.34	100.08	98.54	98.74	102.69	92.91	89.41	99.18	98.56	99.02	90.36	93.49	96.93	98.59
^{141}Pr	8.34	8.60	8.47	8.70	8.08	8.09	7.73	8.62	8.53	8.29	8.68	8.73	8.57	8.68	8.04	7.52	8.42	8.25	8.20	8.05	8.37	8.60	8.30
^{146}Nd	26.77	30.10	27.31	27.64	28.06	27.33	27.22	30.01	26.35	29.10	27.59	26.84	27.98	27.82	28.41	23.42	28.13	26.45	25.32	25.02	28.67	26.10	26.83
^{149}Sm	4.26	4.61	4.33	3.84	4.14	4.39	5.57	4.77	3.78	4.41	4.80	4.21	5.03	4.67	3.68	3.63	4.64	4.56	5.14	4.63	4.89	4.72	4.17
^{151}Eu	0.66	0.80	0.79	0.74	0.90	0.85	0.93	0.84	0.62	0.90	0.79	0.70	0.57	0.86	0.78	0.75	0.86	0.86	0.74	0.60	0.79	0.77	0.78
^{157}Gd	2.64	2.67	2.93	2.44	2.68	2.97	3.32	3.39	2.67	2.67	2.79	3.21	2.67	3.05	3.19	2.57	3.07	2.61	2.42	2.69	2.80	2.38	2.87
^{159}Tb	0.50	0.53	0.48	0.50	0.52	0.50	0.43	0.55	0.51	0.42	0.49	0.42	0.54	0.50	0.49	0.38	0.44	0.45	0.55	0.45	0.49	0.48	0.41
^{163}Dy	3.26	2.87	3.13	2.94	2.91	2.91	2.64	3.42	2.64	2.97	2.98	2.97	2.41	2.61	2.92	2.78	2.66	2.49	2.53	2.36	3.16	2.88	2.84
^{165}Ho	0.55	0.48	0.53	0.49	0.57	0.57	0.55	0.69	0.51	0.64	0.52	0.63	0.60	0.72	0.53	0.52	0.57	0.52	0.65	0.50	0.66	0.60	0.67
^{167}Er	1.55	1.75	1.90	1.71	1.28	2.01	1.57	1.61	1.76	1.66	1.73	1.50	1.51	1.98	1.73	1.32	2.06	1.32	1.57	1.55	1.67	1.58	1.53
^{169}Tm	0.25	0.27	0.24	0.24	0.31	0.25	0.24	0.29	0.17	0.31	0.25	0.26	0.28	0.33	0.22	0.21	0.30	0.22	0.27	0.27	0.29	0.26	0.24
^{173}Yb	1.97	1.95	1.90	1.62	1.32	2.06	2.78	2.22	1.88	2.02	1.80	1.82	1.51	2.29	1.76	1.79	1.92	1.75	1.88	1.91	2.53	1.73	1.86
^{175}Lu	0.29	0.30	0.34	0.21	0.25	0.31	0.20	0.28	0.21	0.28	0.28	0.29	0.32	0.35	0.31	0.29	0.28	0.19	0.25	0.24	0.36	0.28	0.26
^{177}Hf	4.30	5.54	4.30	4.11	3.95	5.03	5.33	9.26	4.06	4.44	4.45	4.73	4.57	3.92	3.66	4.29	3.71	4.20	4.67	4.80	4.35	4.24	4.16
^{181}Ta	1.31	1.07	1.48	1.47	1.35	1.42	1.62	1.70	1.25	1.35	1.37	1.54	1.34	1.42	1.31	1.40	1.26	1.37	1.39	1.33	1.33	1.33	1.19
^{208}Pb	25.11	29.61	24.86	26.56	31.85	27.58	31.57	28.29	27.34	29.45	26.08	26.94	25.82	27.90	25.27	28.60	27.41	26.79	27.98	24.48	24.56	26.49	24.73
^{232}Th	16.23	17.33	17.18	17.19	18.04	17.70	18.84	22.12	15.83	16.66	17.19	17.03	17.28	17.74	16.29	14.53	15.96	16.90	16.55	16.15	16.69	16.69	15.36
^{238}U	4.77	5.41	5.08	5.39	6.04	4.71	5.46	4.81	5.16	5.24	5.15	5.37	5.31	5.50	5.06	5.12	5.41	5.45	5.34	4.66	4.42	4.97	4.80

Table 6d

	70	71	72	73	74	75	76	77	78	79	80	81	82	83	84	85	86	87	88	89	90	91	92
^{7}Li	48.13	40.20	38.32	33.35	31.13	33.49	65.86	38.21	62.70	43.19	66.05	68.02	68.50	74.86	56.87	44.73	55.30	56.95	43.61	27.02	22.86	38.51	35.25
^{11}B	39.92	44.89	38.67	45.51	42.72	35.94	52.41	42.54	40.82	41.70	46.06	42.55	74.42	58.44	45.53	44.97	51.70	45.95	43.19	37.22	43.69	41.42	38.38
^{23}Na	36579	35974	38370	36074	32078	30246	35906	31426	34883	34080	38414	38173	45942	38537	38635	34093	36252	35833	34613	32166	31498	32757	36656
^{25}Mg	949	908	930	878	936	1032	990	891	1041	966	1151	1218	1878	1336	1051	1012	988	999	979	830	703	1034	1023
^{29}Si	465937	457216	467500	460550	474759	440701	462465	434913	463107	460494	503052	514313	767413	519921	491875	449494	497317	476861	449848	464144	424494	420946	461175
^{45}Sc	4.18	3.70	3.92	3.44	4.06	2.76	3.62	3.38	3.81	3.64	3.74	3.46	8.21	4.00	3.17	3.02	4.44	4.21	3.99	3.73	4.11	4.33	4.36
^{49}Ti	988.21	945.16	980.63	948.25	963.39	862.99	898.34	886.01	960.74	907.49	948.23	990.85	1385.32	985.01	945.60	877.58	1021.61	1002.54	915.95	969.79	950.12	903.98	1090.24
^{51}V	1.10	0.99	0.84	1.20	1.04	0.94	0.98	1.18	0.98	1.14	1.06	1.32	3.03	2.04	1.30	1.13	1.26	1.35	1.33	0.93	0.93	1.37	1.46
^{53}Cr	<1.94	2.58	<3.49	<2.13	<1.58	2.38	<1.46	4.22	2.23	<1.31	<1.36	4.41	<1.70	31.56	1.70	<1.07	<1.62	<1.49	<1.71	<1.91	<1.67	1.85	<2.38
^{59}Co	0.91	1.01	0.77	0.82	0.85	0.82	0.99	0.69	1.16	0.93	1.21	1.11	1.09	1.61	0.84	0.86	0.92	0.97	0.87	0.63	0.62	0.81	0.93
^{60}Ni	0.19	<0.37	<0.27	<0.29	0.45	0.45	0.42	0.95	0.17	0.23	0.14	1.67	2.48	7.05	0.39	0.56	<0.130	0.57	0.43	0.54	<0.00	<0.152	0.76
^{66}Zn	71.87	79.26	68.01	71.23	62.61	57.13	70.85	73.60	73.43	76.40	86.35	86.02	272.06	321.18	78.23	77.63	71.84	72.73	60.59	99.88	50.29	56.65	89.83
^{85}Rb	216.02	210.49	218.88	214.40	202.90	191.66	210.90	200.94	220.46	208.91	242.52	257.00	282.54	245.96	231.10	206.26	221.31	207.99	199.05	207.42	185.66	187.50	209.87
^{88}Sr	142.89	132.26	142.28	139.53	128.27	127.05	127.83	127.94	126.22	128.54	121.51	112.40	120.05	121.10	114.13	124.27	132.89	125.34	138.83	124.56	140.62	119.19	126.89
^{89}Y	17.04	16.34	17.68	17.21	15.96	21.07	15.94	15.52	16.47	15.96	15.15	15.60	16.81	14.90	16.37	15.65	16.72	15.87	16.19	15.81	14.78	15.19	18.33
^{90}Zr	179.31	167.36	174.07	171.53	159.43	206.38	155.43	148.24	155.09	158.99	148.63	154.04	149.24	140.09	155.91	155.45	162.47	153.16	158.49	165.62	148.07	152.66	190.76
^{93}Nb	18.84	17.22	19.75	19.18	18.08	17.40	18.38	17.51	18.00	19.15	19.72	19.75	36.02	22.65	19.54	18.37	20.73	19.41	19.41	19.58	18.08	17.26	21.52
^{133}Cs	5.76	5.32	5.73	5.18	5.16	5.14	5.28	5.00	5.95	5.53	7.16	6.66	7.51	6.11	5.47	5.28	5.80	5.59	5.51	5.25	4.81	4.78	5.39
^{137}Ba	844.69	806.53	876.05	841.19	771.13	750.64	795.69	762.34	801.39	809.69	821.03	883.84	857.60	782.36	844.88	796.67	838.42	811.49	773.24	822.06	797.73	743.04	855.33
^{139}La	50.84	46.79	51.72	49.99	46.05	49.11	46.91	44.38	45.73	47.25	45.80	46.43	45.09	43.32	47.14	46.32	47.28	45.51	45.14	47.13	44.66	44.10	49.61
^{140}Ce	99.56	95.83	101.68	98.28	91.57	86.77	93.63	88.98	94.88	92.43	98.10	101.68	106.11	99.78	104.38	97.48	104.41	100.20	98.04	98.95	87.76	90.58	100.45
^{141}Pr	8.95	7.94	8.54	8.51	8.27	8.51	7.94	7.54	8.15	8.28	8.00	8.41	8.40	8.14	8.53	8.43	8.52	8.61	7.94	8.44	7.76	7.90	8.41
^{146}Nd	26.87	27.61	29.76	27.03	25.78	27.67	25.61	24.78	28.09	26.10	25.04	25.80	27.98	26.31	27.16	26.88	27.48	25.14	27.34	27.48	24.51	25.92	27.71
^{149}Sm	4.64	4.13	5.48	4.71	4.55	4.23	4.28	4.26	4.52	4.76	4.13	5.36	4.01	3.77	4.56	4.23	4.36	3.48	3.78	4.34	4.49	4.71	4.13
^{151}Eu	0.75	0.84	0.96	0.79	0.70	0.39	0.68	0.82	0.83	0.79	0.75	0.86	0.97	0.61	0.81	0.79	0.84	0.70	0.84	0.78	0.93	0.66	0.94
^{157}Gd	2.96	3.52	2.32	2.73	2.88	3.49	2.99	3.07	3.08	2.84	3.30	2.30	2.76	2.46	3.11	2.77	3.20	3.19	2.70	2.91	2.10	3.29	2.60
^{159}Tb	0.48	0.48	0.46	0.39	0.40	0.46	0.50	0.38	0.56	0.56	0.50	0.54	0.33	0.43	0.42	0.45	0.41	0.41	0.48	0.39	0.46	0.37	0.35
^{163}Dy	3.11	2.61	3.23	2.87	2.74	3.65	2.63	2.46	3.26	2.75	2.76	3.37	2.89	2.53	3.24	2.27	2.81	2.84	2.74	2.57	2.85	2.46	2.80
^{165}Ho	0.53	0.53	0.64	0.57	0.61	0.69	0.62	0.47	0.68	0.63	0.55	0.71	0.70	0.56	0.54	0.50	0.56	0.58	0.47	0.57	0.67	0.66	0.67
^{167}Er	1.58	1.58	1.59	2.05	1.56	2.00	1.36	1.41	1.20	1.73	1.50	1.68	1.74	1.62	1.89	1.46	1.68	1.90	1.59	1.72	1.67	1.28	1.55
^{169}Tm	0.16	0.27	0.22	0.26	0.29	0.35	0.29	0.23	0.21	0.25	0.23	0.30	0.24	0.22	0.23	0.26	0.27	0.24	0.22	0.23	0.29	0.26	0.20
^{173}Yb	1.77	2.13	2.36	1.61	1.89	1.96	1.90	1.59	1.51	2.08	1.58	2.08	1.90	1.71	1.99	1.70	1.84	2.08	1.59	1.98	1.56	2.09	1.51
^{175}Lu	0.27	0.27	0.36	0.26	0.24	0.38	0.25	0.27	0.28	0.31	0.28	0.33	0.26	0.27	0.31	0.34	0.31	0.23	0.25	0.29	0.25	0.26	0.27
^{177}Hf	4.79	4.44	4.64	4.22	4.70	5.95	4.15	4.00	3.81	4.47	3.71	3.90	3.61	3.73	4.19	3.73	3.94	4.16	4.27	4.39	3.16	4.02	5.07
^{181}Ta	1.29	1.40	1.37	1.30	1.05	1.32	1.13	1.04	1.07	1.20	1.15	1.07	1.51	1.09	1.21	1.20	1.37	1.47	1.27	1.33	1.21	1.14	1.49
^{208}Pb	26.62	41.13	27.50	26.25	27.51	24.44	26.99	24.04	24.77	26.72	29.33	33.73	57.32	32.15	31.68	25.75	29.02	26.76	24.14	26.28	21.87	22.34	27.79
^{232}Th	16.15	16.23	17.44	17.13	15.68	18.00	15.65	14.61	14.57	16.15	15.09	14.58	14.83	14.62	15.95	16.01	16.65	16.28	15.78	17.35	15.77	15.97	17.92
^{238}U	4.89	4.94	5.28	4.92	4.94	4.41	4.94	4.66	4.50	5.12	5.33	5.44	6.32	6.34	5.78	4.88	5.55	5.37	4.85	5.21	4.77	4.66	5.16

Table 6e

	93	94	95	96	97	98	99	100	101	102	103	104	105	106	107	108	109	110	111	112
^{7}Li	45.73	58.30	35.47	57.06	40.81	68.11	44.10	70.68	23.84	29.51	38.46	53.24	36.54	62.16	33.70	38.67	25.30	57.85	44.59	37.92
^{11}B	44.20	41.52	44.71	40.80	38.10	53.42	40.95	44.02	48.13	37.36	42.23	38.03	40.77	44.71	45.21	38.42	52.30	37.11	43.16	47.90
^{23}Na	37060	33683	32720	34941	28614	38825	36903	39680	38064	32457	38060	31993	35274	35942	35986	35308	34556	38462	35261	37641
^{25}Mg	995	883	895	969	686	1002	733	927	684	945	1377	908	910	1080	900	1107	936	1059	910	1012
^{29}Si	431630	437493	466787	454435	362093	488190	444460	491218	445426	492724	694862	423837	415526	471776	474512	452758	613992	423275	467731	472478
^{45}Sc	3.86	4.11	3.94	3.77	3.24	4.50	4.58	3.61	3.62	3.27	4.94	3.57	2.92	4.45	3.26	3.41	4.36	3.45	3.55	3.35
^{49}Ti	906.44	885.77	949.18	925.55	694.49	930.48	1038.90	1112.19	1017.01	1188.28	1240.13	952.73	948.40	1039.80	987.92	956.58	1364.70	893.07	1022.21	956.40
^{51}V	1.18	1.39	0.88	<0.22	0.76	1.27	1.12	1.51	1.00	0.95	1.49	0.99	0.87	1.42	1.14	1.34	1.81	0.97	1.15	0.92
^{53}Cr	<2.69	<1.45	<1.72	<1.83	<1.45	<1.94	<3.54	<3.58	<3.74	1.97	<2.42	<1.64	<2.02	<1.38	<1.92	<2.21	3.59	<2.43	3.75	<2.05
^{59}Co	0.72	0.65	0.92	0.78	0.64	0.90	0.73	<0.32	0.86	0.55	1.38	0.82	0.65	1.01	0.41	0.91	0.68	0.73	0.73	<0.24
^{60}Ni	<0.33	0.76	<9.19	<0.31	0.75	0.95	<0.37	<0.00	<0.47	0.64	1.27	<0.21	0.71	0.79	<0.31	1.59	3.79	<0.00	0.71	<0.192
^{66}Zn	93.25	62.58	66.40	75.85	44.47	67.15	55.80	59.26	55.31	52.79	85.55	55.95	57.15	73.83	76.33	154.56	185.32	70.33	65.27	65.42
^{85}Rb	191.13	195.39	206.51	198.13	157.98	230.46	226.40	273.64	211.38	175.53	197.98	192.77	185.55	216.72	199.12	189.05	215.41	197.48	197.93	203.31
^{88}Sr	121.34	128.39	130.62	135.18	118.14	120.14	143.21	127.26	145.79	130.42	143.40	129.09	136.11	129.34	140.50	129.41	129.32	129.50	134.42	134.51
^{89}Y	17.04	16.39	16.54	17.28	12.51	15.77	18.79	20.48	18.24	15.57	20.07	16.65	19.42	19.36	17.58	16.73	19.93	18.82	16.90	18.17
^{90}Zr	168.85	155.46	170.95	177.74	117.29	158.79	190.21	209.42	191.21	211.33	199.05	166.64	189.27	175.41	185.95	169.05	309.66	184.11	173.50	179.21
^{93}Nb	18.60	18.11	19.07	19.90	14.32	19.47	23.10	26.16	24.44	28.68	35.80	21.78	22.85	23.93	20.88	21.07	30.88	21.31	22.37	22.34
^{133}Cs	4.94	5.04	5.33	5.32	3.85	5.46	5.45	6.01	5.38	4.60	5.33	5.23	4.99	5.98	5.15	5.21	6.05	4.93	4.83	5.53
^{137}Ba	777.50	775.91	826.05	828.12	585.73	784.36	916.54	969.69	896.51	762.62	793.07	797.21	817.10	848.63	833.65	774.09	800.43	802.00	819.68	829.90
^{139}La	48.61	45.34	48.57	49.63	34.19	44.20	48.27	51.29	48.36	40.05	44.55	42.58	47.22	44.78	47.61	41.83	44.34	46.67	43.05	45.54
^{140}Ce	92.60	92.90	98.02	97.98	69.03	95.35	98.44	106.02	93.95	82.53	85.73	89.18	91.39	97.16	95.94	88.63	88.61	88.42	89.20	93.27
^{141}Pr	8.25	7.94	8.40	8.48	6.03	8.04	9.66	9.86	10.06	7.86	8.70	8.63	8.93	8.56	9.24	8.37	8.18	8.69	8.62	9.36
^{146}Nd	27.27	24.73	28.03	28.40	19.19	26.43	28.86	30.97	29.65	25.81	29.52	27.21	29.41	27.92	30.83	27.26	24.89	28.65	28.40	29.07
^{149}Sm	4.31	4.50	4.53	5.24	3.52	5.05	5.21	5.00	4.60	3.88	4.77	5.25	4.95	4.85	4.11	4.24	4.66	5.43	4.29	4.98
^{151}Eu	0.60	0.80	0.70	0.78	0.61	0.53	0.69	0.74	0.85	0.72	0.80	0.64	0.74	0.70	0.66	0.44	0.70	0.81	0.70	0.74
^{157}Gd	2.60	2.44	3.84	3.27	2.57	2.97	2.55	3.57	2.95	2.37	3.42	2.79	4.03	2.42	2.74	3.44	2.67	3.17	2.99	2.77
^{159}Tb	0.45	0.50	0.52	0.55	0.36	0.45	0.49	0.45	0.42	0.44	0.45	0.50	0.58	0.50	0.51	0.44	0.39	0.60	0.40	0.48
^{163}Dy	2.91	2.74	3.02	2.87	2.21	2.72	3.36	3.43	2.77	2.73	3.72	3.13	2.45	2.88	3.05	2.93	2.92	3.13	2.98	3.29
^{165}Ho	0.58	0.51	0.61	0.60	0.41	0.54	0.73	0.68	0.71	0.51	0.76	0.51	0.63	0.62	0.69	0.49	0.59	0.69	0.63	0.61
^{167}Er	1.45	1.56	1.60	2.03	1.19	1.80	2.07	1.91	2.16	1.70	2.26	1.77	1.70	1.84	2.23	1.71	2.25	1.92	1.73	2.22
^{169}Tm	0.21	0.25	0.27	0.23	0.20	0.27	0.31	0.31	0.29	0.23	0.32	0.25	0.23	0.22	0.30	0.27	0.27	0.32	0.22	0.26
^{173}Yb	1.99	1.35	2.24	2.06	1.32	1.92	1.75	2.20	1.86	1.29	1.96	2.02	1.86	1.90	2.03	1.49	1.83	2.13	1.94	2.08
^{175}Lu	0.19	0.25	0.27	0.34	0.22	0.23	0.23	0.22	0.26	0.21	0.35	0.17	0.32	0.31	0.27	0.29	0.26	0.31	0.30	0.30
^{177}Hf	4.77	4.60	4.54	5.10	3.05	4.33	5.24	4.96	5.26	5.79	6.43	3.85	5.13	4.37	4.71	4.57	8.77	4.87	4.68	3.85
^{181}Ta	1.51	1.26	1.41	1.39	1.05	1.25	1.66	1.85	1.75	2.01	2.40	1.85	1.36	1.67	1.34	1.49	2.17	1.57	1.69	1.52
^{208}Pb	27.93	25.91	26.17	25.40	19.46	26.67	22.93	24.76	22.74	20.75	32.99	21.11	24.34	28.28	26.29	27.65	37.65	24.95	24.24	25.61
^{232}Th	17.70	16.31	18.28	18.47	12.72	16.43	18.42	19.63	18.71	15.18	17.28	16.35	17.63	17.99	19.35	16.17	16.99	18.08	17.76	17.62
^{238}U	5.03	5.35	5.30	4.99	3.92	5.51	5.31	5.59	5.14	4.39	4.74	4.93	4.88	5.74	5.65	5.24	5.31	5.03	5.31	5.87

Table 7

Variable	LA139	CE140	ND146	SM149	EU151	GD157	TB159	YB173	LU175
^{139}La	1	0.6649	0.7133	0.4746	0.2950	0.3404	0.4364	0.4580	0.3527
^{140}Ce	0.6649	1	0.4862	0.2514	0.3817	0.1514	0.1603	0.3011	0.1525
^{146}Nd	0.7133	0.4862	1	0.441	0.2148	0.4084	0.4284	0.4943	0.3718
^{149}Sm	0.4746	0.2514	0.4410	1	0.1470	0.1611	0.4301	0.2755	0.3164
^{151}Eu	0.2950	0.3817	0.2148	0.1470	1	-0.0092	0.1018	0.1328	0.0409
^{157}Gd	0.3404	0.1514	0.4084	0.1611	-0.0092	1	0.3511	0.3104	0.2397
^{159}Tb	0.4364	0.1603	0.4284	0.4301	0.1018	0.3511	1	0.1904	0.2632
^{173}Yb	0.4580	0.3011	0.4943	0.2755	0.1328	0.3104	0.1904	1	0.2955
^{175}Lu	0.3527	0.1525	0.3718	0.3164	0.0409	0.2397	0.2632	0.2955	1

Table 8

Rock	**#**	**De La Roche *et al.* (1980) classification**
Volcanic glasses from mortars	50	Rhyolites
Volcanics from Mount Arci	7	Rhyolites
	111	Alkali- Rhyolites
	37	Alkali- Rhyolites
Volcanics from Saint Antioco	6	Rhyolites
	22	Alkali- Rhyolites

Table 9a,b

(a)

Variable	TN	MA	SA
CaO	16.546	-10.842	-2.697
FeO_T	63.419	63.97	85.609
P_2O_5	-191.734	-246.048	-282.898
Al_2O_3	37.784	39.945	45.11
Constant	-295.945	-289.794	-401.319

(b)

Group	Correct percent	# TN	# MA	# SA
Theatre	100	50	0	0
Mt. Arci	100	0	155	0
S.Antioco	92.86	1	1	26
Total	99.14	51	156	26

Table 10a,b

(a)

Variable	**Root 1**	**Root 2**
CaO	4.5298	1.755
FeO_T	-0.7997	3.9348
P_2O_5	10.7059	-6.1706
Al_2O_3	-0.5462	0.9192
Constant	3.9207	-18.0525

(b)

y = ax + b	**a**	**b**
Straight line 1	-5.606425	10.015314
Straight line 2	1.347037	0.469467
Straight line 3	0.056704	2.24111

Table 11a,b

(a)

Variable	TN	MA	SA
Sr	2.041	0.904	0.685
Ce	1.071	0.275	0.766
V	0.593	0.846	-0.196
Ba	-0.092	-0.069	0.01
Rb	0.752	0.687	0.444
Y	-1.865	-1.032	-0.712

(b)

Group	Percent correct	# TN	# MA	# SA
Theatre	100	112	0	0
Mt. Arci	100	0	37	0
S.Antioco	100	0	0	14
Total	100	112	37	14

Table 12a,b

(a)

Variable	**Root 1**	**Root 2**
Sr	0.0963	0.085
Ce	0.059	-0.0275
V	-0.0072	0.1284
Ba	-0.0029	-0.0118
Rb	0.0085	0.036
Y	-0.0726	-0.0838
Constant	-12.6758	-4.7147

(b)

y = ax + b	**a**	**b**
Straight line 1	10.327408	30.872576
Straight line 2	-1.24852	-3.943814
Straight line 3	0.591842	1.588636